A GEOLOGICAL DESCRIPTION OF POINT PLEASANT PARK

Neil Tobey

Submitted in Partial Fulfillment of the Requirements
for the Degree of Bachelor of Science, Honours
Department of Earth Sciences
Dalhousie University, Halifax, Nova Scotia
March 2006

Dalhousie University

Department of Earth Sciences
Halifax, Nova Scotia
Canada B3H 3J5
(902) 494-2358
FAX (902) 494-6889

DATE: March 13, 2006

AUTHOR: Neil Tobey

TITLE: A Geological Description of Point Pleasant Park

Degree: B Sc   Convocation: May   Year: 2006

Permission is herewith granted to Dalhousie University to circulate and to have copied for non-commercial purposes, at its discretion, the above title upon the request of individuals or institutions.

_____
Signature of Author

Acknowledgements

I would like to acknowledge the following people who have helped to make this thesis possible. I would like to thank Dr. Rebecca Jamieson for agreeing to take me on as her honours student when she did. I would like to thank Glenn Hart for providing the base maps for my thesis. I would like to thank Dr. Wach, Dr. Gibling, and Hasley Vincent for their much needed sedimentary and stratigraphy help. I would like to thank Patricia Stoffyn for her help on the microprobe. I would like to thank Gordon Brown for his help in preparing the thin sections. And last but not least I would like to thank my friends and family for their continuous support during the past 8 months.

A Geological Description of Point Pleasant Park

Neil Tobey

Point Pleasant Park has been a landmark of the city of Halifax for over 200 years. Originally built as a military base in 1796, Point Pleasant Park was leased to the people of Halifax in 1873 by Queen Victoria for a shilling a year for 999 years.   The Park was recommissioned during the two world wars and since has been a municipal park for all of the residents in Halifax to enjoy. The devastation brought about by Hurricane Juan provided an opportunity to study the bedrock geology within Point Pleasant Park. The bedrock geology of the Halifax peninsula was originally assigned to the Cunard member of the Halifax Formation. After careful observation, the bedrock geology within the park was has been assigned to a different unit, informally named the Bluestone member after an old quarry on the western side of the North West Arm. The Bluestone member is an interlayered metasiltstone-slate turbidite unit lying gradationally on top of the Cunard member. Two subdivisions of the Bluestone member have been identified within the Park. Unit A is interlayered metasiltstone and slate containing abundant calcareous concretions. This unit starts at the southern tip of the park and continues north until the last occurrence of calcareous concretions at Cable Rock. Unit B is similar in lithology to unit A but has no observed concretions. The lithology of the park has been folded into a large-west plunging syncline with the fold axis located at the northern edge of the park. Two different metamorphic events have affected the rocks within the park. Regional metamorphism occurred along with the folding during the Acadian Orogeny (ca. 390 Ma) and has metamorphosed the Bluestone member to greenschist (chlorite zone) facies. Contact metamorphism caused by the intrusion of the South Mountain Batholith (ca. 380 Ma) overprinted the regional metamorphism producing cordierite, which has weathered out to give the rocks their characteristic "spotted" appearance.

Table of Contents

List of Figures

List of Tables

1. Introduction:

1.1 Purpose and Scope of Study

The purpose of this thesis is to provide a systematic and descriptive analysis of the geology of Point Pleasant Park with reference to lithology, stratigraphy, structure, and metamorphism.

The opportunity to study the park presented itself after the devastation of the park by Hurricane Juan in September of 2003. Because of Hurricane Juan, some new outcrops were exposed, and light levels in wooded areas improved, which allowed for a better systematic description of the geology in Point Pleasant Park. Initial field observations made in the summer of 2004 revealed the presence of previously unreported calcareous concretions within some of the rock units which raised the possibility of describing a new unit within the Halifax Formation on the southern Halifax peninsula. Until then, the bedrock underlying the entire peninsula was assigned to the Cunard Member of the Halifax Formation. This study also contributes to the study of the contact aureole and the effect of the intrusion of the South Mountain Batholith on the rocks beneath the city of Halifax (Jamieson et al, 2005; Hart, 2006). Another benefit of this study is to provide a geological description of a historical site, which could be incorporated into tourist information on the park.

1.2 Geographical Location and Historical Significance of Study Area

Point Pleasant Park covers an area of approximately $1km^2$ at the southern tip of the Halifax peninsula. The area now included in the park was originally

established as a military base after the City of Halifax was founded in 1749. In 1873, Queen Victoria leased the park to the people of Nova Scotia for a shilling a year. The park was re-commissioned as a military base during World Wars 1 and 2. The study area encompasses the entire park plus a few outcrops between the park and the railway cut (Fig 1.1).

1.3 Geological Summary of Point Pleasant Park

Point Pleasant Park is underlain by the Halifax Formation of the Meguma Group, a deep sea fan complex deposited on the outer paleocontinental shelf of Gondwana during the Cambrian/Ordovician period (Schenk, 1997). As described below, the rocks in Point Pleasant Park are assigned to the Bluestone member (informal name) of the Halifax Formation, which overlies the Cunard Member (Jamieson et al, 2005). The Bluestone member is an interbedded sequence of metasiltstone and slate with local calcareous concretions present in outcrops at the southern end of the park.

In general, the rocks within Point Pleasant Park lie on the southern limb of a large west-plunging syncline referred to as the Point Pleasant Park Syncline (Fig. 4.2). The bedding strikes approximately 230° and dips 20 – 40° NW. Cleavage is well exposed in the outcrops, except along the western side of park where it has been annealed by contact metamorphism. The cleavage strikes approximately 230°, but dips at a steeper angle (60 – 80° to the NW).

Regional metamorphism of the Meguma Group occurred during the Acadian Orogeny (410 – 380 Ma) when the Meguma Terrane collided with

Laurentia (Williams, 1979). Metamorphic grade varies from greenschist to amphibolite facies throughout the Meguma Terrane with higher grades at the NE and SW ends. In the study area the regional grade is chlorite zone of the greenschist facies. Intrusion of the South Mountain Batholith (380 ± 3 Ma, Carruzzo et al, 2003) created a contact aureole in the Halifax Formation, part of which is well exposed within Point Pleasant Park.

1.4 Methods

1.4.1 Field Mapping

During the summer of 2004 (May – August) and the winter of 2005/2006 (December - January), detailed mapping of Point Pleasant Park was performed. Overall 41 different outcrops were examined. Of these, 21 were sampled. GPS readings were taken, and a general description of each outcrop was made, noting general lithological and structural features. Bedding, cleavage, and lineation readings were taken, depending on what was exposed at each outcrop.

1.4.2 Map Preparation

Once the field data were gathered, geological maps of the park were created using AutoCAD R14, Fieldlog, Idrisi, and Pathfinder. Charlie Walls provided an original base map of the park. These maps were used in a poster for the GAC-MAC conference at Dalhousie University in May, 2005. Since then these maps have been updated by Glenn Hart, and will be used in this thesis. GPS data were downloaded from the portable GPS and location corrections were made to the points using Pathfinder. The corrected points were then put into

Fieldlog along with the associated structural data. Three major maps were produced: an outcrop map (Fig 1.1), a bedding map (Fig 4.2a), and a structural map (Fig 4.2b). Two cross – sections through the park were constructed (Fig 4.4 and 4.5).

1.4.3 Petrography and Mineral Chemistry

Thin sections from all 21 samples collected from the park were examined for mineralogy and texture. Appendix C and D summarise the data collected. Five representative samples were selected for microprobe analysis to determine the range of mineral compositions across Point Pleasant Park.

1.5 Organization of the Thesis

Chapter 2 explains the regional geological setting of Point Pleasant Park. Chapter 3 describes the lithology and stratigraphy of the sedimentary rocks within Point Pleasant Park. Chapter 4 discusses the structural geology of the rocks within the park. Chapter 5 discusses the metamorphism and petrography including mineral chemistry. Chapter 6 summarises the data.

Mineral Assmblages in Point Pleasant Park   1:7000

Legend

Bluestone

Mineral Assemblages

+ Chl + Crd + Bt
+ Crd + Bt

Rock Units

Bluestone
SMB
Point Pleasant Park

Roads/Paths

Trails
Railway

Ogilvie Towers   PPP04 - 18

PPP04 - 15

PPP04 - 1

Francklyn Street   PPP04 - 20

PPP04 - 14

PPP04 - 9
Black Rock Beach

PPP04 - 13

PPP04 - 12

PPP04 - 10

PPP04 - 11

PPP04 - 16, 17a, 17bPPP04 - 2

Cable Rock

PPP04 - 3

PPP04 - 21

PPP04 - 5a, 5bPPP04-6,7
Battery Point

PPP04 - 8

Measured Section

PPP04 - 4

Kilometers

0   0.125   0.25   0.5   0.75   1

Figure 1.1 - Map of study area and surrounding areas showing mineral assemblages. Map includes PPP04 sample locations and numbers. Base map provided by Glenn Hart

Map version 2.1 by: Glenn Hart, 2005

2. Regional Geology of the Meguma Terrane

2.1 Introduction

The Meguma Terrane, the most outboard of the various Appalachian terranes, was accreted during the Devonian Acadian Orogeny (Williams, 1979). The Meguma Terrane consists of Paleozoic sedimentary and granitic rocks, including the Meguma Group, the Annapolis Group, the Horton Group, the Windsor Group, and the South Mountain Batholith (Fig 2.1). Meguma Group rocks that were folded and regionally metamorphosed during the Acadian Orogeny (ca. 410 – 370 Ma, Hicks et al, 1999) underlie the study area, located at the southern end of the Halifax peninsula. The rocks were metamorphosed a second time due to the intrusion of the South Mountain Batholith.

The nomenclature of the Meguma Terrane has been the topic of interest for quite some time, but for the purpose of this thesis, I will be using the terms Meguma Group, Goldenville Formation, and Halifax Formation. O'Brien (1986) proposed a third formation within the Meguma Group in the Mahone Bay area, termed the Green Bay Fm. This corresponds to the Goldenville – Halifax Transition (GHT) but the term Green Bay Fm has not become widely used. The study area of this thesis lies within the Halifax Formation.
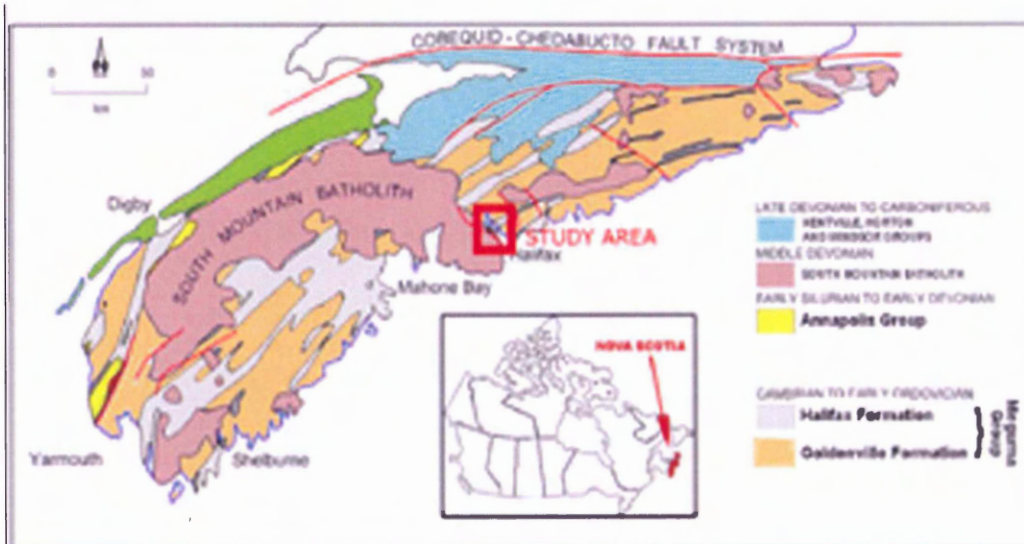
Regional geology map of the Meguma Terrane with the Avalon Terrane north of the Cobequid-Chedabucto Fault.
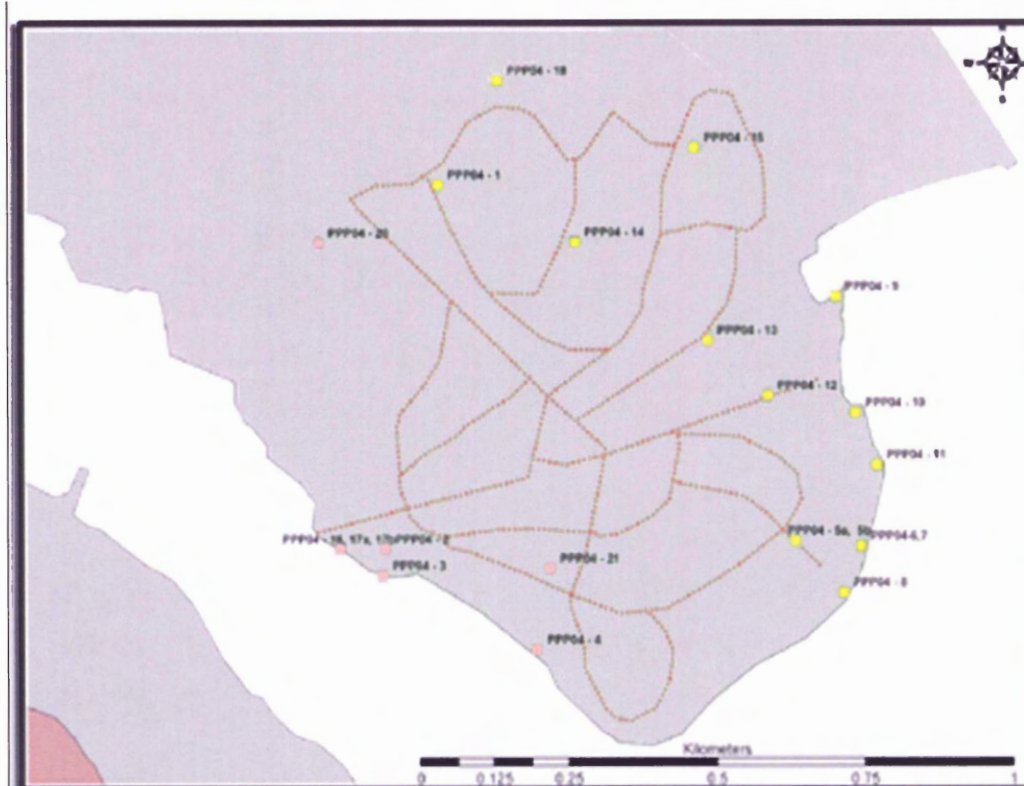
Geological Map of Point Pleasant Park. Point Pleasant Park is Part of the Bluestone member (dark gray) of the Halifax Formation. Intrusion of the South Mountaion Batholith (pink) created a contact aureole within the park

Figure 2.1a – Regional and local geological maps. Original maps provided by Glenn Hart

Regional Geological History

Stratigraphic	Plutonic	Deformation	Metamorphic

Flexural Slip

Windsor Group
(339-323 mya)
Horton Group

South Mountain Batholith
(380 mya:
Peraluminous granite,
granodiorite to
leucogranite)

Contact Metamorphism
(380 mya: marked by
first appearance of
cordierite)

Kentville Fm
(420-410mya)
White-Rock Fm.
(462-410 mya)

Annapolis Grp.

Regional Up-right folding.
(410-380 mya:
NE-SW trending,
upright folds plunging
southwest)

Regional Metamorphism
(410 -380 mya:
Greenschist to north to
amphibolite to south)

Halifax Fm.

Goldenville Fm.

Meguma Grp.
(540-462 mya)

Devonian / Ordovician

Local Halifax Geological History

Stratigraphic	Plutonic	Deformation	Metamorphic

Flexural Slip

South Mountain Batholith
(380 mya
Halifax Pluton)

Contact Metamorphism
(380 mya: marked by
first appearance of
cordierite)

Bluestone member
(487 mya*)

Halifax Formation

Meguma Group

Regional Up-right folding.
(410-380 mya:
NE-SW trending,
upright folds plunging
southwest)

Regional Metamorphism
(410-380 mya:
Chlorite zone)

Devonian / Ordovician

* Age of 487 mya based on Rhabdinopora flabelliformis (graptolite) in the Bear River member which correlates to the Feltzen member (Bluestone member) of the Halifax Formation in South West Nova Scotia (M. Melchin and C. White personal communication to R. Jamelson, February 2006).

Figure 2.1b – Regional and local geological histories. Original diagram modified from Glenn Hart

2.2 Meguma Group

2.2.1 Goldenville Formation

The Goldenville Formation is the ca. 9000 m thick basal unit of the Meguma Group (Schenk, 1997). It is exposed at the northern end of the Halifax peninsula, and does not lie within the study area. The Goldenville Formation is divided into three distinct members: the New Harbour member, the Rissers member, and the West Dublin member (Schenk, 1997). The deep-water ichnofossil *Oldhamia* places the lower middle Goldenville Fm in the early Cambrian (White et al, 2006). White et al (2006) have suggested that basal part of the Goldenville extends into the Neoproterozoic. The New Harbour member is a basin floor fan deposit comprising 7000m of quartzo - feldspathic wacke. The wacke units typically form massive T_a and T_b Bouma units with thinner layers of silty/sandy slates (Schenk, 1997). Both the Rissers and the West Dublin members are slope fan deposits, each approximately 1000m think (Schenk, 1997). The Rissers member consists of black slate that coarsens upward to sandy turbidites, typically T_{a-c} (Schenk, 1997). The West Dublin member consists of thick turbidites (T_{ab}) with thin interbedded turbidite sequences (T_{a-e}) (Schenk, 1997).

2.2.2 Halifax Formation

The Halifax Formation has been interpreted as a large prograding wedge of shale and siltstone (Schenk, 1991) up to 8000 m thick. In the Mahone Bay area, the Halifax Formation has been subdivided into three dominant members: the Moshers Island Member, the Cunard Member and the Feltzen Member

(O'Brien, 1988). In Halifax, only the Cunard Member has been formally recognized. However, the results of this study and others (Jamieson et al, 2005; Hart, 2006) suggest that a second lithological unit, here termed the Bluestone member, underlies Point Pleasant Park and the Purcells Cove - Williams Lake area. Stratigraphic and structural data described below suggest that this unit may be equivalent to the Feltzen Member.

2.2.3 Moshers Island Member

The Moshers Island Member is a 500 m thick pale gray to bluish gray slate unit that conformably overlies the Goldenville Formation (Schenk, 1997). Beds are slate rich, with thinner sandy layers. The slaty layers are 10 – 40 cm thick and the sandier units are 10 – 15 cm thick (Hicks, 1996). Carbonate concretions and thin carbonate lenses occur throughout the Moshers Island Member (Hicks, 1996). This member is metalliferous, containing significant amounts of Ba, Zn, Cu, Pb, and large amounts of Mn (2-12%) (Schenk, 1997).

2.2.4 Cunard Member

The Cunard Member is a relatively thick (500 – 8000 m) grey to black slate unit with interbedded fine-grained turbidites (T_{a-e}) that conformably overlies the Moshers Island Member (Schenk, 1997; Hicks 1996). It underlies most of the peninsula of Halifax, but not the study area. Thinly bedded sandy layers contain significant amounts of sulfides, up to 50% in some areas (Hicks, 1996). A strong cleavage present in the slaty layers is less well developed in the sandier layers (Hicks, 1996). In the Digby area, the Bear River member, correlative with the Feltzen member, contains the graptolite *Rhabdinopora flabelliformis,* diagnostic

of the Early Tremadoc (ca 487 Ma) (White et al, 2006; C. White & M. Melchin,

pers. comm. to R. Jamieson, 2006).

2.2.5 Feltzen member

The Feltzen Member is a 2000 m thick interbedded siltstone and slate unit

lying conformably on top of the Cunard Member (Schenk, 1997). Outcrops are

typically dark grey-blue grey. The amount of siltstone in this unit is considerably

higher than in the Cunard Member, up to 20% in some areas (Hicks, 1996).

Siltstone layers are typically rhythmically interbedded with slate, and can be up to

20cm thick. Slaty units are either finely laminated, or homogeneous (O'Brien,

1988). The Feltzen Member, though not formally defined in the Halifax area,

shows several distinct similarities with the rocks in Point Pleasant Park.

2.2.6 Bluestone Member

Based on observations described in Chapter 3, the rocks in Point Pleasant

Park have been assigned to the Bluestone member of the Halifax Formation, an

informally defined unit named for the Bluestone Quarry on the western side of the

North West Arm directly across from Point Pleasant Park.

2.3 Annapolis Group

The uppermost stratified unit in the Meguma Terrane is the Annapolis

Group which is restricted to the Annapolis Valley and SW Nova Scotia. This

group is not present in the study area, but is described here in brief for

completeness. It includes the White Rock Formation, a slate, quartzite, and

metavolcanic unit (MacDonald et al, 2002) which has been dated (U-Pb, zircon)

at 442 ± 4 Ma (Keppie, & Krogh, 2000) and 438 ± 3 Ma (MacDonald et al, 2002).

The Torbrook Formation lies conformably above the White Rock Formation and

consists of metasiltstones, slates, and marbles (White & Barr, 2003). Numerous

mafic sills intrude the Torbrook Formation. Early Devonian shelly fossils are

found within the unit (MacDonald et al, 2002). The Annapolis Group has been

folded with the Meguma Group, placing a lower limit of Early Devonian on the

age of regional deformation (Hicks et al, 1999).

2.4 South Mountain Batholith

The South Mountain Batholith (SMB) is a large (~7300 km^2) peraluminous

granitic pluton that intruded the Meguma Group during the later stages of the

Acadian Orogeny (ca. 380 ± 3 Ma; Carruzzo et al, 2003; Kontak et al, 2002). The

closest outcrops to the study area are near Purcell's Cove on the western side of

the North West Arm. Thirteen different plutons make up the SMB, which consists

largely of biotite granodiorite, biotite monzogranite, and more evolved

monzogranite and leucogranite (Kontak et al, 2002; Clarke et al, 2004). The

pluton directly affecting Point Pleasant Park is the Halifax Pluton (Kontak et al,

2002). The rocks of the Halifax Pluton are subdivided into two different phases

(Kontak et al, 2002). Phase 1 is a zoned sequence of peraluminous biotite

monzogranite and biotite granodiorite with muscovite and cordierite (Kontak et al,

2002). Phase 2 is a biotite-muscovite leucomonzogranite (Kontak et al, 2002).

2.5 Regional Deformation and Metamorphism

Regional large-scale NE/SW trending folds associated with the Acadian Orogeny occur throughout the Meguma Group (Horne & Culshaw, 2001). The folds are typically upright chevron folds with axial planar cleavage in the slaty layers, as evident in Point Pleasant Park. Late stage flexural – slip folding occurred in SW Nova Scotia and within the study area (Horne & Culshaw, 2001).

Regional metamorphism associated with the Acadian Orogeny occurred ca. 410 – 370 Ma (Hicks et al, 1999). Regional grade varies from greenschist to amphibolite facies (Williams, 1979) with high grade at the SW and NE ends and low grade in the middle of the terrane. Within the study area, the regional grade is chlorite zone of greenschist facies. The intrusion of the South Mountain Batholith (ca. 380 Ma) created a contact aureole within the Meguma Group. The outer limit of the contact aureole is marked by the presence of cordierite "spots" (Jamieson et al, 2005).   The study area lies entirely within the contact aureole.

3. Lithology and Stratigraphy of Point Pleasant Park

3.1 Introduction

Although Point Pleasant Park has been used for undergrad field studies for Dalhousie and Saint Mary University for many years, lithological units within Point Pleasant Park have not been formally described or subdivided. Here a preliminary subdivision is proposed. Two distinct units (A and B, with A being the basal unit) have been identified (Fig. 3.1). Both units are rhythmically interbedded meta-siltstone/slates, but unit A contains abundant calcareous concretions. The thickness of the Bluestone member is difficult to determine due to the lack of continuity of outcrops.

3.2 Unit A

3.2.1 Slate – Siltstone

Unit A extends from Battery Point and continues along dip until the last known outcrop containing calcareous nodules, on the North West Arm at Cable Rock (Fig 4.3). It consists of rhythmically interbedded meta-siltstone and slate. Both types of layers range from a few centimetres to tens of centimetres thick (Fig 3.2). Typically, meta-siltstone layers occupy 50% of the outcrop, but in some areas they can occupy up to 70% (PPP04 – 5a & b, Fig 3.1). Concentrations of sulphide minerals in coarser-grained layers have produced substantial iron staining on outcrops. A measured section from this unit is presented in Appendix A.

Mineral Assmblages in Point Pleasant Park   1:7000
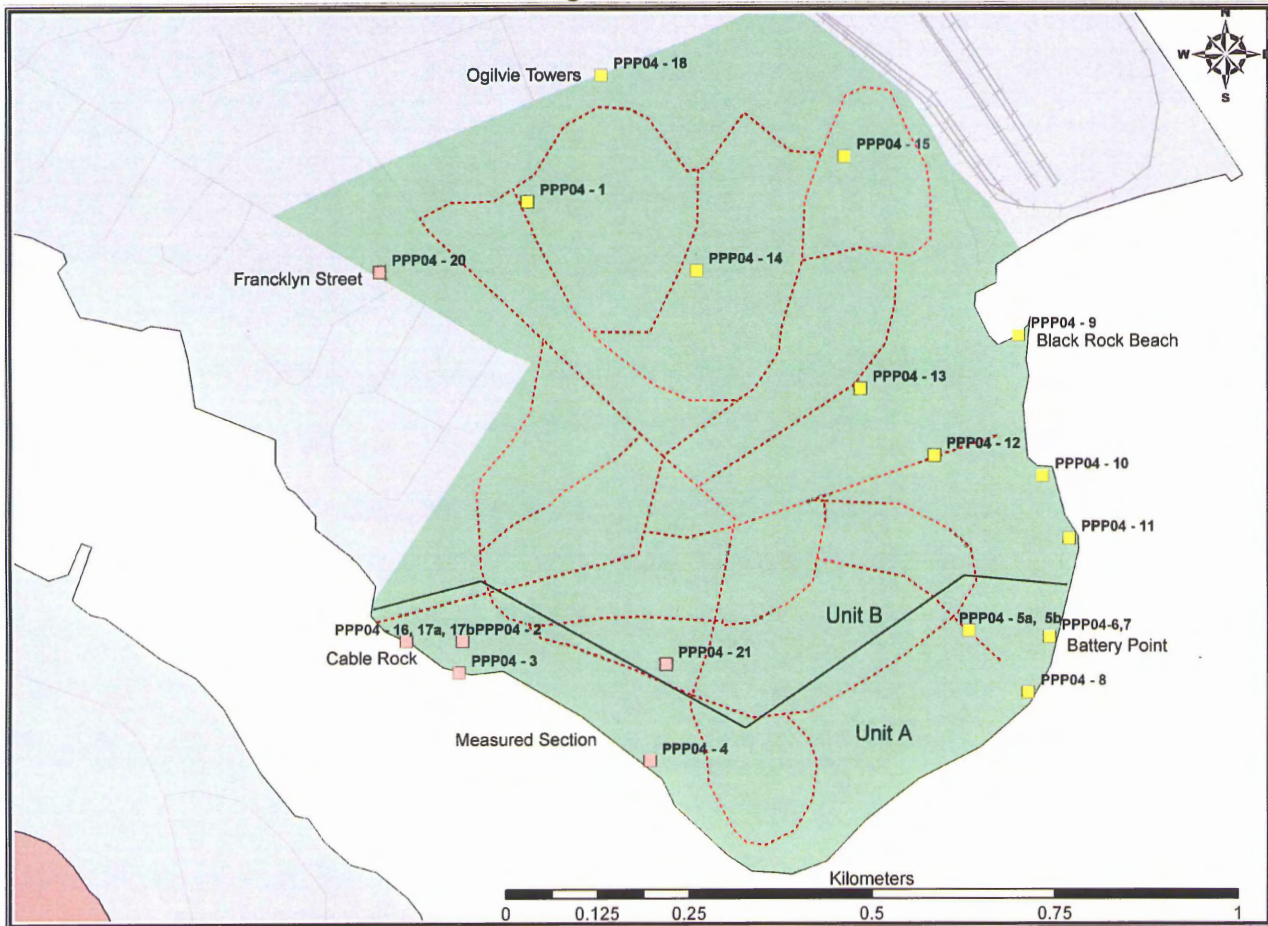
Ogilvie Towers ▪ ▪ PPP04 - 18

PPP04 - 15

PPP04 - 1

PPP04 - 20
Francklyn Street

PPP04 - 14

PPP04 - 9
Black Rock Beach

PPP04 - 13

PPP04 - 12

PPP04 - 10

PPP04 - 11

Unit B

PPP04 - 16, 17a, 17b PPP04 - 2

Cable Rock   PPP04 - 3

PPP04 - 21

PPP04 - 5a, 5b PPP04-6,7
Battery Point

PPP04 - 8

Measured Section   PPP04 - 4   Unit A

Kilometers

0   0.125   0.25   0.5   0.75   1

Legend

Bluestone

Mineral Assmblages

▪ + Chl + Crd + Bt
▪ + Crd + Bt

Rock Units   **Roads/Paths**

▪ Bluestone   —— Trails

▪ SMB   —— Railway

▪ Point Pleasant Park

Figure 3.1 – Map showing the informal division between units A & B. Map Provided by Glenn Hart

Map version 2.1 by: Glenn Hart, 2005

At outcrop scale, several different turbidite sequences can be identified, with T_{b-c} Bouma units dominating. The basal contact of each sequence is marked by a scoured surface, indicating that erosion took place. In the T_c units, ripple sets are typically 1-5 cm in amplitude and have a 5 cm wavelength (Fig 3.3). Based upon the orientation of the crests of these ripples, the paleo-flow direction has been interpreted as approximately trending 125°. Interpretation of the Bouma sets has to be taken with some caution because slaty cleavage and metamorphic recrystallization have modified primary grain size and fine structure. Detrital grain size is hard to determine due to recrystallization, however a first guess based upon thin section observations, is fine grained (0.5 – 1 mm), based upon thin section observations in PPP04 - 5.

Figure 3.2 – Metasiltstone (light) and slate (dark) from a turbidite unit in the measured section in unit A.

Figure 3.3 - Crossbedding in metasiltstone from turbidite layer in the measured section. Younging direction is up. Pits are weathered cordierite

3.2.2 Calcareous Concretions

The presence of calcareous concretions distinguishes unit A from unit B. The concretions are lensoidal with diameters typically 10 – 20 cm (Fig 3.4 & 3.5). Colour zoning is evident in hand sample scale reflecting variations in mineralogy, described in Chapter 5. Colour zoning varies depending on the location of the concretions. Concretions in lower grade samples range in colour from green cores to bluish gray rims. Some concretions in higher-grade samples have orange rims with a black core.

Two different types of concretions have been observed, with both being present beneath the fortification at Battery Point. Type I concretions appear to have a crosscutting relationship with sedimentary layering. These concretions

are approximately 20 cm in diameter (Fig 3.4). Type II form pinch and swell structures within sedimentary layers, with the concretions in the thicker parts. These concretions vary in size from 10 – 30 cm in diameter (Fig 3.5).

The mineralogy of the concretions differs from their host rocks. The nodules contain garnet, biotite, muscovite, chlorite, calcite, ilmenite, and a sulfide. No cordierite is present in the concretions. Other aspects of mineralogy are discussed in Chapter 5.

Based on studies elsewhere (Pye et al, 1990), the concretions probably formed during diagenesis of host sediments. Precipitation on a shell fragment (or other nucleation site) of material (ions) from a supersaturated fluid creates a spherical growth within permeable sandier layers. These nodules typically form at shallow burial depth (Pye et al, 1990).

Figure 3.4 – Type I concretions present at the Battery Point outcrop (PPP04 – 6, 7a, 7b, 7c). Concretion cuts sandy layer's primary features at outcrop scale, not visible in photo
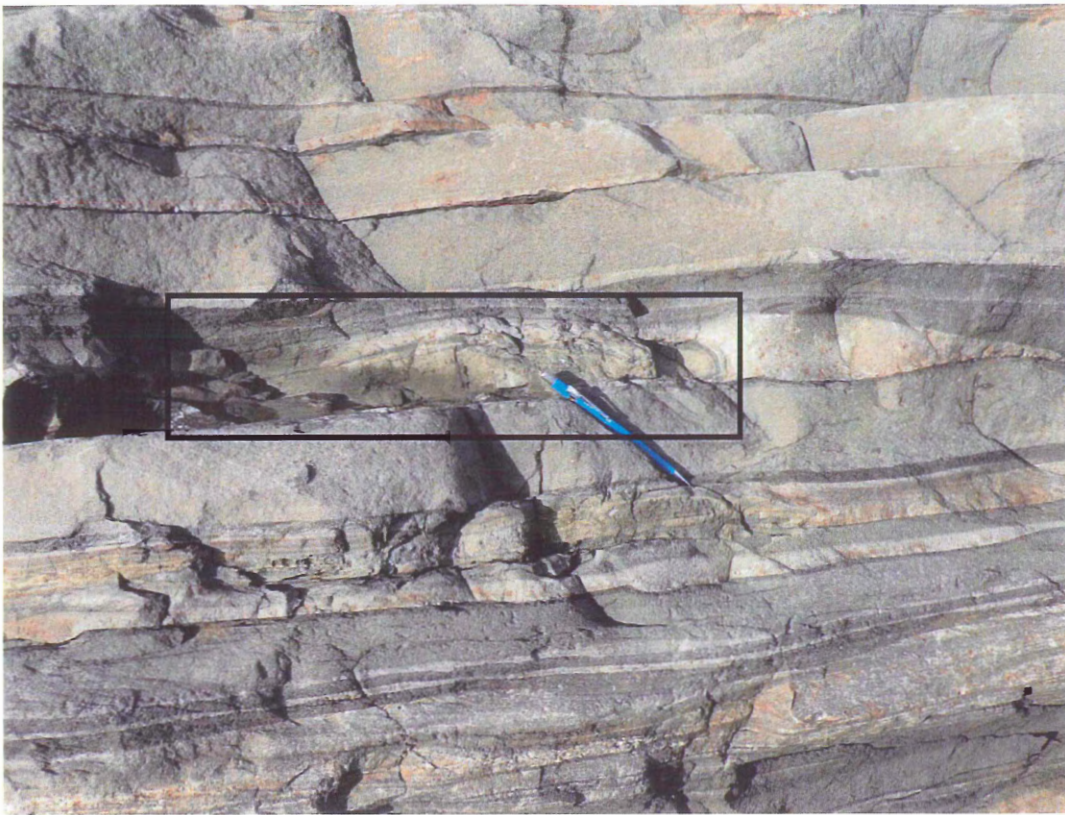
Figure 3.5 – Type II concretions present at the Battery Point outcrop (PPP04 – 6, 7a, 7b, 7c). Outlined concretion formed in swell structure pinching out at the edge of the photo

3.3 Unit B

Unit B overlies unit A, but the contact is not well defined. Here the base of unit B is taken to be immediately above the last known layer containing calcareous concretions (Cable Rock). All outcrops north of PPP04 – 5, including those north of the park, are also assigned to unit B. Unit B has interbedded metasiltstone/slate layers similar in appeerence to those in unit A (Fig 3.6), but this unit lacks calcareous concretions. Turbiditic sequences are similar to unit A in appearance, thickness, and abundance. Also, siltstone layers in unit B have a more grayish colour, where as in unit A they have a brownish green colour. Climbing ripples are similar in dimension to those in unit A (Fig. 3.3). There was no section measured in this unit because of the lack of continuous outcrops

Detrital grain size is also hard to determine in unit B due to the amount of

recrystallization present in the outcrops.

Figure 3.6 – Interlayered metasiltstone (light) and slate (dark) from Black Rock Beach in unit B. Pencil for scale

4. Structure

4.1 Introduction

Horne and Culshaw (2001) analyzed the structure of the peninsula of Halifax as far as the northern limit of this study area (Fig. 4.1). Their work showed the Halifax Formation was deformed into km-scale NE/SW trending, upright, tight, chevron-like folds during the Acadian Orogeny. Flexural – slip folding occurred at the later stages of the Acadian Orogeny (Horne & Culshaw, 2001), which is evident by the offset in some cordierite grains (Horne & Culshaw, 2001).

Two large structures were analyzed on the peninsula of Halifax by Horne and Culshaw (2001). The Lawrencetown anticline appears north of the Dalhousie University campus well outside of the study area. The study area lies within a NE/SW-trending syncline, labelled the Point Pleasant Park syncline, with the hinge line located at the northern edge of the park (Fig 4.2). At the southern edge of the park, bedding dips shallowly to the north. Bedding becomes nearly horizontal around the Quarry Pond and changes to a southerly dip north of the Quarry Pond. The slaty cleavage, characteristic of fine-grained units of the Halifax Formation, is axial planar to these upright folds.
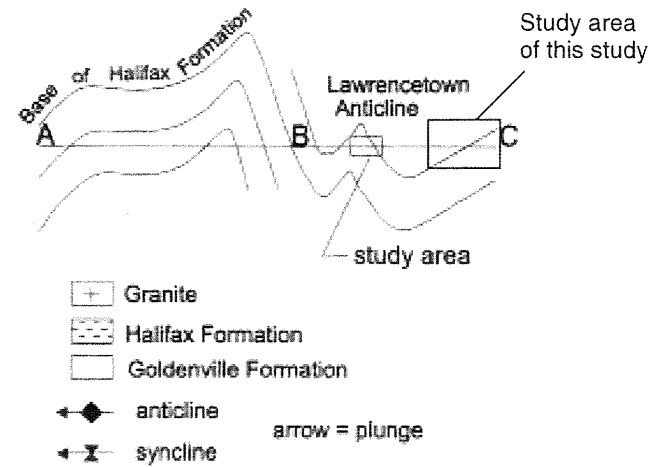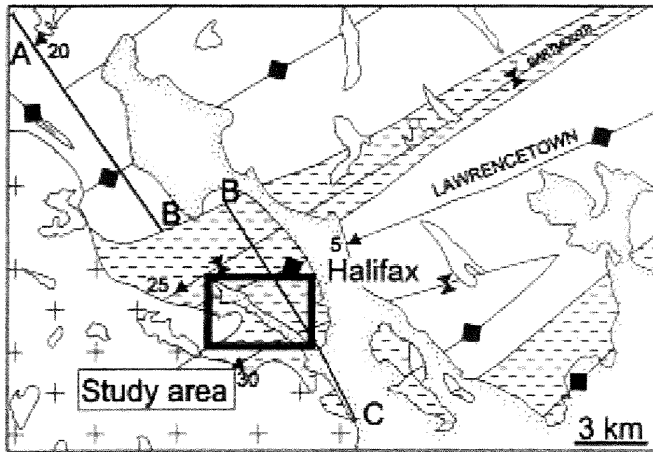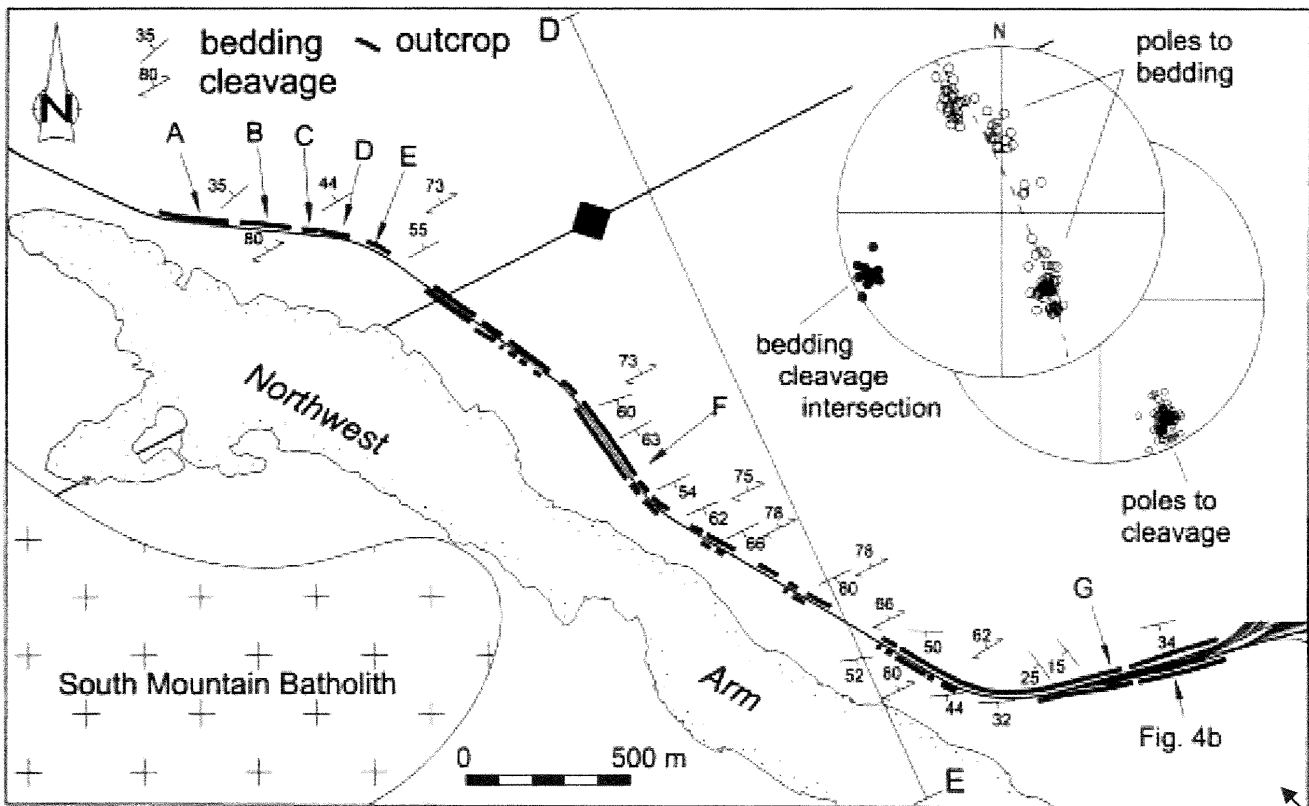
Figure 4.1 – Structural map of the peninsula of Halifax up to the northern limit of this study area. Taken from Horne and Culshaw (2001). Figure A shows the study area of Horne and Culshaw (2001) and figure B shows the structural information on the peninsula of Halifax until Point Pleasant Park. Horne and Culshaw suggested that the axis of the Point Pleasant Syncline lies north of the park, but this study suggests that the axis of the syncline lies at the northern border of the park.

Structure in PPP   1:7500
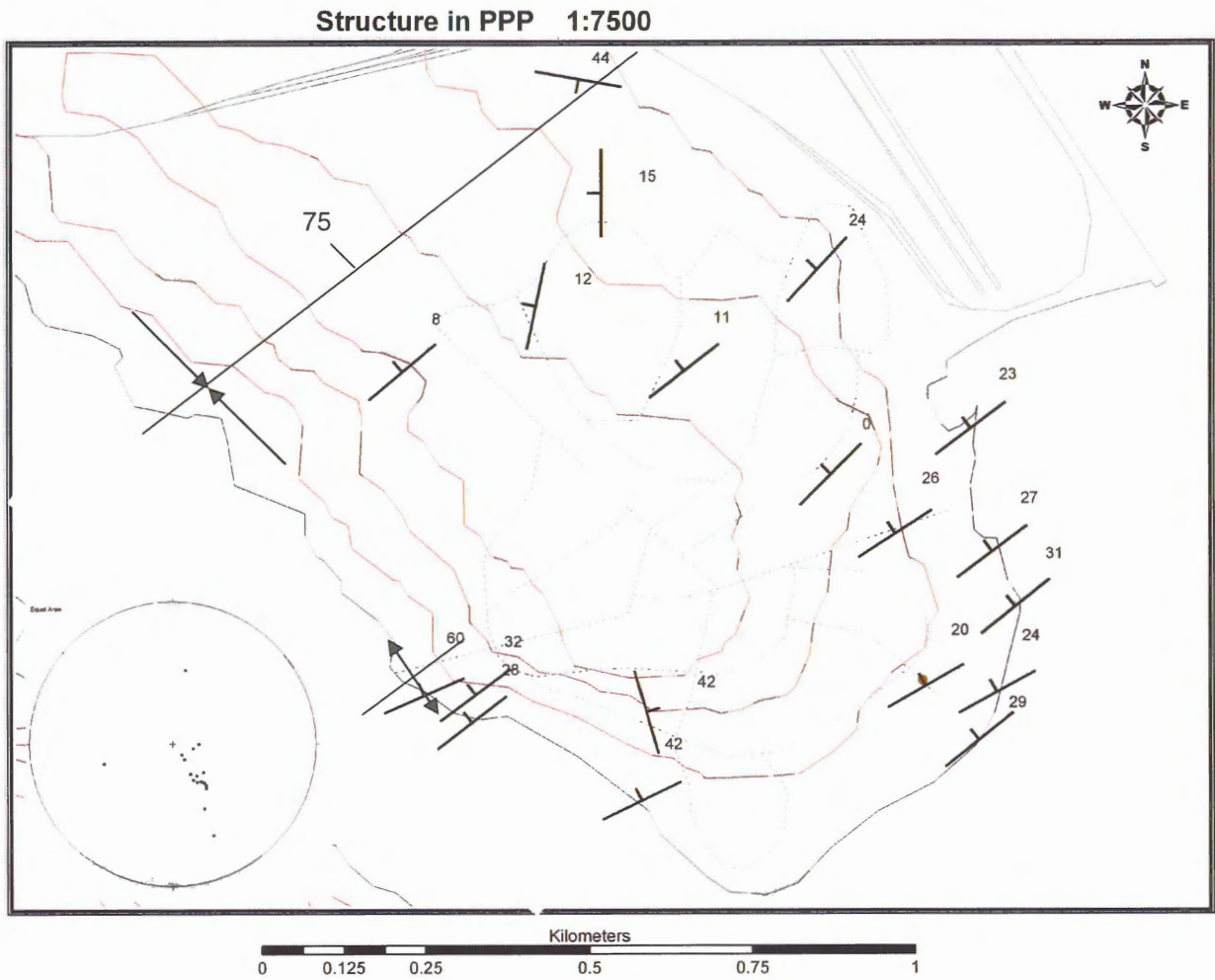
Figure 4.2a – Orientation of bedding of Point Pleasant Park. Line indicates trace of the axial surface.
Maps provided by Glenn Hart

Structure in PPP 1:7500
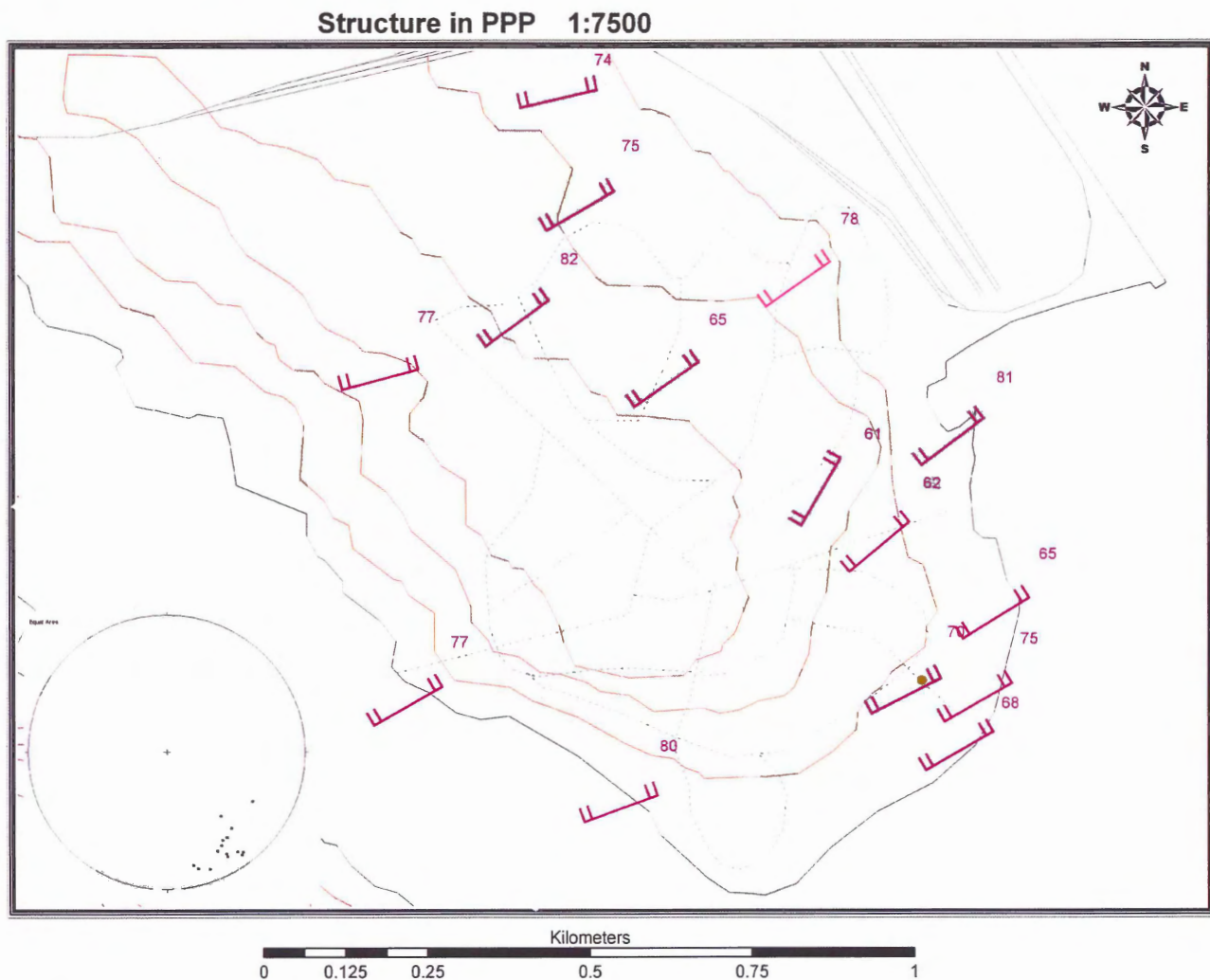
Figure 4.2b – Orientation of cleavage. Cleavage is axial planar to the orientation of the hinge and dips to the NW. Maps provided by Glenn Hart

4.2 Cross Section

Two cross - sections within the park were constructed. Both begin at the southern tip of the park (Battery Point, PPP04 – 6, 7a, 7b, 7c) and end at the northern edge of the study area. Section A - A' lies along the harbour side of the park (Fig 4.3) and shows a simple syncline. Section B – B' lies along the North-

West Arm (Fig 4.3) and has a more complex structural pattern. The same syncline can be seen in cross-section B, along with a small parasitic anticline.

By convention, the bedding and cleavage readings are displayed as strike/dip with the strike measurement taken following the right-hand rule. The dips noted in outcrop description are the measured dips, which have been corrected for projection onto plane of cross - section (Appendix B). Cross - sections can be seen in Figures 4.4 and 4.5
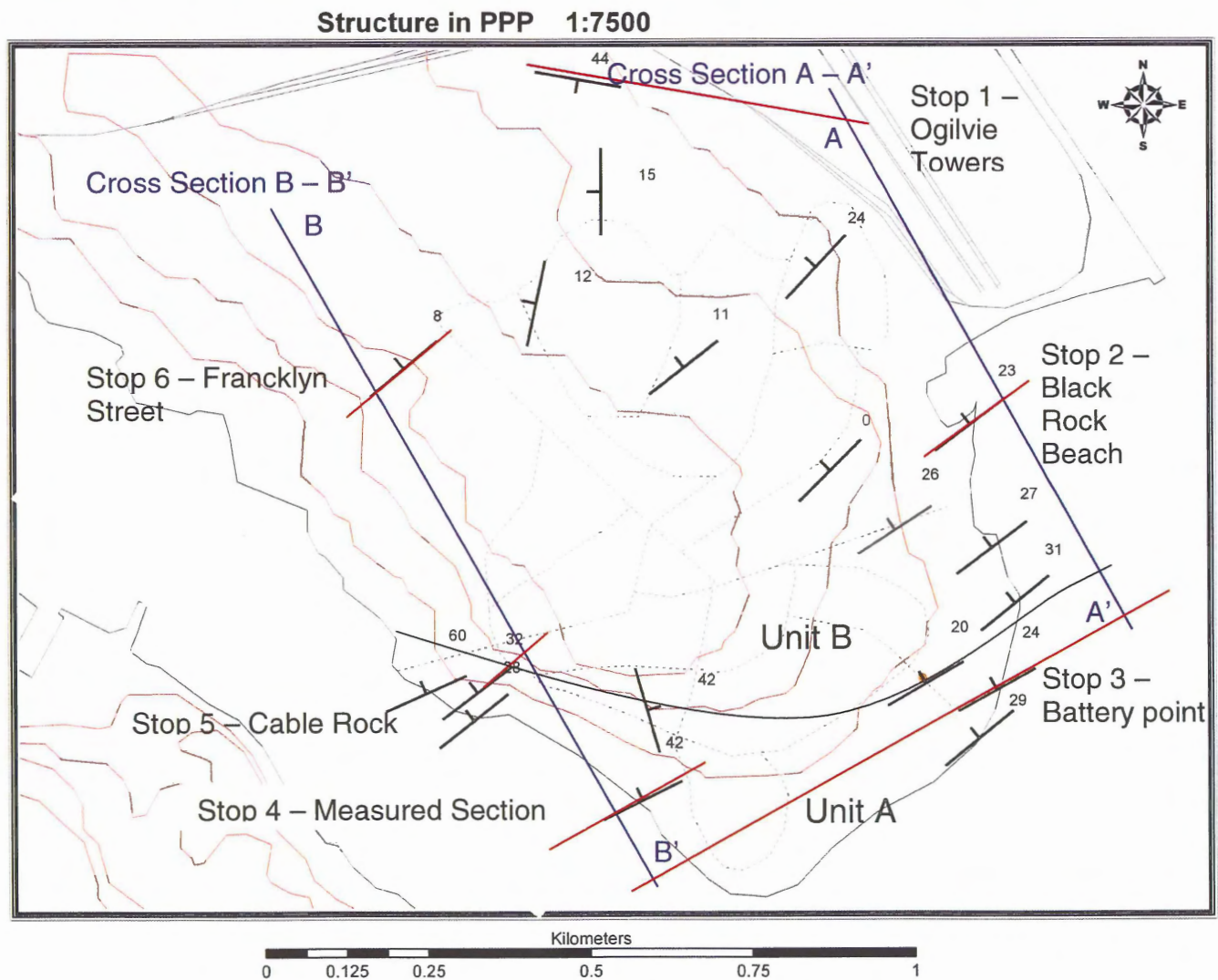
Figure 4.3 – Location of cross – sections A – A' and B – B'. Blue lines indicate cross sections. Base map provided by Glenn Hart.
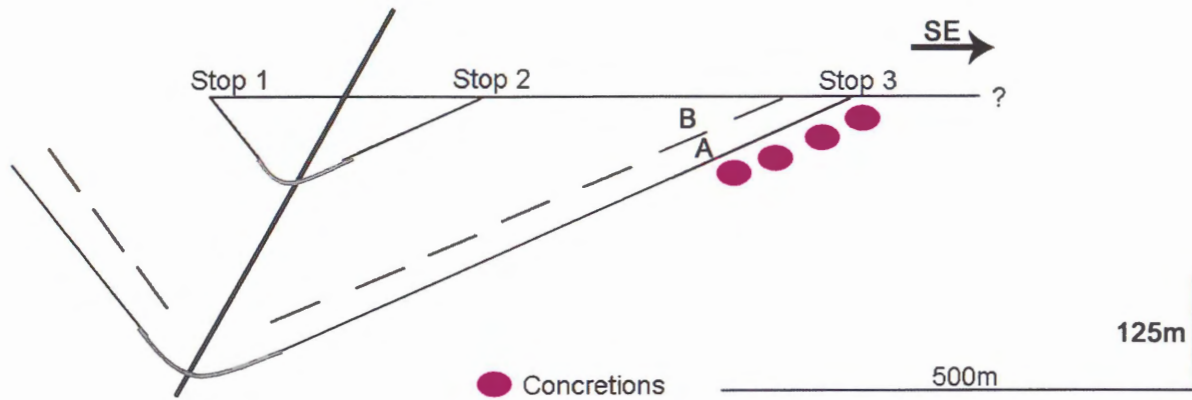
Figure 4.4 – Cross - section A-A' is located dominantly in unit B, and is the only section that crosses both the lithological boundary and shows the change in dip of the beds across the synclinal axis. Bedding between stops 2 and 3 is fairly consistent in reference to the overall bedding within the park. Solid lines represent bedding and dashed lines represent possible lithological boundary.
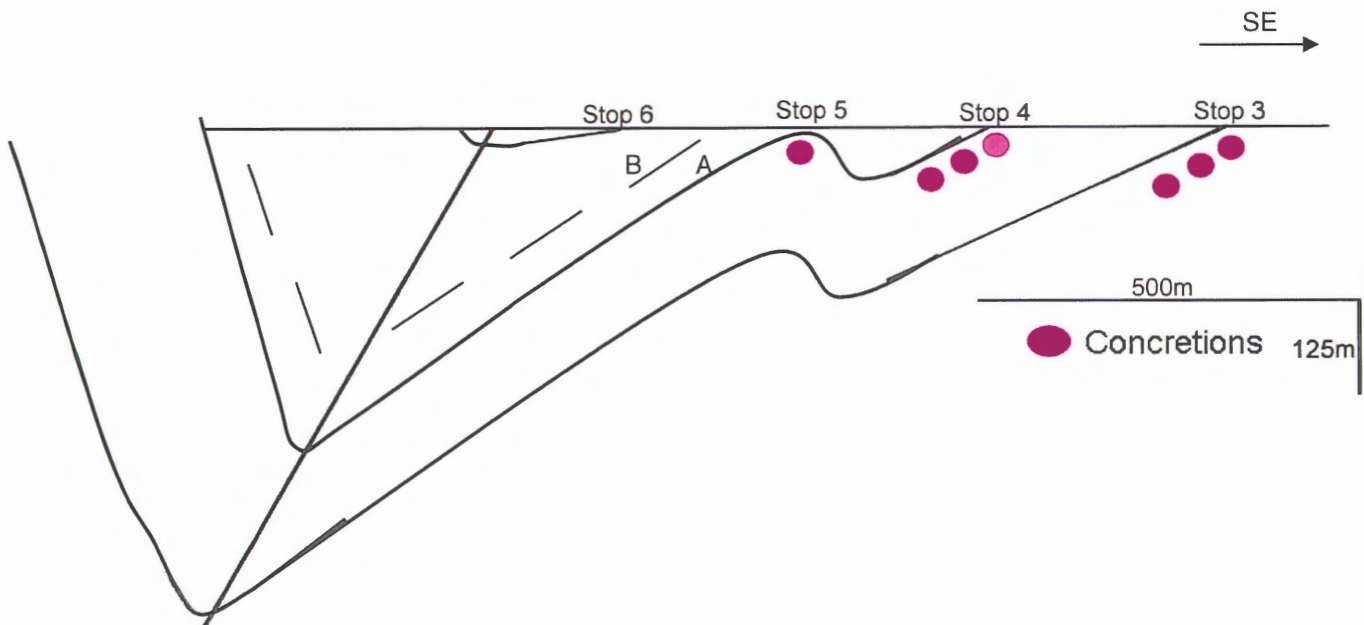
Figure 4.5 – Cross - section B-B' is located dominantly in unit A, and shows a parasitic anticline at the Cable Rock outcrop (stop 5). . Solid lines represent bedding and dashed lines represent possible lithological boundary.

4.2.1 Stop 1 – Ogilvie Towers

The Ogilvie Towers outcrop, in the parking lot of the Ogilvie Towers building, is located at the norrthernost edge of the study area. This is an outcrop of unit B, and is located on the northern limb of the Point Pleasant Park syncline (Fig 4.6). Bedding is oriented 100/44, dipping to the south. Cleavage is present in this outcrop and is oriented 257/74 dipping to the NW. The outcrop is heavily weathered on some surfaces.

Figure 4.6 – Ogilvie Towers outcrop located in unit B. Bedding is present as the flat surface and dips to the south. Photo taken looking at cleavage surface. Park is located to the south.

4.2.2 Stop 2 – Black Rock Beach

Black Rock Beach is located at the south end of the Container Pier parking lot. Black Rock itself is a glacially sculpted outcrop of unit B, on the southern limb of the syncline (Fig 4.7). Here the bedding is oriented 233/23 dipping to the NW. A strong slaty cleavage oriented at 233/81 is dipping steeply to the NW. The surface is scoured by glacial striations trending approximately parallel to the dip of the bedding.

Figure 4.7– Black Rock Beach outcrop. Flat surface in photo is slightly oblique to the bedding plane. Bedding is offset by a strong slaty cleavage.

4.2.3 Stop 3 – Battery Point

Battery Point, at the southern tip of the park, marks the southernmost point on both cross-sections (Fig 4.8). This is the only stop along cross - section A – A' that contains calcareous concretions. Here the bedding is oriented 241/24 dipping to the NW. A strong slaty cleavage is present in the pelitic layers oriented 238/85 and dipping to the NW. Both types of concretions are present at this stop, but only type 2 concretions are seen in Fig 4.8.
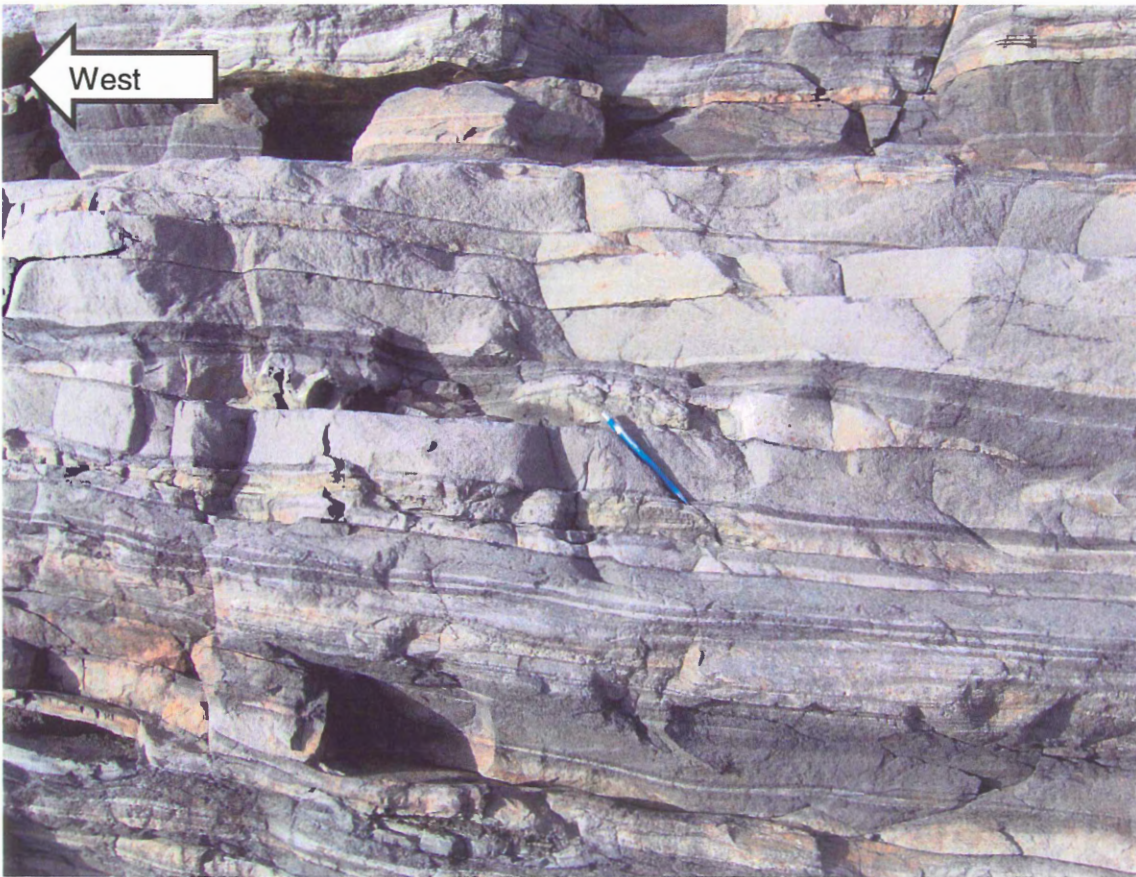
Figure 4.8– Battery Point outcrop located along the shoreline at the southern tip of the Halifax peninsula underneath an old gun battery used in both world wars. Photo shows a type 2 concretion. Cleavage is parallel to the plane of the photo, but bedding is obvious.

4.2.4 Stop 4 – Measured Section

The measured section presented in Appendix A in is located along the western shore of the park between Battery Point and Cable Rock, within rocks of unit A (Fig 4.9). In the measured section, the bedding is oriented 262/25 (on average) dipping to the NW. Cleavage in this section is for the most part annealed due to recrystallization and growth of cordierite during contact metamorphism.
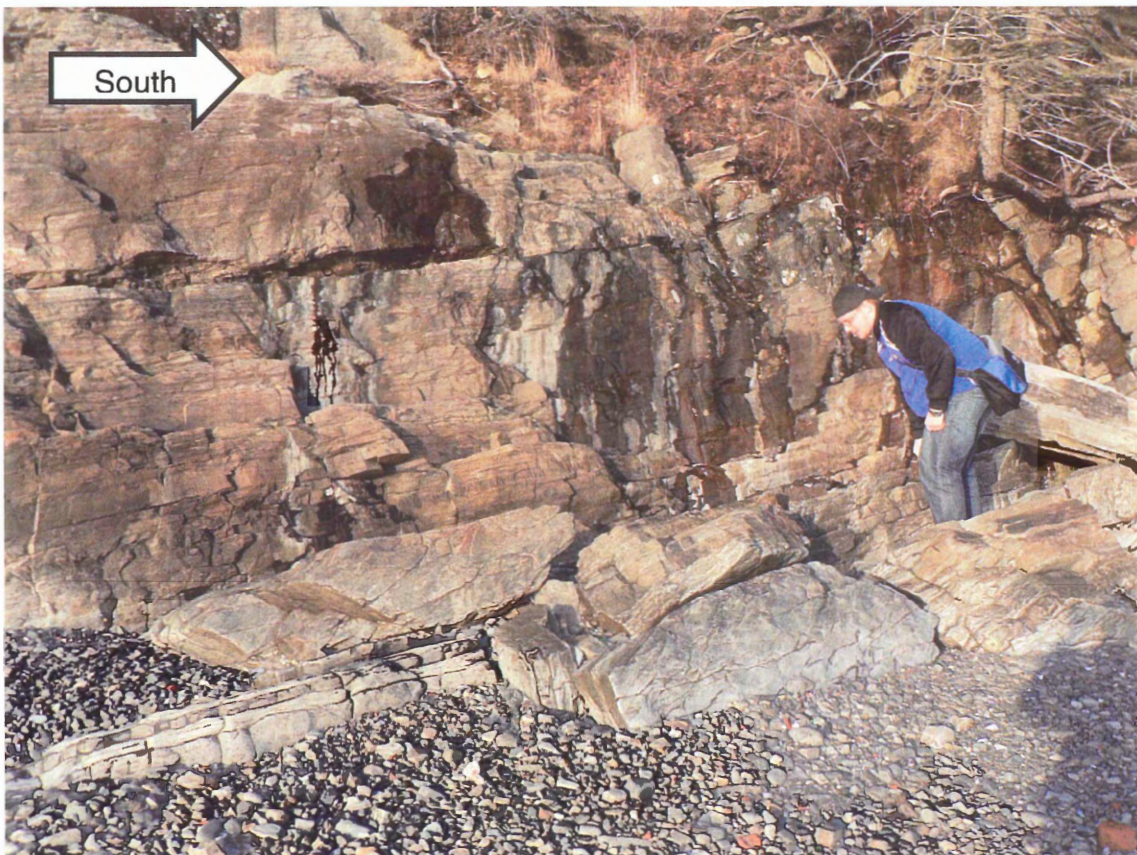
Figure 4.9– Measured section outcrop. Bedding is evident. Cleavage is heavily annealed due to the intrusion of the SMB, but is represented as faint lines.

4.2.5 Stop 5 – Cable Rock

Cable Rock is located NW of the measured section in unit A. Bedding in this section is oriented 248/35 dipping to the NW. Cleavage in this section has been annealed. A small parasitic anticline within the large Point Pleasant Park syncline is present at this stop with the fold axis oriented 248/42 NE (Fig 4.10). Glacial striations are present on the surface of this outcrop. Concretions are present at this outcrop, but due to the annealing of the cleavage and the weathering on the surface of the outcrop, determination between type 1 and 2 concretions is difficult.

Figure 4.10 - Small anticline at Cable Rock located on the western side of the outcrop next to the shoreline. Anticline is easily accessible at lower tides. Photo taken looking east looking towards the park

4.2.6 Stop 6 – Franckyln Street

The northernmost outcrop on cross section B – B' is on Francklyn Street, which marks the western boundary of the park. The outcrop is within unit A (Fig 4.11). Here, the bedding is oriented 235/08 and dips to the NW. The cleavage at this outcrop is oriented 255/77 dipping to the NW. Figure 4.1 shows the bedding dipping north. The fold hinge lies north of this outcrop and south of outcrops on Point Pleasant Drive because the bedding changes dip directions between this stop and outcrops on Point Pleasant Drive.

Figure 4.11 – Francklyn Street outcrop located at the western boundary of the park. Photo shows bedding dipping to the north. Cleavage is not evident in the photo, but is present in the outcrop

5. Metamorphism

5.1 Introduction

Regional metamorphism of the Meguma Group occurred during the Acadian Orogeny (ca. 415-370 Ma; Williams, 1979; Hicks et al, 1999). Regional grade varies from greenschist to amphibolite facies (Muecke & Keppie, 1979). Within the study area, the regional grade is greenschist facies (chlorite zone) with overprinting contact metamorphism caused by the intrusion of the South Mountain Batholith (SMB) at ca. 380 Ma (Jamieson et al, 2005; Carruzzo et al, 2003). The presence of cordierite grains marks the outer limit of the aureole (Jamieson et al, 2005). The SMB outcrops near Purcell's Cove on the western side of the North West Arm. Although it can be seen from the park, there are no outcrops of the SMB in Point Pleasant Park.

The outcrops exhibiting the highest level of metamorphism are located along the shores of the North West Arm. In these outcrops, large cordierite grains are present with some samples exhibiting a "fried egg" texture suggesting two different phases of cordierite growth. The cordierite1-in isograd, marked by the first appearance of cordierite "spots", lies north of the park (Jamieson et al, 2005). A second cordierite isograd (cordierite2) is inferred to lie within the park (Fig 5.1). Bedding in these samples is preserved but cleavage has been annealed due to cordierite growth resulting from the intrusion of the SMB.

Using the electron microprobe at Dalhousie University, five different thin sections were analysed for mineralogy. PPP04 – 5b and 19 lie along cross-section A. PPP04 – 3 is located along cross section B. PPP04 – 7c and 17b are

from calcareous concretions present in two different areas and have significantly different mineralogy than their host rocks. PPP04 – 7c is from the outcrop at Battery Point and 17b is from the outcrop at Cable Rock.

5.2 Bulk Rock Geochemistry

The bulk rock geochemistry of Bluestone member slates in Point Pleasant Park is broadly similar to that of the underlying Cunard Member slates. The Cunard member has higher Al_2O_3, S, C, and lower SiO_2 (Table 5.1). This change in bulk rock geochemistry from the underlying Cunard Member is discussed further by Hart (2006).

	Cunard			Bluestone
Sample	SS Dark	IWK03	Mbe	PPP04-5b
SiO_2	59.76	57.88	54.81	61.34
TiO_2	0.99	0.97	1.01	0.99
Al_2O_3	21.87	23.46	25.29	20.11
Fe_2O_3t	4.31	5.52	4.52	5.37
FeOt	3.88	4.97	4.07	4.83
MnO	0.04	0.05	0.06	0.06
MgO	0.91	1.79	1.32	1.2
CaO	0.48	0.15	0.23	0.16
Na_2O	1.2	1.18	1.47	1.21
K2O	3.71	3.87	4.11	4.69
P2O5	0.07	0.09	0.06	0.08
LOI	5.63	4.86	6.31	3.81
Carbon	0.49	0.46	0.46	0.07
Sulphur	0.36	1.12	0.14	0.11
Total FeOt,LOI	98.54	99.27	98.73	98.48

Table 5.1 – Bulk rock composition from slate samples on the peninsula of Halifax. Analysis performed at St Mary's University. Out of the 7 samples analyzed, 4 were provided by Glenn Hart for general comparison of the Cunard and Bluestone.

Figure 5.1 - Map showing change in mineral assemblage marked by the presence of a second generation of cordierite (Cordierite 2 in isograd).
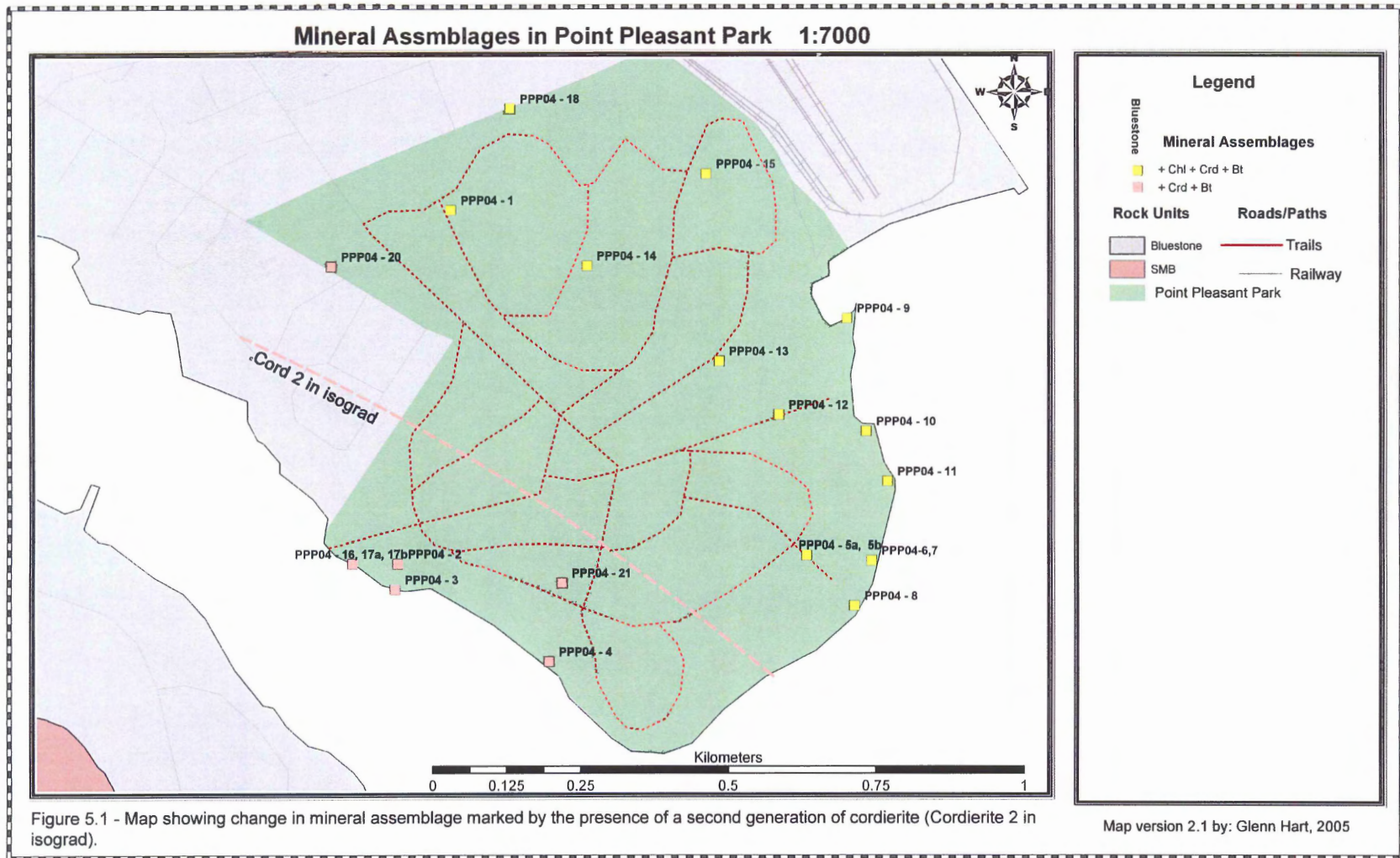
5.3 Below Cordierite2 in Isograd

5.3.1 PPP04 – 19

PPP04 – 19 is from the parking lot at Ogilvie Towers at the northernmost edge of the study area (stop 1, Fig 4.6). This sample is from the lowest grade part of the contact aureole in the study area. The sample contains muscovite + biotite + altered cordierite + quartz + chlorite ± opaque minerals. Large altered xenoblastic cordierite porphyroblasts (Fig 5.2) give the rocks a spotted appearance. However, no fresh cordierite was found in this sample. The cordierite has been replaced by finely intergrown muscovite/chlorite. No chlorite was analyzed in the matrix. Smaller xenoblastic biotite and muscovite grains are present in both the remnant cordierite grains and within the matrix. These grains are commonly intergrown, forming "stacks" (Fig 5.3). The rest of the sample consists of a fine – grained matrix of muscovite, opaque minerals, and quartz. Chemical variations among different grains of the same mineral are minimal. Average biotite, muscovite, and chlorite compositions are listed in Table 5.2.

Elements	Biotite	Elements	Muscovite	Elements	Chlorite
SiO_2	33.26	SiO_2	46.66	SiO_2	31.52
TiO_2	1.19	TiO_2	0.09	TiO_2	0.04
Al_2O_3	22.00	Al_2O_3	36.95	Al_2O_3	29.45
Cr_2O_3	0.09	Cr_2O_3	0.01	Cr_2O_3	0.01
FeO	24.16	FeO	0.88	FeO	20.61
MnO	0.19	MnO	0.00	MnO	0.28
MgO	6.58	MgO	0.38	MgO	5.77
CaO	0.00	CaO	0.00	CaO	0.12
Na_2O	0.17	Na_2O	1.00	Na_2O	0.27
K_2O	6.82	K_2O	9.24	K_2O	0.70
Total	**94.46**	**Total**	**95.21**	**Total**	**88.77**
11 Oxygen		11 Oxygen		14 Oxygen	
Si	2.58	Si	3.07	Si	3.11
Ti	0.07	Ti	0.00	Ti	0.00
Al	2.01	Al	2.87	Al	3.42
Cr	0.01	Cr	0.00	Cr	0.00
Fe	1.57	Fe	0.05	Fe	1.70
Mn	0.01	Mn	0.00	Mn	0.02
Mg	0.76	Mg	0.04	Mg	0.85
Ca	0.00	Ca	0.00	Ca	0.01
Na	0.03	Na	0.13	Na	0.05
K	0.68	K	0.78	K	0.09
Total	**7.70**	**Total**	**6.94**	**Total**	**9.25**
Cation Ratio	**n = 3**	**Cation Ratio**	**n = 3**	**Cation Ratio**	**n = 1**
Fe	67.32	Na	14.14	Fe	66.68
Mg	32.68	K	85.86	Mg	33.32

Table 5.2 – Average mineral compositions for sample PPP04 – 19. Each box contains the weight percent followed by the cations corrected to the correct number of oxygen and then the cation ratios. Cation ratios are calculated as (Fe/(Fe+Mg))*100 or (Na/(Na+K))*100
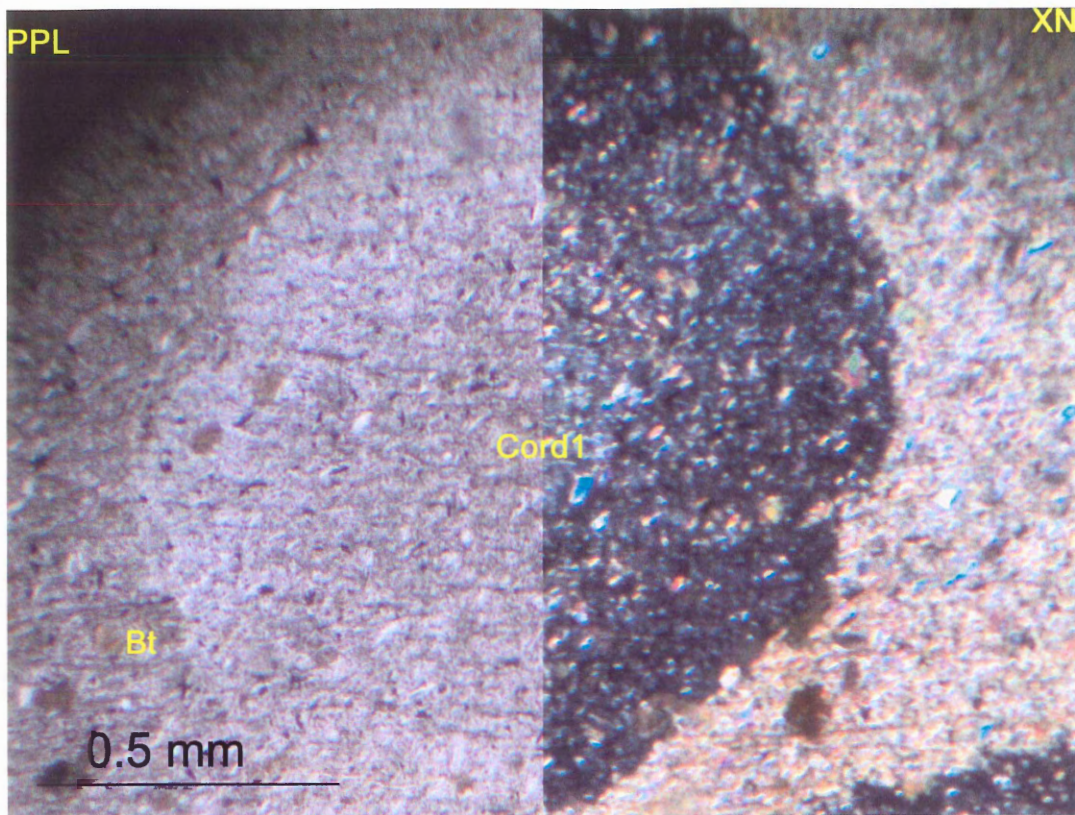
Figure 5.2 – Thin section photo of PPP04 – 19 in transmitted light. Large altered xenoblastic cordierite grains present with smaller biotite and muscovite grains surrounded by a fine-grained matrix.
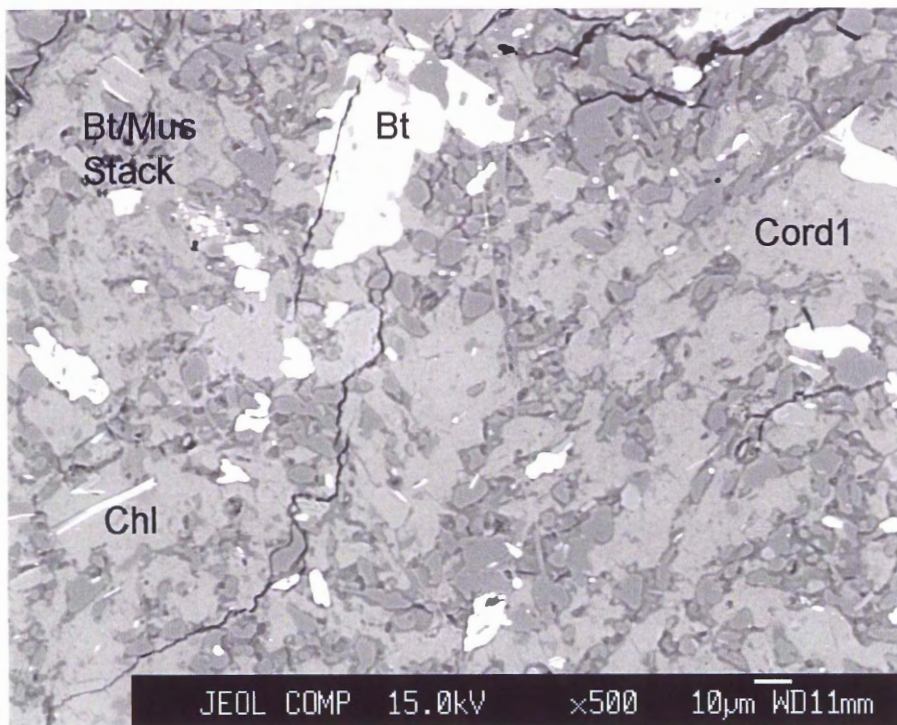
Figure 5.3 – BSE image of PPP04 – 19. Photo taken within an altered cordierite grain.

5.3.2 PPP04 – 5b

Sample PPP04 – 5b was taken along from an outcrop 200m north of the

Battery Point outcrop (Fig 1.1). This sample contains similar mineralogy and

textures to PPP04 – 19 (muscovite + biotite + altered cordierite + quartz). No

chlorite was found within the sample except in chlorite/muscovite intergrowths

similar to PPP04 – 19. Large, xenoblastic relict cordierite grains give the rocks a

spotted appearance (Fig 5.4 & 5.5). Smaller muscovite and biotite grains are

present inside and outside the relict cordierites as individual grains and in

muscovite/biotite stacks. The matrix consists of fine-grained quartz + muscovite

+ biotite. Average chemical compositions of biotite and muscovite are shown in

Table 5.3.

Elements	Biotite	Cations	11 Oxygen	Elements	Muscovite	Cations	11 oxygen
SiO_2	33.94	Si	2.64	SiO_2	47.06	Si	3.11
TiO_2	1.23	Ti	0.07	TiO_2	0.09	Ti	0.00
Al_2O_3	20.66	Al	1.90	Al_2O_3	36.29	Al	2.82
Cr_2O_3	0.04	Cr	0.00	Cr_2O_3	0.00	Cr	0.00
FeO	23.18	Fe	1.51	FeO	0.88	Fe	0.05
MnO	0.12	Mn	0.01	MnO	0.00	Mn	0.00
MgO	6.92	Mg	0.80	MgO	0.47	Mg	0.05
CaO	0.00	Ca	0.00	CaO	0.00	Ca	0.00
Na_2O	0.20	Na	0.03	Na_2O	0.85	Na	0.11
K_2O	7.88	K	0.78	K_2O	9.24	K	0.78
Total	**94.16**	**Total**	**7.74**	**Total**	**94.88**	**Total**	**6.92**
		Cation Ratio	n = 4			Cation Ratio	n = 3
		Fe	65.26			Na	12.18
		Mg	34.74			K	87.82

Table 5.3 – Average mineral compositions for sample PPP04 – 5b. Each box contains the weight percent followed by the cations corrected to the correct number of oxygen and then the cation ratios. Cation ratios are calculated as (Fe/(Fe+Mg))*100 or (Na/(Na+K))*100
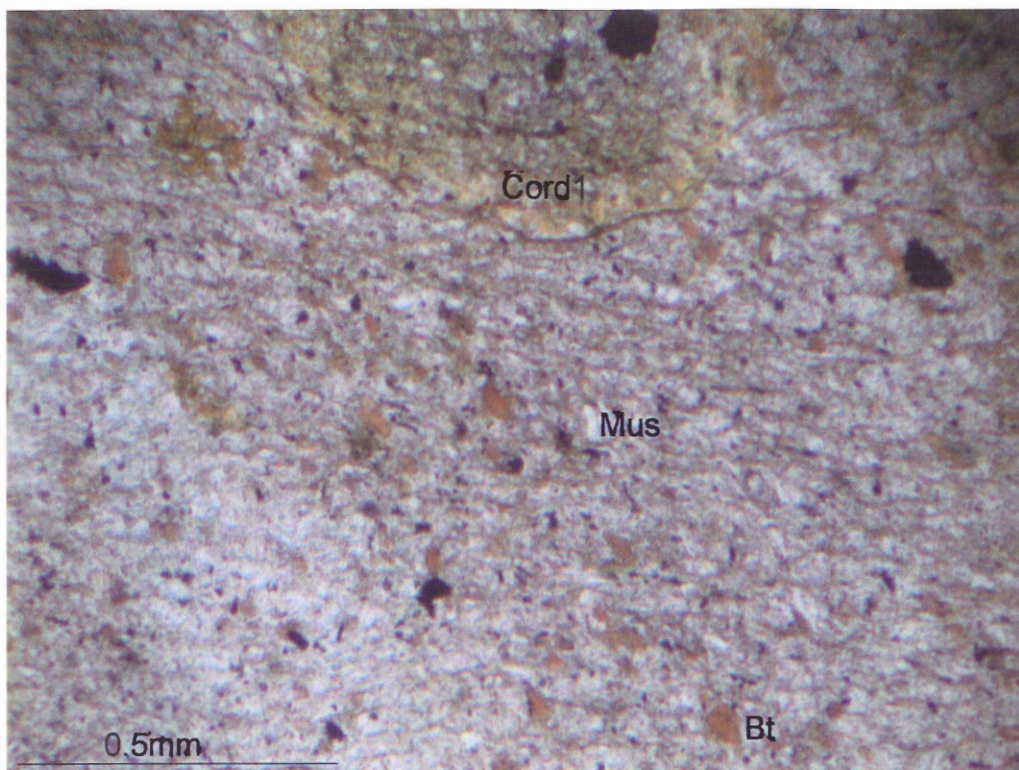
Figure 5.4 – Thin section photo of PPP04 – 5b. Large altered cordierite grains with smaller biotite and muscovite grains
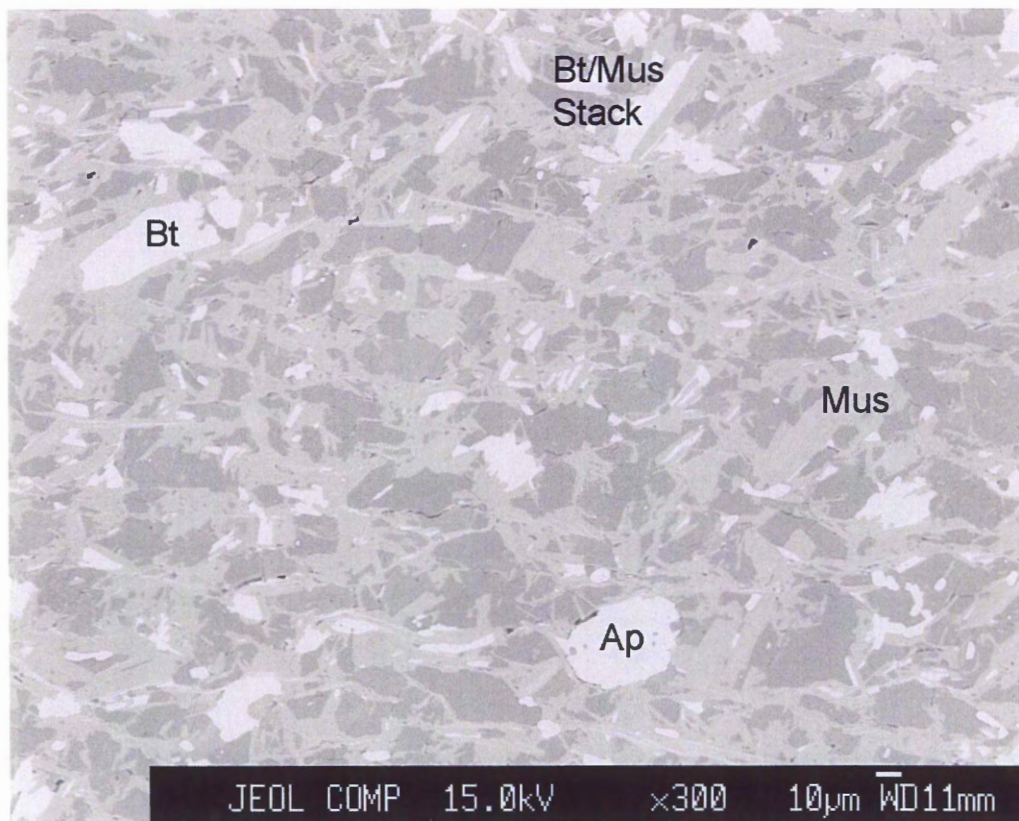
Figure 5.5 – BSE image of PPP04 – 5b. Matrix assemblage shows biotite, muscovite, quartz, and apatite.

5.4 Above Cordierite2 in Isograd

5.4.1 PPP04 – 3

Sample PPP04 – 3, the highest-grade sample analyzed, was taken from the shores of the North West Arm at stop 4 along cross section B (Fig 4.9). This sample contains cordierite + feldspar + muscovite + biotite + quartz. The only fresh cordierite analyzed was found in this sample (Fig 5.6). Two different analyses were obtained from fresh cordierite. Potassium rich (2-3 Wt%) and potassium poor compositions could be an intergrowth of cordierite and feldspar. Cordierites in this sample display "fried egg" texture (Fig 5.7). Biotite and muscovite are present both as individual grains and as stacks. Minor apatite and oxides are present (Fig 5.8). The fine-grained matrix contains muscovite, biotite, and quartz. Average chemical compositions are presented in Table 5.4.
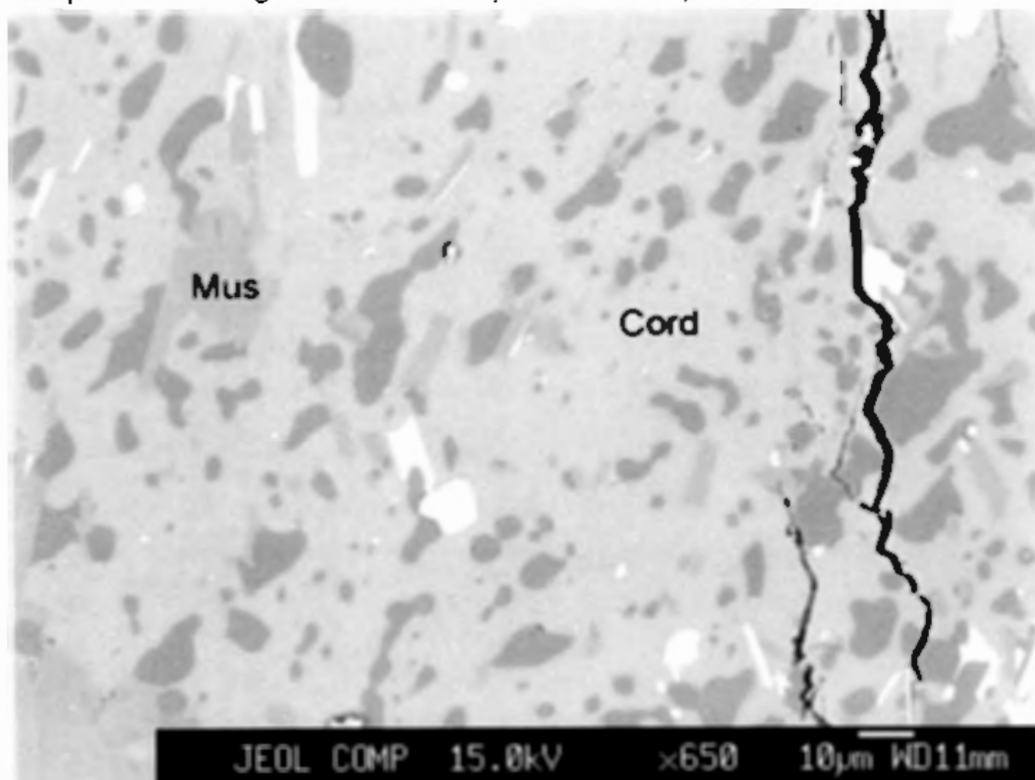
Figure 5.6 – BSE image of PPP04 – 3. Fresh cordierite containing inclusions of quartz and feldspar

Elements	Biotite	Cordierite K	Cordierite	Elements	Muscovite	Na - Plag	K-Feldspar
SiO_2	33.67	48.21	47.66	SiO_2	47.42	64.21	65.33
TiO_2	2.21	0.02	0.03	TiO_2	0.55	0.02	0.07
Al_2O_3	20.82	32.42	33.25	Al_2O_3	36.17	21.98	19.37
Cr_2O_3	0.11	0.00	0.03	Cr_2O_3	0.14	0.00	0.00
FeO	24.59	10.28	12.64	FeO	1.03	0.09	1.08
MnO	0.12	0.26	0.43	MnO	0.01	0.00	0.00
MgO	5.22	3.91	5.06	MgO	0.39	0.00	0.11
CaO	0.03	0.04	0.02	CaO	0.00	2.59	0.01
Na_2O	0.09	0.35	0.25	Na_2O	0.47	10.21	2.91
K_2O	8.28	2.37	0.26	K_2O	9.45	0.11	11.39
Total	**95.16**	97.85	**99.64**	**Total**	**95.63**	**99.21**	**100.26**
Cations	11 Oxygen	18 Oxygen	18 Oxygen	Cations	11 Oxygen	8 Oxygen	8 Oxygen
Si	2.62	5.04	4.96	Si	3.11	2.85	2.97
Ti	0.13	0.00	0.00	Ti	0.03	0.00	0.00
Al	1.91	4.05	4.08	Al	2.80	1.15	1.04
Cr	0.01	0.00	0.00	Cr	0.01	0.00	0.00
Fe	1.60	0.98	1.10	Fe	0.06	0.00	0.04
Mn	0.01	0.03	0.04	Mn	0.00	0.00	0.00
Mg	0.61	0.68	0.79	Mg	0.04	0.00	0.01
Ca	0.00	0.00	0.00	Ca	0.00	0.12	0.00
Na	0.01	0.06	0.05	Na	0.06	0.88	0.26
K	0.82	0.21	0.03	K	0.79	0.01	0.66
Total	**7.71**	**11.07**	**11.05**	**Total**	**6.89**	**5.02**	**4.97**
Cation Ratios	n = 9	n = 5	n = 3	Cation Ratios	n = 7	n = 4	n = 1
Fe	72.53	59.17	58.32	Ca	0.03	12.23	0.00
Mg	27.47	40.83	41.68	Na	7.04	87.13	28.01
				K	92.93	0.63	71.99

Table 5.4 - Average mineral compositions from sample PPP04 – 3. Each box contains the weight percent followed by the cations corrected to the correct number of oxygen and then the cation ratios. Cation ratios are calculated as (Fe/(Fe+Mg))*100 or (Na/(Na+K))*100
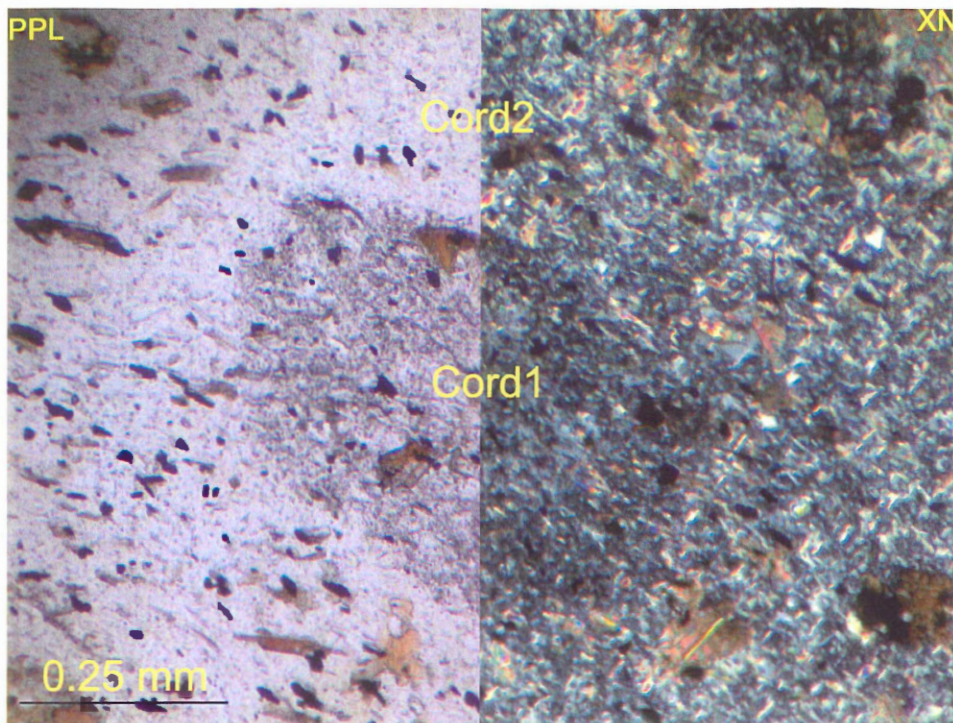
Figure 5.7 – "Fried Egg" cordierites present above cordierite2 in isograd in sample PPP04 - 3.
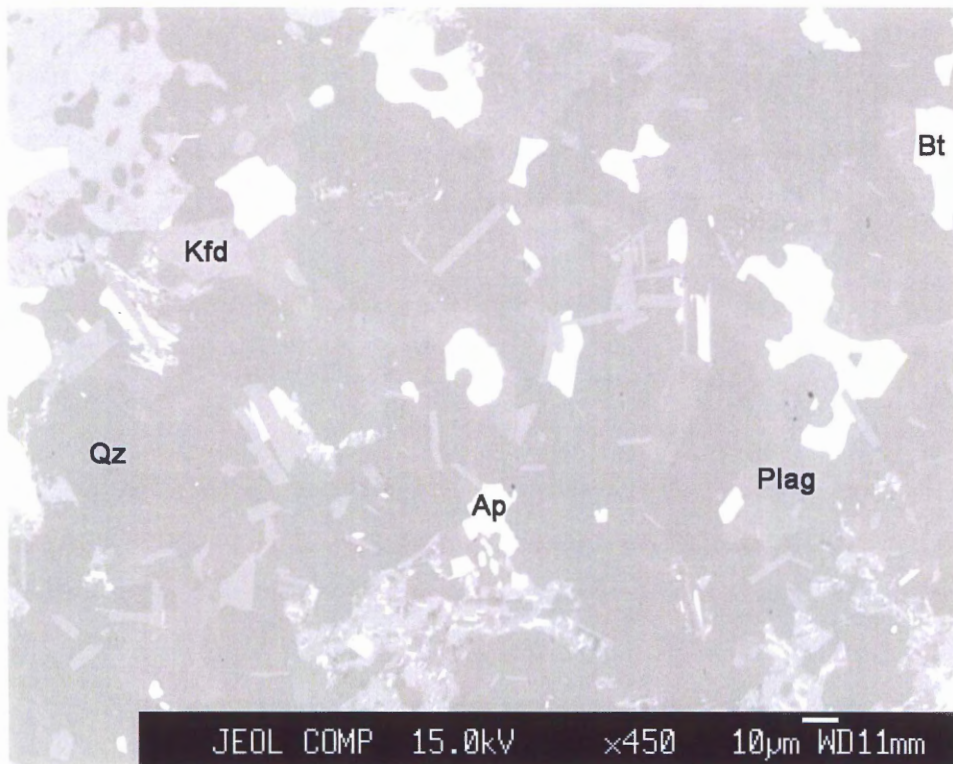
Figure 5.8 – BSE image of PPP04 – 3. Matrix shows feldspars, quartz, biotite, and apatite

5.4.2 P – T Estimates for the Cordierite2 in Isograd

The presence of inclusion-poor rims on cordierite ("fried egg" texture) is interpreted to represent a second growth of cordierite, and defines the location of the cordierite2 in isograd. Above the cordierite2 in isograd the mineral assemblage is biotite + muscovite + cordierite (1 & 2) + K-feldspar + quartz and below the cordierite2 in isograd the mineralogy is biotite + muscovite + chlorite + cordierite 1 + quartz. Biotite is present in all samples, and is not included in the reaction. Using TWQ, one reaction was determined (Fig 5.9):

2 chlorite + 8 muscovite + 16 quartz ↔ 8 K-feldspar + 5 cordierite +16 H_2O.
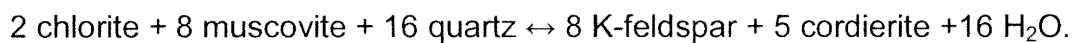
The South Mountain Batholith was emplaced at a pressure of 3.2 – 3.8 kbar (Raeside & Mahoney 1996) which translates to ca. 10 km depth. At these pressures, an approximate temperature for the inferred reaction at the cordierite2-in isograd is ca. 550 °C (Fig 5.9). This value is hotter than preliminary biotite-in isograd temperature estimates suggested by Jamieson et al (2005) and equal to the T estimate for the Cunard biotite isograd calculated by Glenn Hart (2006). This temperature value is also lower than the Bluestone andalusite-in isograd calculated by Glenn Hart (2006). This temperature also agrees with the given mineralogy of the samples analyzed.
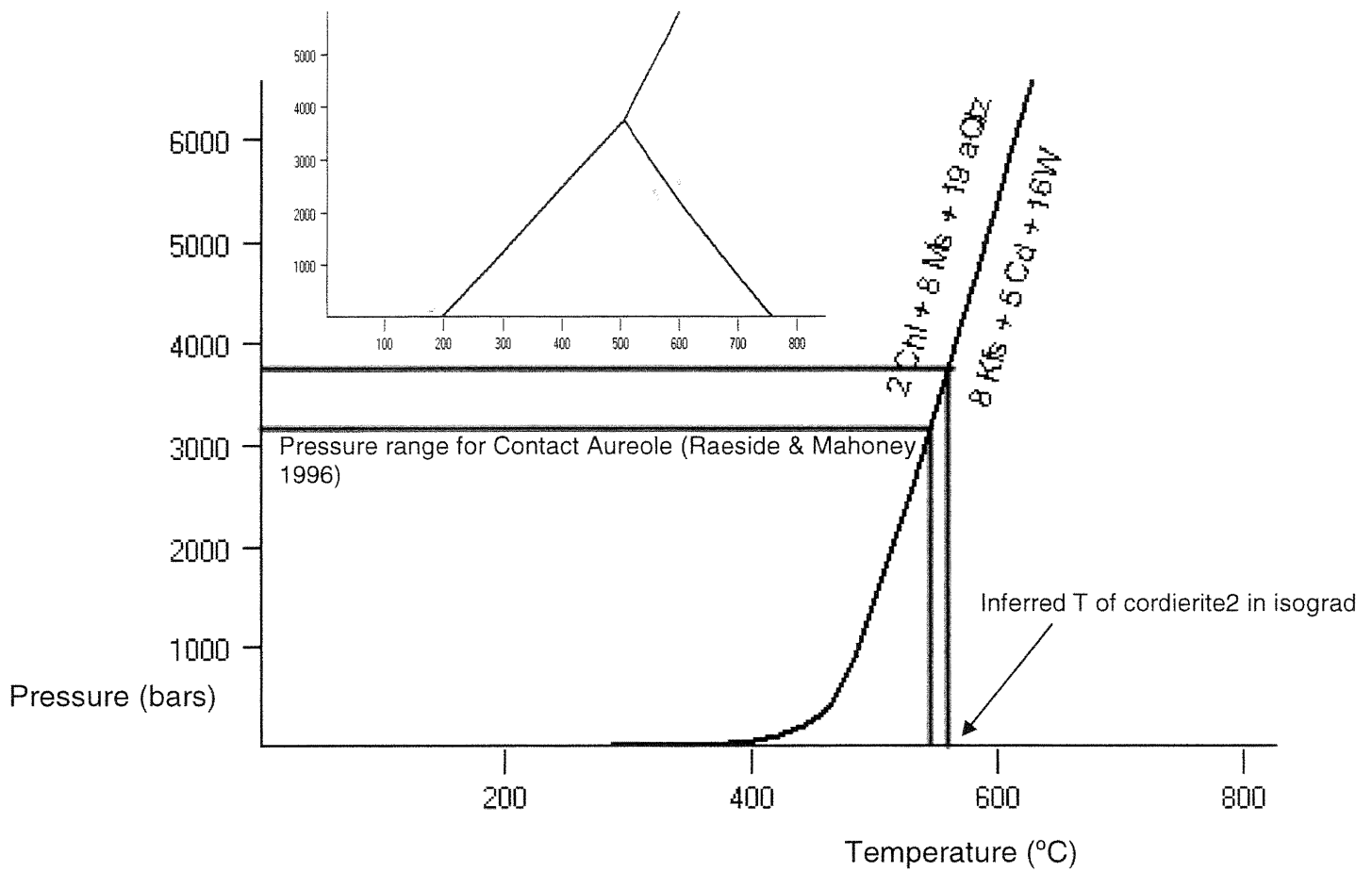
Figure 5.9 – Reaction: 2 chlorite + 8 muscovite + 16 quartz ↔ 8 K – feldspar + 5 cordierite +16 H_2O. Graph constructed using TWQ, and assumes end member composition for chlorite, muscovite, K-feldspar, and cordierite.

5.5 Calcareous Concretions

A characteristic feature of the Bluestone member is the presence of calcareous concretions in unit A. Two samples from different grades were analyzed by the electron microprobe (PPP04 – 7c and PPP04 – 17b), since they are too fine grained to determine mineralogy by optical techniques.

5.5.1 PPP04 – 7c

Sample PPP04 – 7c is from the Battery Point outcrop (stop 3, Fig 4.8). This concretion, displays three different zones in thin section (Fig 5.10) with zone

1 being from the core of the concretion and zone three from the rims. The zoning within the concretions reflects the change in bulk composition from a calcic core to a more pelitic rim.
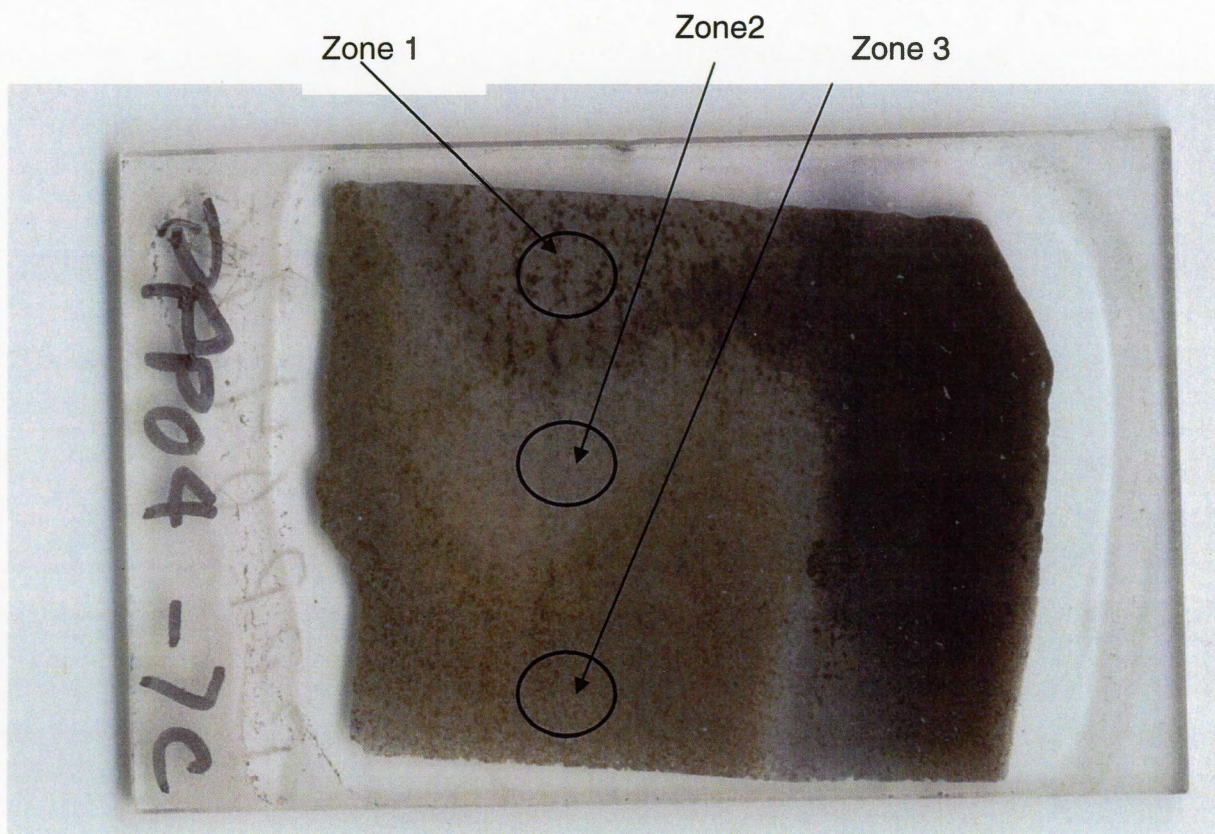
Figure 5.10 – Thin section of PPP04 – 7c with the three different mineralogic zones defined.

Zone 1 (core) contains garnet + chlorite + quartz ± epidote ± anorthite ± titanite ± apatite. Garnet appears for the first time, and is limited to the concretions, probably due to the change in bulk composition allowing Ca to stabilize the formation of garnet. Variation in mineral chemistry within zone 1 is minimal for all minerals except garnet. Within all three zones, two different garnet compositions were found. Both populations have low Mg. Population one

is a high-Ca-low Fe + Mn garnet and population two is low-Ca-high Fe + Mn

garnet (Fig 5.11). These two analyses are from garnet cores. However, since

the garnets are fine grained, some analyses could be from rims of garnets that

were obliquely cut. No detailed element mapping of the garnets was performed

and the grain size limits the interpretation of these analyses. A single high-Mn

low Ca – Fe garnet was analyzed from zone 1. An unknown calc-silicate mineral

(UCSM) was also analyzed. Table 5.5 gives average values for the two garnet

populations and Table 5.6 gives average chemical analysis for zone 1.

Elements	P 1 gt	P 2 gt	Cations	12 Oxygen	12 Oxygen
SiO_2	38.38	38.00	Si	2.99	3.00
TiO_2	0.45	0.33	Ti	0.03	0.02
Al_2O_3	20.54	20.73	Al	1.88	1.93
Cr_2O_3	0.03	0.04	Cr	0.00	0.00
FeO	5.84	10.20	Fe	0.38	0.67
MnO	6.64	9.51	Mn	0.44	0.64
MgO	0.04	0.08	Mg	0.01	0.01
CaO	27.76	20.80	Ca	2.32	1.76
Na_2O	0.00	0.00	Na	0.00	0.00
K_2O	0.01	0.01	K	0.00	0.00
Total	**99.69**	**99.69**	**Total**	**8.04**	**8.02**
			Cation Ratio	**n = 5**	**n = 6**
			Fe	12.11	21.89
			Mn	14.00	20.69
			Mg	0.16	0.29
			Ca	73.73	57.12
			Total	100.00	100.00

Table 5.5 – Average values for the two different garnet populations in PPP04 – 7c. Cation ratios are calculated as (Fe/(Fe+Mg+Mn+Ca))*100 or (Na/(Na+K+Ca))*100

Elements	Z1 Chlorite	Z1 UCSM	Epidote	Elements	Z1 Ca - Plag	Elements	Z1 Titanite
SiO_2	26.80	36.30	37.95	SiO_2	43.78	SiO2	30.47
TiO_2	0.01	0.00	0.06	TiO_2	0.00	TiO2	34.17
Al_2O_3	22.49	27.01	27.29	Al_2O_3	36.19	Al2O3	3.28
Cr_2O_3	0.00	0.00	0.01	Cr_2O_3	0.00	Cr2O3	0.50
FeO	20.29	7.66	7.61	FeO	0.09	FeO	0.50
MnO	1.89	0.61	0.41	MnO	0.00	MnO	0.10
MgO	15.92	6.07	0.01	MgO	0.00	MgO	0.05
CaO	0.11	16.84	23.85	CaO	19.51	CaO	28.81
Na_2O	0.03	0.00	0.00	Na_2O	0.57	Na2O	0.02
K_2O	0.00	0.00	0.00	K_2O	0.00	K2O	0.00
Total	**87.53**	**94.50**	**97.19**	**Total**	**100.14**	**Total**	**97.90**
Cations	14 Oxygen	11 Oxygen	13 Oxygen	Cations	8 Oxygen	Cations	5 Oxygen
Si	2.76	2.59	3.15	Si	2.02	Si	1.01
Ti	0.00	0.00	0.00	Ti	0.00	Ti	0.86
Al	2.73	2.27	2.67	Al	1.97	Al	0.13
Cr	0.00	0.00	0.00	Cr	0.00	Cr	0.01
Fe	1.75	0.46	0.53	Fe	0.00	Fe	0.01
Mn	0.16	0.04	0.03	Mn	0.00	Mn	0.00
Mg	2.45	0.64	0.00	Mg	0.00	Mg	0.00
Ca	0.01	1.29	2.12	Ca	0.97	Ca	1.03
Na	0.01	0.00	0.00	Na	0.05	Na	0.00
K	0.00	0.00	0.00	K	0.00	K	0.00
Total	**9.87**	**7.28**	**8.51**	**Total**	**5.02**	**Total**	**3.06**
Cation Ratio	n = 2	n = 1	n = 1	Cation Ratio	n = 1		n = 1
Fe	40.00	18.84	19.68	Ca	94.97		
Mn	3.77	1.50	1.09	Na	5.03		
Mg	55.97	26.60	0.05	K	0.00		
Ca	0.27	53.06	79.18	Total	100.00		
Total	100.00	100.00	100.00				

Table 5.6 - Average mineral compositions for zone 1 of sample PPP04 – 7c. Each box contains the weight percent followed by the cations corrected to the correct number of oxygen and then the cation ratios. Cation ratios are calculated as $(Fe/(Fe+Mg+Mn+Ca))*100$ or $(Na/(Na+K+Ca))*100$
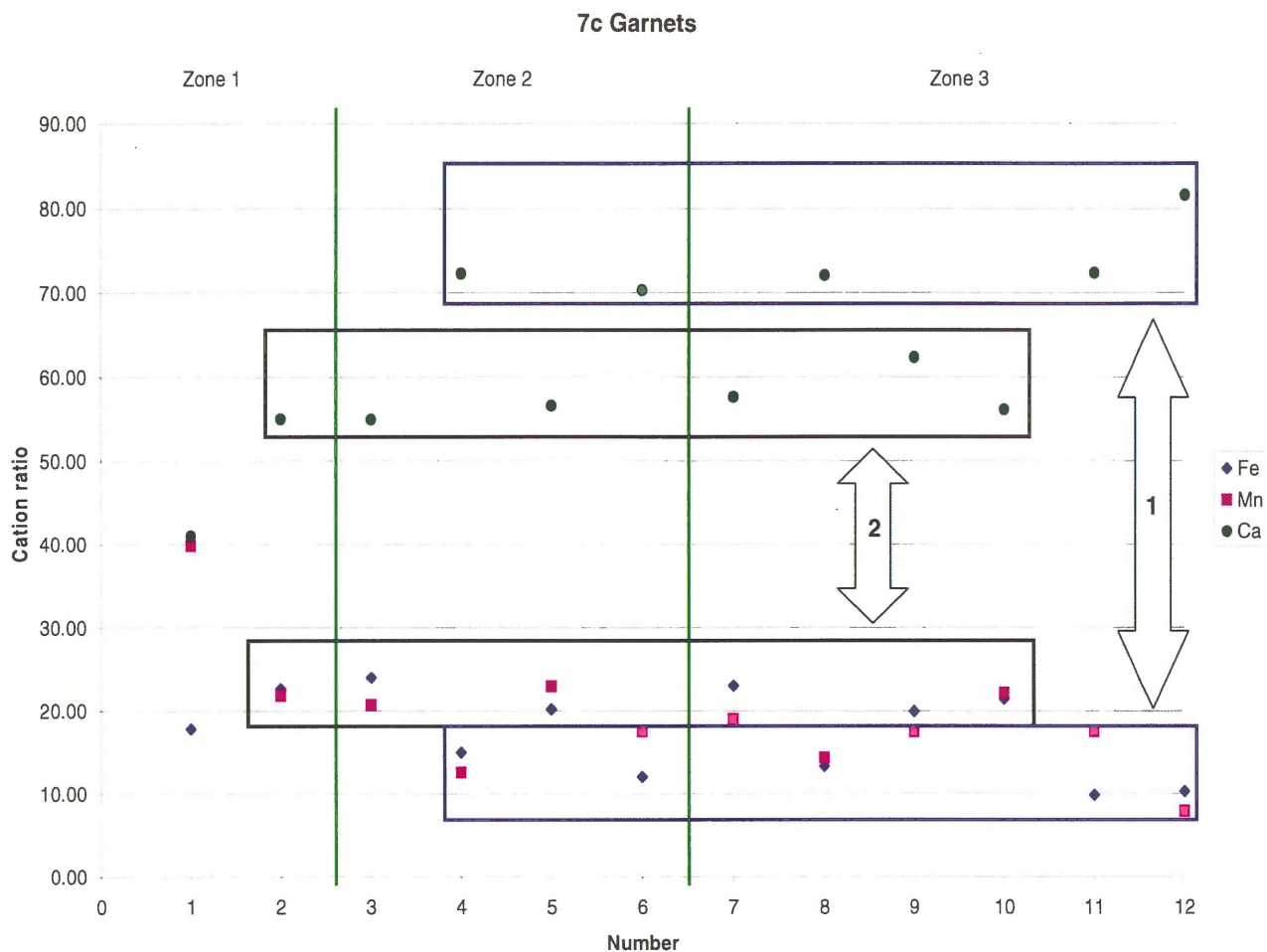
Figure 5.11 – Graph showing the two different populations of garnet analyzed in PPP04 – 7c. Population 1 is a High Ca, low Fe and Mn garnets. Population 2 is a lower Ca, higher Fe-Mn garnet. Mg values were constant throughout the samples and are not plotted on this graph.

Zone 2 contains garnet + chlorite + epidote + quartz ± calcite ± apatite.

No biotite, titanite, or feldspar was analyzed in this zone. Both types of garnet

are found in this zone. Minimal variation in mineral composition is present.

Average mineral compositions for zone 2 can be seen in Table 5.7.

Elements	Z2 Chlorite	Cations	14 Oxygen	Elements	Z2 Epidote	Cations	13 Oxygen
SiO2	25.90	Si	2.74	SiO2	37.92	Si	3.14
TiO2	0.00	Ti	0.00	TiO2	0.01	Ti	0.00
Al2O3	22.04	Al	2.74	Al2O3	28.14	Al	2.75
Cr2O3	0.00	Cr	0.00	Cr2O3	0.00	Cr	0.00
FeO	24.18	Fe	2.15	FeO	6.82	Fe	0.47
MnO	1.75	Mn	0.16	MnO	0.61	Mn	0.04
MgO	13.35	Mg	2.10	MgO	0.00	Mg	0.00
CaO	0.05	Ca	0.00	CaO	23.54	Ca	2.09
Na2O	0.00	Na	0.00	Na2O	0.00	Na	0.00
K2O	0.00	K	0.00	K2O	0.00	K	0.00
Total	**87.28**	**Total**	**9.89**	**Total**	**97.03**	**Total**	**8.49**
		Cation Ratio	**n = 2**			**Cation Ratio**	**n =1**
		Fe	48.51			Fe	18.13
		Mn	3.57			Mn	1.65
		Mg	47.80			Mg	0.00
		Ca	0.11			Ca	80.22
		Total	100			Total	100.00

Table 5.7 - Average mineral compositions for zone 2 of sample PPP04 – 7c. Each box contains the weight percent followed by the cations corrected to the correct number of oxygen and then the cation ratios. Cation rations are calculated as (Fe/(Fe+Mg+Mn+Ca))*100 or (Na/(Na+K+Ca))*100

Zone 3 contains garnet + chlorite + epidote + quartz ± titanite. No biotite, apatite, calcite, or feldspar was analyzed this zone. Both types of garnet are found in this zone. Minimal variation in mineral composition is present throughout the zone. Average mineral compositions for zone 3 can be seen in Table 5.8.

Elements	Z3 Chlorite	Z3 Epidote	Elements	Z3 Titanite
SiO2	26.38	38.11	SiO2	31.03
TiO2	0.01	0.15	TiO2	30.11
Al2O3	22.87	27.38	Al2O3	5.49
Cr2O3	0.00	0.00	Cr2O3	0.01
FeO	20.32	7.40	FeO	1.15
MnO	1.93	0.33	MnO	0.57
MgO	15.74	0.01	MgO	0.04
CaO	0.07	23.89	CaO	29.05
Na2O	0.00	0.00	Na2O	0.00
K2O	0.00	0.00	K2O	0.00
Total	**87.32**	**97.27**	**Total**	**97.45**
Cations	**14 Oxygen**	**13 Oxygen**	**Cations**	**5 Oxygen**
Si	2.73	3.16	Si	1.04
Ti	0.00	0.01	Ti	0.76
Al	2.79	2.67	Al	0.22
Cr	0.00	0.00	Cr	0.00
Fe	1.76	0.51	Fe	0.03
Mn	0.17	0.02	Mn	0.02
Mg	2.43	0.00	Mg	0.00
Ca	0.01	2.12	Ca	1.04
Na	0.00	0.00	Na	0.00
K	0.00	0.00	K	0.00
Total	**9.88**	**8.50**	**Total**	**3.10**
Cation Ratio	**n = 3**	**n = 1**		**n = 1**
Fe	40.31	19.28		
Mn	3.88	0.88		
Mg	55.65	0.05		
Ca	0.16	79.79		
Total	100	100.00		

Table 5.8 - Average mineral compositions for zone 3 of sample PPP04 – 7c. Each box contains the weight percent followed by the cations corrected to the correct number of oxygen and then the cation ratios. Cation ratios are calculated as (Fe/(Fe+Mg+Mn+Ca))*100 or (Na/(Na+K+Ca))*100

5.5.2 PPP04 – 17b

Sample PPP04 – 17b is a concretion from the Cable Rock outcrop (stop 5 – Fig 4.10) above the cordierite2-in isograd. This sample contains four different mineralogic zones (Fig 5.12), with zone 1 being the core of the concretion and zone 4 being the rim.
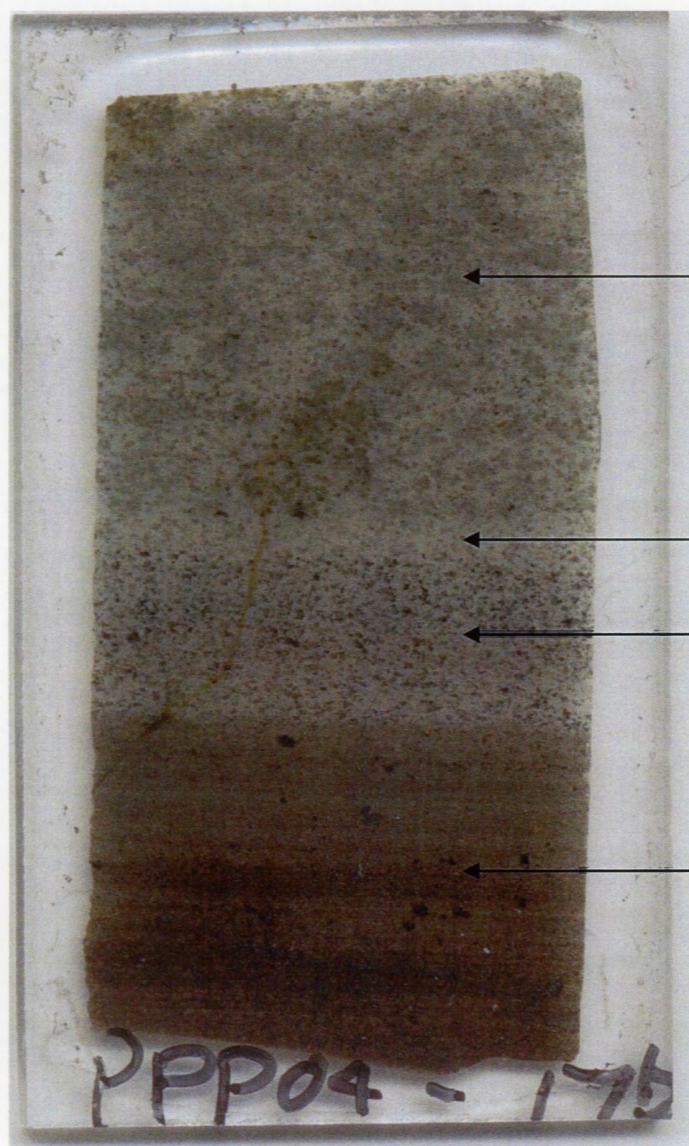
Figure 5.12 – Photo of PPP04 – 17 with the four different mineralogic zones

Zone 1

Zone 2

Zone 3

Zone 4

Zone 1 contains garnet + Ca - plagioclase + epidote + unknown calc-silicate + titanite + quartz. Little variation in mineral composition is found in this zone. Similar unknown calc-silicate minerals were analyzed in this zone as in zone 1 of PPP04 – 7c. This sample does not contain the two populations of garnets found in sample 7c. Average mineral compositions are listed in Table 5.9.

Element	Z1 Epidote	Z1 UCSM	Element	Z1 Ca - Plag	Element	Z1 Titanite
SiO2	38.66	36.20	SiO2	43.09	SiO2	30.56
TiO2	0.04	0.01	TiO2	0.00	TiO2	34.36
Al2O3	28.88	26.27	Al2O3	36.77	Al2O3	3.29
Cr2O3	0.02	0.02	Cr2O3	0.00	Cr2O3	0.20
FeO	6.47	9.31	FeO	0.13	FeO	0.57
MnO	1.12	0.51	MnO	0.00	MnO	0.19
MgO	0.01	6.65	MgO	0.01	MgO	0.01
CaO	23.09	15.49	CaO	20.25	CaO	28.82
Na2O	0.05	0.05	Na2O	0.16	Na2O	0.04
K2O	0.00	0.00	K2O	0.00	K2O	0.00
Total	**98.33**	**94.51**	**Total**	**100.41**	**Total**	**98.04**
Cation	13 Oxygen	11 Oxygen	Cation	8 Oxygen	Cation	12 Oxygen
Si	38.66	2.59	Si	1.99	Si	2.44
Ti	0.04	0.00	Ti	0.00	Ti	2.06
Al	28.88	2.22	Al	2.00	Al	0.31
Cr	0.02	0.00	Cr	0.00	Cr	0.01
Fe	6.47	0.56	Fe	0.00	Fe	0.04
Mn	1.12	0.03	Mn	0.00	Mn	0.01
Mg	0.01	0.71	Mg	0.00	Mg	0.00
Ca	23.09	1.19	Ca	1.00	Ca	2.46
Na	0.05	0.01	Na	0.01	Na	0.01
K	0.00	0.00	K	0.00	K	0.00
Total	**98.33**	**7.30**	**Total**	**5.02**	**Total**	**7.34**
Cation Ratio	n = 2	n = 1	Cation Ratio	n = 1		n = 4
Fe	17.32	22.42	Ca	98.58		
Mn	3.00	1.26	Na	1.42		
Mg	0.02	28.55	K	0.00		
Ca	79.66	47.78				

Table 5.9 - Average mineral compositions for zone 1 of sample PPP04 – 17b. Each box contains the weight percent followed by the cations corrected to the correct number of oxygen and then the cation ratios. Cation rations are calculated as (Fe/(Fe+Mg+Mn+Ca))*100 or (Na/(Na+K+Ca))*100

Zone 2 contains Ca - plag + muscovite + titanite + a sulfide + quartz. Little variation in mineral chemistry is found in this zone. The only plagioclase analysis in this section gives higher than expected Fe and Mg values, suggesting an intergrowth with plagioclase and something else (possibly chlorite). No garnet or

epidote was found in this zone. Table 5.10 gives average chemical compositions of the minerals analyzed.

Element	Z2 Ca - Plag	Z2 Muscovite	Element	Z2 Titanite
SiO2	44.71	46.40	SiO2	30.72
TiO2	0.00	0.00	TiO2	33.00
Al2O3	31.65	34.96	Al2O3	4.35
Cr2O3	0.00	0.00	Cr2O3	0.19
FeO	3.21	0.73	FeO	0.52
MnO	0.08	0.07	MnO	0.20
MgO	2.83	0.78	MgO	0.01
CaO	13.98	1.30	CaO	29.21
Na2O	0.91	0.50	Na2O	0.01
K2O	0.82	8.38	K2O	0.00
Total	**98.18**	**93.11**	**Total**	**98.20**
Cation	**8 Oxygen**	**11 Oxygen**	**Cation**	**12 Oxygen**
Si	2.12	3.12	Si	2.44
Ti	0.00	0.00	Ti	1.97
Al	1.77	2.77	Al	0.41
Cr	0.00	0.00	Cr	0.01
Fe	0.13	0.04	Fe	0.03
Mn	0.00	0.00	Mn	0.01
Mg	0.20	0.08	Mg	0.00
Ca	0.71	0.09	Ca	2.49
Na	0.08	0.06	Na	0.00
K	0.05	0.72	K	0.00
Total	**5.06**	**6.89**	**Total**	**7.37**
Cation Ratio	**n = 1**	**n = 1**		**n = 2**
Ca	84.25	10.66		
Na	9.87	7.40		
K	5.88	81.93		

Table 5.10 - Average mineral compositions for zone 2 of sample PPP04 – 17b. Each box contains the weight percent followed by the cations corrected to the correct number of oxygen and then the cation ratios. Catiorn ratios are calculated as (Fe/(Fe+Mg+Mn+Ca))*100 or (Na/(Na+K+Ca))*100

Zone 3 contains Ca - plagioclase + Mn-ilmenite + a sulfide + chlorite +

quartz. Chlorite compositions vary in this zone from Fe_{39} Mg_{59} to Fe_{47} Mg_{51}. Mn-

rich ilmenite is present in zone 3 (Mn_{56} Fe_{44}). The rest of the minerals have

minimal variation in chemical composition. Average mineral compositions

including ranges in chlorite composition are listed in Table 5.11.

Element	P1 Chlorite	P2 Chlorite	Element	Z3 Ca - Plag	Element	Z3 Ilmenite
SiO2	30.75	28.56	SiO2	46.47	SiO2	0.11
TiO2	0.98	0.61	TiO2	0.03	TiO2	52.36
Al2O3	17.99	19.92	Al2O3	33.74	Al2O3	0.04
Cr2O3	0.14	0.09	Cr2O3	0.02	Cr2O3	0.26
FeO	18.38	22.42	FeO	0.26	FeO	20.05
MnO	0.71	0.88	MnO	0.01	MnO	25.53
MgO	15.62	13.69	MgO	0.02	MgO	0.01
CaO	0.11	0.17	CaO	16.75	CaO	0.13
Na2O	0.11	0.10	Na2O	2.06	Na2O	0.02
K2O	2.83	1.26	K2O	0.00	K2O	0.02
Total	**87.63**	**87.71**	**Total**	**99.36**	**Total**	**98.55**
Cation	14 Oxygen	14 Oxygen	Cation	8 Oxygen	Cation	3 Oxygen
Si	3.16	2.98	Si	2.15	Si	0.00
Ti	0.08	0.05	Ti	0.00	Ti	1.00
Al	2.18	2.45	Al	1.84	Al	0.00
Cr	0.01	0.01	Cr	0.00	Cr	0.01
Fe	1.58	1.95	Fe	0.01	Fe	0.43
Mn	0.06	0.08	Mn	0.00	Mn	0.55
Mg	2.39	2.13	Mg	0.00	Mg	0.00
Ca	0.01	0.02	Ca	0.83	Ca	0.00
Na	0.02	0.02	Na	0.18	Na	0.00
K	0.37	0.17	K	0.00	K	0.00
Total	**9.87**	**9.84**	**Total**	**5.02**	**Total**	**1.99**
Cation Ratio	n = 1	n = 1	Cation Ratio	n = 1	Cation Ratio	n = 1
Fe	39.04	46.77	Ca	81.80	Fe	43.69
Mn	1.52	1.88	Na	18.20	Mn	56.31
Mg	59.16	50.89	K	0.00		
Ca	0.28	0.47				

Table 5.11 - Average mineral compositions for zone 3 of sample PPP04 – 17b. Each box contains the weight percent followed by the cations corrected to the correct number of oxygen and then the cation ratios. Cation ratios are calculated as (Fe/(Fe+Mg+Mn+Ca))*100 or (Na/(Na+K+Ca))*100

Zone 4 contains chlorite + Mn-ilmenite + Na - plagioclase + pyrrhotite + quartz. Only one chlorite was analyzed from this section so the range in chemical composition is unknown. Mn – rich ilmenite is similar to that found in zone 3. Also, there is a change from Ca - plag in zones one, two, and three to Na - plagioclase in zone 4. Table 5.12 gives average chemical compositions for the minerals found in zone 4.

Element	Z4 Chlorite	Element	Z4 Na - Plag	Element	Z4 Ilmenite
SiO2	28.72	SiO2	59.95	SiO2	0.09
TiO2	4.55	TiO2	0.00	TiO2	52.24
Al2O3	18.35	Al2O3	24.96	Al2O3	0.03
Cr2O3	0.09	Cr2O3	0.00	Cr2O3	0.28
FeO	20.16	FeO	0.20	FeO	20.43
MnO	1.06	MnO	0.00	MnO	25.20
MgO	11.69	MgO	0.00	MgO	0.01
CaO	3.90	CaO	6.26	CaO	0.11
Na2O	0.00	Na2O	8.17	Na2O	0.03
K2O	0.57	K2O	0.06	K2O	0.03
Total	**89.10**	**Total**	**99.60**	**Total**	**98.44**
Cation	**14 Oxygen**	**Cation**	**8 Oxygen**	**Cation**	**3 Oxygen**
Si	2.94	Si	2.68	Si	0.00
Ti	0.35	Ti	0.00	Ti	1.00
Al	2.22	Al	1.32	Al	0.00
Cr	0.01	Cr	0.00	Cr	0.01
Fe	1.73	Fe	0.01	Fe	0.44
Mn	0.09	Mn	0.00	Mn	0.54
Mg	1.79	Mg	0.00	Mg	0.00
Ca	0.43	Ca	0.30	Ca	0.00
Na	0.00	Na	0.71	Na	0.00
K	0.08	K	0.00	K	0.00
Total	**9.63**	**Total**	**5.02**	**Total**	**2.00**
Cation Ratio	**n = 1**	**Cation Ratio**	**n = 2**	**Cation Ratio**	**n = 1**
Fe	42.82	Ca	29.62	Fe	44.47
Mn	2.29	Na	70.06	Mn	55.53
Mg	44.27	K	0.32		
Ca	10.62				

Table 5.12 - Average mineral compositions for zone 4 of sample PPP04 – 17b. Each box contains the weight percent followed by the cations corrected to the correct number of oxygen and then the cation ratios. Cation ratios are calculated as (Fe/(Fe+Mg+Mn+Ca))*100 or (Na/(Na+K+Ca))*100

6. Discussion and Conclusion

6.1 Discussion

6.1.1 Stratigraphy

The Bluestone member resembles published descriptions of the Feltzen Member (O'Brien, 1986) described in Chapter 2. Both are located stratigraphically above the Cunard Member (Fig 2.2). Both are interlayered meta-siltstone and slates with calcareous concretions present (O'Brien, 1988). Both members look similar to each other in outcrops and have higher siltstone content than the underlying Cunard Member. On this basis, it is proposed that the Bluestone member is correlative with the Feltzen, and possibly an extension of the Feltzen Member. More work is needed to determine whether or not the Bluestone member is really the Feltzen Member or a new lithological unit.

6.1.2 Structure

Based upon the overall structure in the park, outcrops containing calcareous conretions should appear in outcrops north of the railway tracks. However, no concretions have been discovered. There are four possible reasons for the absence of these concretions. First, there could be unrecognized structures that would offset unit A, for example a normal fault. This would bring unit B above unit A and thus unit A would not be on the surface. Second, there could be a lack of outcrops due to urbanization of Halifax. As the city grew, a lot of the outcrops could have been destroyed to make way for buildings and homes. Thirdly, there could be a lack of recognition of concretions outcrops in the sparse, heavily weathered urban outcrops. And finally, there could be a localized facies

change in the lithology from calcareous rich to calcareous poor from the southern tip of the peninsula north.

6.1.3 Metamorphism

Samples 19 and 5b exhibit typical chlorite zone mineralogy. The only difference is the presence of fresh chlorite in sample 19. Sample 3 shows the change in mineralogy as you cross the cordierite2 in isograd. The PT estimate obtained from TWQ is a preliminary measurement, which requires more refinement.

Mineral zoning in both analyzed concretions is probably due to the change in bulk composition from core to rim of the concretions, which is reflected in the change in mineral assemblage from core to rim. Sample PPP04 – 7c appears to be relatively Ca – rich throughout the sample. This sample also does not show Mn – zoning. All the Mn in the concretion appears to be within the garnets. Chlorite appears to be the only mineral that is not Ca-rich. There is a change in the abundance of Ca – rich minerals from zone 1 (core) to zone 3 (rim). Zone 1 has the most abundant Ca – rich minerals (epidote, plagioclase, titanite, calcite, and garnet), where zone 3 has the least abundant Ca – rich minerals (epidote, titanite, and garnet).

Sample PPP04 – 17b changes from a Ca – rich core (zone 1) to an Mn – rich rim (zone 4). The Ca in this concretion is dominantly in the plagioclase and titanite of zone 1 and 2. Zone 3 is a transition zone where Ca –rich plagioclase and Mn – rich ilmenites are both present. In zone 4 there is a change from Ca – rich plag to Na – rich plag. Mn – rich ilmenites are also present in zone 4.

The difference in the composition of the two concretions could be a diagenetic process, or it could be a metasomatic process. Pending on the chemistry of the fluid that formed the concretions during diagenesis, the mineralogy could be quite different, or the influx of metamorphic fluid could have formed the concretions. Some recrystallization probably took place due to the degree of metamorphism on each concretion.

6.2 Conclusions

A previously unrecognized lithological unit has been identified underlying the southern part of the Halifax peninsula, including Point Pleasant Park:

1. The new unit, referred to here as the Bluestone member, is stratigraphically equivalent to the Feltzen Member of the Halifax Formation identified in the Mahone Bay region. It overlies the Cunard Member and grades into it somewhere between Point Pleasant Park and the Dalhousie campus.

2. Two different divisions of the Bluestone member can be recognized within Point Pleasant Park based on the presence of calcareous concretions in the lower unit A and their absence from the overlying unit B.

3. P-T conditions were estimated for the cordierite2 in isograd located ca. 500m from the contact with the SMB. This isograd marks a second growth of cordierite. Using TWQ, the reaction yielded temperatures of 540 - 560°C for a pressure range of 3.2 – 3.8 kbars.

4. Zoning within the calcareous concretions is marked by changes in mineral assemblage, which is represented in color zoning at outcrop scale. This change in mineral composition is most likely due to a change in bulk composition of the concretion from dominantly Ca – rich cores to the Ca – poor rims.

6.3 Suggestions for Future Work

Further work in Point Pleasant Park should include a more detailed study of the Bluestone member north of the park to determine if unit A outcrops outside of the park, specifically noting the presence or absence of calcareous concretions. A more detailed analysis of the outcrops within the park is needed, looking in particular for the presence of concretions to better determine the boundary between units A and B. Also, a more detailed mineralogic study of the calcareous concretions within the park should be performed to determine their origin and the cause of the zoning within the concretions. A more detailed mineralogic study of units A and B is also needed, looking in particular for the presence of fresh cordierite in order to put a more precise location of the cordierite2 in isograd. Finally, a pamphlet summarizing the findings of this study should be created and this pamphlet should be made available to the general public.

References

Carruzzo, S., Kontak, D..J., Reynolds, P.H., Clarke, D.B., Dunning, G. R., Selby, D., and Creaser, R.A. (2003) U/Pb, Re/Os, and Ar/Ar dating of the South Mountain Batholith and its mineral deposits. Geochimica et Cosmochimica Acta, Volume 67, Issue 18, Supplement 1, p.A54 , Goldschmidt Conference 2003

Clarke, D.B., MacDonald, M.A., and Erdmann, S. (2004) Chemical variation in Al_2O_3–C_aO–Na_2O–K_2O space: controls on the peraluminosity of the South Mountain Batholith. Canadian Journal of Earth Sciences, 41, pp. 785–798

Hart, G. (2006) Andalusite in the South Mountain Batholith contact aureole, Halifax NS: A tale of two isograds. Unpublished B.Sc. thesis, Dalhousie University, Halifax, NS.

Hicks, R.J. (1996). Low-grade metamorphism in the Meguma Group, southern Nova Scotia. Unpublished M.Sc. thesis, Dalhousie University, Halifax, N.S.

Hicks, R.J., Jamieson, R.A., and Reynolds, P.H. (1999). Detrital and metamorphic $^{40}Ar/^{39}Ar$ ages from muscovite and whole-rock samples, Meguma Supergroup, southern Nova Scotia. Canadian Journal of Earth Sciences, 36, pp. 23–32.

Horne, N. and Culshaw, C. (2001) Flexural – slip folding in the Meguma Group, Nova Scotia, Canada. Journal of Structural Geology, 23, pp 1631 – 1652.

Jamieson, R.A., Tobey, N.W., and ERTH 3020 (2005) Contact metamorphism of the Halifax Formation on the southeast margin of the Halifax Pluton, Halifax, Nova Scotia. GAC/MAC, May 2005, Dalhousie University, Halifax, NS.

Keppie, J. D. and Krogh, T. E. (2000) 440 Ma igneous activity in the Meguma Terrane, Nova Scotia, Canada: part of the Appalachian overstep sequence; American Journal of Science, 300, pp. 528-538.

Keppie, J.D., and Muecke, G.K. (*Compilers*) (1979) Metamorphic map of Nova Scotia. Scale 1 : 500 000. Nova Scotia Department of Mines and Energy.

Kontak, D.J., Dostal, J., Kyser, T.K., and Archibald, D.A. (2002) A petrological, geochemical, isotopic and fluid-inclusion study of 370 Ma pegmatite–aplite sheets, Peggys Cove, Nova Scotia, Canada. Canadian Mineralogist, 40, pp. 1249-1286

MacDonald, L.A, Barr, S.M., White, C.E., and Ketchum, J.W.F (2002) Petrology, age, and tectonic setting of the White Rock Formation, Meguma terrane, Nova Scotia: evidence for Silurian continental rifting. Canadian Journal of Earth Sciences, 39, pp. 259–277

O'Brien, B. H. (1986) Preliminary report on the geology of the Mahone Bay area, Nova Scotia, *in* Current Research, Part A, Geological Survey of Canada Paper 86-1A, pp. 439–444.

O'Brien, B.H. (1988) A study of the Meguma Terrane in Lunenburg County, Nova Scotia. Geological Survey of Canada, Open File 1823.

Point Pleasant Park (N.A.) Retrieved from http://www.pahs.ednet.ns.ca/PPP/ on February 15th, 2006

Pye, K., Dickson, J.A.D., Schiavon, N., Coleman, M.L., and Cox, M. (1990) Formation of siderite – Mg – calcite – iron sulphide concretions in intertidal marsh and sandflat sediments, north Norfolk, England. Sedimentology, 37, pp. 325 – 343.

Raeside, R. P. and Mahoney, K.M. (1996): The contact metamorphic aureole of the South Mountain Batholith, southern Nova Scotia. Geol. Assoc. Can. – Mineral. Assoc. Can., Program Abstr. 21, A77.

Schenk, P.E. (1991) Events and sea-level changes on Gondwana's margin: the Meguma Zone (Cambrian to Devonian) of Nova Scotia, Canada. Geological Society of America Bulletin, 103, pp. 512–521.

Schenk, P.E. (1997) Sequence stratigraphy and provenance on Gondwana's margin: The Meguma zone (Cambrian–Devonian) of Nova Scotia, Canada: Geological Society of America Bulletin, 109, pp. 395–409.

White, C.E., Barr, S.M., and Toole, R.M. (2006) New constraints on deciphering the origin of the Meguma Group in southwestern Nova Scotia. Atlantic Geoscience Society, Abstracts, February 2006, Wolfville Nova Scotia

Williams, H. (1979) The Appalachian Orogen in Canada. Canadian Journal of Earth Sciences, 16, pp. 792–807.

250 m from Cable Rock

Note	Structur	Facie

Sample 2 just above section

Nodule

Wavey bedding

Highly Fractured

Several 2cm pinch and swells, sample 1

Several 2cm pinch and swells

5 fining upward cycles

Pinch and

T_c

T_b

T_c

T_b

T_c

T_b

T_b

T_b

T_b

T_c

T_b

T_c

T_b

T_c

T_b

T_c

T_b

T_c

T_b

T_c

T_b

T_c

350 m from Cable Rock

VF   F

100 cm

Vertical Scale

		Degrees			Degrees
Stop 1	Angle	51	**Stop 2**	Angle	82
	Apparent Dip	44		Apparent Dip	23
	True Dip	51		True Dip	23
		Degrees			Degrees
Stop 3	Angle	90	**Stop 4**	Angle	111
	Apparent Dip	24		Apparent Dip	25
	True Dip	24		True Dip	27
		Degrees			Degrees
Stop 5	Angle	83	**Stop 6**	Angle	84
	Apparent Dip	35		Apparent Dip	8
	True Dip	35		True Dip	8

Appendix C: Microprobe Data

Table A: Microprobe data for biotites from samples PPP04 – 19, 5b, & 3. Cation ratios calculated as $(Fe/Fe+Mg)*100$

Comment	ppp19 biotite 7	ppp19 mica 14	ppp19 mica 16	ppp3 mica 9	ppp3 matrix 16	ppp3 matrix 17	ppp3 matrix 18
SiO2	33.39	32.77	33.62	33.95	33.01	34.07	33.21
TiO2	1.28	1.23	1.06	1.65	2.20	2.16	2.27
Al2O3	21.22	20.95	23.83	21.05	20.29	20.41	19.90
Cr2O3	0.18	0.04	0.04	0.09	0.15	0.13	0.14
FeO	23.63	24.98	23.86	24.87	26.27	25.17	25.36
MnO	0.21	0.19	0.18	0.19	0.15	0.08	0.10
MgO	6.43	6.77	6.53	5.55	5.15	5.10	5.45
CaO	0.00	0.00	0.00	0.04	0.04	0.05	0.06
Na2O	0.19	0.10	0.23	0.05	0.05	0.06	0.04
K2O	7.89	6.46	6.12	8.66	6.88	8.38	7.63
Total	94.41	93.51	95.47	96.11	94.20	95.61	94.18
Number of cations corrected for 11 oxygen							
Si	2.60	2.58	2.55	2.62	2.60	2.64	2.62
Ti	0.07	0.07	0.06	0.10	0.13	0.13	0.13
Al	1.95	1.94	2.13	1.91	1.88	1.87	1.85
Cr	0.01	0.00	0.00	0.01	0.01	0.01	0.01
Fe	1.54	1.64	1.51	1.60	1.73	1.63	1.67
Mn	0.01	0.01	0.01	0.01	0.01	0.01	0.01
Mg	0.75	0.79	0.74	0.64	0.61	0.59	0.64
Ca	0.00	0.00	0.00	0.00	0.00	0.00	0.01
Na	0.03	0.02	0.03	0.01	0.01	0.01	0.01
K	0.78	0.65	0.59	0.85	0.69	0.83	0.77
Total	7.75	7.71	7.63	7.76	7.67	7.71	7.71
Cation Ratio							
Fe	67.34	67.42	67.19	71.55	74.09	73.47	72.31
Mg	32.66	32.58	32.81	28.45	25.91	26.53	27.69
Total	100.00	100.00	100.00	100.00	100.00	100.00	100.00

ppp3 dark 21	ppp3 dark 22	ppp3 light 29	ppp3 light 32	ppp3 light 33	ppp5b 1	ppp5b 3	ppp5b 9	ppp5b 11
33.36	33.56	34.30	33.51	34.07	34.17	33.97	33.80	33.81
2.45	2.47	2.62	2.04	2.06	1.10	1.30	1.32	1.20
20.67	21.10	21.22	21.66	21.11	20.88	20.56	20.82	20.40
0.06	0.04	0.13	0.09	0.13	0.07	0.05	0.04	0.01
23.70	24.42	23.94	24.13	23.49	23.64	23.38	23.03	22.66
0.11	0.12	0.10	0.10	0.11	0.14	0.11	0.11	0.11
5.08	5.12	5.08	5.24	5.24	6.86	6.88	6.83	7.11
0.00	0.00	0.01	0.02	0.09	0.00	0.00	0.00	0.00
0.05	0.04	0.17	0.17	0.16	0.26	0.22	0.16	0.16
8.61	8.51	8.77	8.60	8.50	7.88	7.89	7.99	7.76
94.08	95.38	96.34	95.56	94.96	95.00	94.33	94.10	93.23
2.62	2.60	2.63	2.59	2.64	2.64	2.64	2.63	2.65
0.14	0.14	0.15	0.12	0.12	0.06	0.08	0.08	0.07
1.91	1.93	1.92	1.97	1.93	1.90	1.88	1.91	1.89
0.00	0.00	0.01	0.01	0.01	0.00	0.00	0.00	0.00
1.56	1.58	1.53	1.56	1.52	1.53	1.52	1.50	1.49
0.01	0.01	0.01	0.01	0.01	0.01	0.01	0.01	0.01
0.60	0.59	0.58	0.61	0.61	0.79	0.80	0.79	0.83
0.00	0.00	0.00	0.00	0.01	0.00	0.00	0.00	0.00
0.01	0.01	0.03	0.03	0.02	0.04	0.03	0.02	0.02
0.86	0.84	0.86	0.85	0.84	0.78	0.78	0.79	0.78
7.71	7.71	7.70	7.74	7.70	7.75	7.75	7.74	7.74
72.34	72.80	72.57	72.07	71.56	65.89	65.59	65.42	64.12
27.66	27.20	27.43	27.93	28.44	34.11	34.41	34.58	35.88
100.00	100.00	100.00	100.00	100.00	100.00	100.00	100.00	100.00

Table B: Muscovite data from samples PPP04 – 19, 5b, & 3. Cation ratios calculated as (Ca/Ca+Na+K)*100

Comment	ppp19 mica 9	ppp19 mica 15	ppp19 mica 17	ppp3 mica 7	ppp3 mica 8	ppp3 matrix 14	ppp3 matrix 19	ppp3 dark 24
SiO2	45.77	47.19	47.00	50.07	47.41	47.17	48.18	45.53
TiO2	0.04	0.08	0.16	0.62	0.63	0.79	0.58	0.16
Al2O3	36.73	37.39	36.73	37.56	36.46	36.13	33.48	36.22
Cr2O3	0.02	0.00	0.00	0.46	0.30	0.09	0.09	0.00
FeO	0.83	0.71	1.10	1.18	1.12	0.93	1.35	0.92
MnO	0.00	0.00	0.00	0.04	0.03	0.01	0.00	0.00
MgO	0.37	0.31	0.47	0.38	0.35	0.28	0.77	0.39
CaO	0.00	0.00	0.00	0.00	0.00	0.01	0.01	0.00
Na2O	1.03	1.00	0.98	0.55	0.53	0.55	0.40	0.31
K2O	9.19	9.44	9.10	8.57	10.26	10.02	9.96	8.68
Total	93.98	96.12	95.53	99.44	97.10	95.97	94.84	92.22
Number of cations corrected for 11 oxygen								
Si	3.06	3.08	3.09	3.14	3.08	3.10	3.20	3.08
Ti	0.00	0.00	0.01	0.03	0.03	0.04	0.03	0.01
Al	2.89	2.87	2.84	2.77	2.80	2.79	2.62	2.89
Cr	0.00	0.00	0.00	0.02	0.02	0.00	0.01	0.00
Fe	0.05	0.04	0.06	0.06	0.06	0.05	0.07	0.05
Mn	0.00	0.00	0.00	0.00	0.00	0.00	0.00	0.00
Mg	0.04	0.03	0.05	0.04	0.03	0.03	0.08	0.04
Ca	0.00	0.00	0.00	0.00	0.00	0.00	0.00	0.00
Na	0.13	0.13	0.12	0.07	0.07	0.07	0.05	0.04
K	0.78	0.79	0.76	0.69	0.85	0.84	0.84	0.75
Total	6.95	6.94	6.93	6.81	6.94	6.92	6.91	6.86
Cation Ratio								
Ca	0.00	0.00	0.00	0.00	0.00	0.12	0.12	0.00
Na	14.53	13.87	14.02	8.92	7.31	7.62	5.76	5.15
K	85.47	86.13	85.98	91.08	92.69	92.26	94.12	94.85

ppp3 dark 26	ppp3 dark 27	ppp5b 4	ppp5b 8	ppp5b 10
46.90	46.67	47.48	46.66	47.06
0.46	0.59	0.02	0.20	0.04
36.94	36.40	37.06	36.68	35.12
0.00	0.00	0.00	0.00	0.00
0.79	0.93	0.89	0.76	1.00
0.00	0.00	0.00	0.00	0.00
0.30	0.29	0.29	0.40	0.70
0.00	0.00	0.00	0.00	0.00
0.44	0.51	1.01	0.87	0.66
9.82	8.80	9.52	9.34	8.87
95.65	94.19	96.28	94.92	93.44
3.08	3.09	3.09	3.08	3.15
0.02	0.03	0.00	0.01	0.00
2.86	2.84	2.85	2.86	2.77
0.00	0.00	0.00	0.00	0.00
0.04	0.05	0.05	0.04	0.06
0.00	0.00	0.00	0.00	0.00
0.03	0.03	0.03	0.04	0.07
0.00	0.00	0.00	0.00	0.00
0.06	0.07	0.13	0.11	0.09
0.82	0.74	0.79	0.79	0.76
6.91	6.86	6.94	6.93	6.89
0.00	0.00	0.00	0.00	0.00
6.39	8.14	13.88	12.48	10.18
93.61	91.86	86.12	87.52	89.82

Table C: Cordierite data from samples PPP04 – 3. Cation ratios calculated as (Fe/Fe+Mg)*100

Comment	ppp3 cordierite 1	ppp3 cordierite 2	ppp3 cordierite 3	ppp3 cordierite 4	ppp3 cordierite 5	ppp3 cordierite 6	ppp3 light 28	ppp3 light 30
SiO2	49.41	47.12	47.83	49.45	47.62	47.55	47.92	47.12
TiO2	0.01	0.04	0.05	0.02	0.00	0.03	0.00	0.02
Al2O3	33.29	32.16	33.27	31.29	33.32	33.16	32.78	32.57
Cr2O3	0.02	0.00	0.04	0.01	0.04	0.00	0.00	0.00
FeO	9.29	8.85	13.13	10.98	12.88	11.92	10.89	11.40
MnO	0.28	0.22	0.45	0.34	0.45	0.41	0.23	0.22
MgO	3.64	3.17	5.08	4.40	5.13	4.98	4.16	4.17
CaO	0.05	0.06	0.01	0.01	0.02	0.02	0.04	0.02
Na2O	0.30	0.31	0.23	0.27	0.25	0.27	0.46	0.43
K2O	2.44	4.56	0.05	1.44	0.00	0.73	1.34	2.06
Total	98.73	96.48	100.15	98.20	99.73	99.06	97.83	98.02
Number of cations corrected for 18 oxygen								
Si	5.14	5.09	4.95	5.19	4.95	4.97	5.05	5.00
Ti	0.00	0.00	0.00	0.00	0.00	0.00	0.00	0.00
Al	4.08	4.09	4.06	3.87	4.08	4.08	4.08	4.08
Cr	0.00	0.00	0.00	0.00	0.00	0.00	0.00	0.00
Fe	0.81	0.80	1.14	0.96	1.12	1.04	0.96	1.01
Mn	0.03	0.02	0.04	0.03	0.04	0.04	0.02	0.02
Mg	0.56	0.51	0.78	0.69	0.80	0.78	0.65	0.66
Ca	0.01	0.01	0.00	0.00	0.00	0.00	0.01	0.00
Na	0.06	0.06	0.05	0.05	0.05	0.05	0.09	0.09
K	0.32	0.63	0.01	0.19	0.00	0.10	0.18	0.28
Total	11.01	11.21	11.04	10.99	11.04	11.06	11.04	11.14
Cation Ratio								
Fe	58.92	61.07	59.18	58.34	58.46	57.33	59.53	60.50
Mg	41.08	38.93	40.82	41.66	41.54	42.67	40.47	39.50

Table D: Feldspar data from samples PPP04 – 3. Cation ratios calculated as (Ca/Ca+Na+K)*100

Comment	ppp3 matrix 12	ppp3 matrix 13	ppp3 dark 23	ppp3 dark 25	ppp3 light 34
SiO2	64.86	63.40	63.43	65.16	65.33
TiO2	0.04	0.04	0.00	0.00	0.07
Al2O3	21.99	21.62	22.75	21.57	19.37
Cr2O3	0.00	0.00	0.00	0.00	0.00
FeO	0.12	0.14	0.05	0.05	1.08
MnO	0.00	0.00	0.00	0.00	0.00
MgO	0.00	0.00	0.00	0.00	0.11
CaO	2.75	2.57	3.01	2.04	0.01
Na2O	10.31	10.40	9.70	10.43	2.91
K2O	0.13	0.15	0.10	0.08	11.39
Total	100.20	98.32	99.03	99.32	100.26
Number of cations corrected for 8 oxygen					
Si	2.85	2.85	2.82	2.88	2.97
Ti	0.00	0.00	0.00	0.00	0.00
Al	1.14	1.14	1.19	1.12	1.04
Cr	0.00	0.00	0.00	0.00	0.00
Fe	0.00	0.00	0.00	0.00	0.04
Mn	0.00	0.00	0.00	0.00	0.00
Mg	0.00	0.00	0.00	0.00	0.01
Ca	0.13	0.12	0.14	0.10	0.00
Na	0.88	0.91	0.84	0.90	0.26
K	0.01	0.01	0.01	0.00	0.66
Total	5.02	5.04	5.00	5.00	4.97
Cation Ratio					
Ca	12.75	11.94	14.53	9.72	0.00
Na	86.55	87.21	84.90	89.88	28.01
K	0.71	0.85	0.57	0.40	71.99

Table E: Chlorite data from PPP04 – 19. Cation ratios calculated as (Fe/Fe+Mg)*100

Elements	19 Chlorite
SiO2	31.52
TiO2	0.04
Al2O3	29.45
Cr2O3	0.01
FeO	20.61
MnO	0.28
MgO	5.77
CaO	0.12
Na2O	0.27
K2O	0.70
Total	88.77
14 Oxygen	
Si	3.11
Ti	0.00
Al	3.42
Cr	0.00
Fe	1.70
Mn	0.02
Mg	0.85
Ca	0.01
Na	0.05
K	0.09
Total	9.25
Cation Ratios	
Fe	66.68
Mg	33.32

Table F: Garnet data from PPP04 – 7c. Cation ratios calculated as (Ca/Ca+Fe+Mn+Mg)*100

Comment	ppp7c 01	ppp7c 02	ppp7c 13	ppp7c 14	ppp7c 16	ppp7c 17	ppp7c 24	ppp7c 26	ppp7c 27	ppp7c 29	ppp7c 30	ppp7c 31
SiO2	36.91	37.92	37.79	38.18	37.81	38.17	38.12	38.61	38.30	38.06	38.53	38.41
TiO2	0.96	0.45	0.12	0.23	0.51	0.67	0.17	0.25	0.16	0.55	0.46	0.67
Al2O3	19.65	20.63	20.99	20.53	20.66	20.41	20.85	20.64	20.52	20.72	20.87	20.23
Cr2O3	0.36	0.08	0.02	0.01	0.03	0.02	0.01	0.00	0.07	0.04	0.08	0.04
FeO	8.04	10.59	11.02	7.26	9.32	5.70	10.78	6.45	9.56	9.94	4.70	5.07
MnO	17.75	10.03	9.38	6.03	10.46	8.21	8.78	6.86	8.29	10.15	8.26	3.86
MgO	0.33	0.12	0.08	0.03	0.06	0.02	0.08	0.05	0.05	0.07	0.06	0.05
CaO	14.43	20.01	19.66	27.40	20.40	25.97	21.04	27.17	23.35	20.35	26.92	31.34
Na2O	0.01	0.00	0.02	0.00	0.00	0.00	0.00	0.00	0.00	0.00	0.00	0.00
K2O	0.00	0.00	0.03	0.02	0.01	0.02	0.00	0.00	0.00	0.00	0.00	0.00
Total	98.44	99.82	99.10	99.68	99.27	99.20	99.82	100.04	100.29	99.87	99.88	99.67
Number of cations corrected for 12 oxygen												
Si	2.99	2.99	3.00	2.98	2.99	2.99	3.00	3.00	3.00	3.00	2.99	2.98
Ti	0.06	0.03	0.01	0.01	0.03	0.04	0.01	0.01	0.01	0.03	0.03	0.04
Al	1.88	1.92	1.96	1.89	1.93	1.89	1.93	1.89	1.89	1.92	1.91	1.85
Cr	0.02	0.00	0.00	0.00	0.00	0.00	0.00	0.00	0.00	0.00	0.00	0.00
Fe	0.54	0.70	0.73	0.48	0.62	0.37	0.71	0.42	0.63	0.65	0.30	0.33
Mn	1.22	0.67	0.63	0.40	0.70	0.54	0.59	0.45	0.55	0.68	0.54	0.25
Mg	0.04	0.01	0.01	0.00	0.01	0.00	0.01	0.01	0.01	0.01	0.01	0.01
Ca	1.25	1.69	1.67	2.29	1.73	2.18	1.77	2.26	1.96	1.72	2.24	2.60
Na	0.00	0.00	0.00	0.00	0.00	0.00	0.00	0.00	0.00	0.00	0.00	0.00
K	0.00	0.00	0.00	0.00	0.00	0.00	0.00	0.00	0.00	0.00	0.00	0.00
Total	8.01	8.02	8.02	8.06	8.01	8.02	8.02	8.04	8.05	8.01	8.03	8.06
Cation Ratio												
Fe	17.83	22.72	24.02	14.98	20.21	12.06	23.03	13.35	19.95	21.41	9.85	10.30
Mn	39.87	21.82	20.71	12.60	22.96	17.56	19.02	14.38	17.50	22.15	17.53	7.94
Mg	1.30	0.43	0.32	0.11	0.24	0.08	0.31	0.19	0.19	0.27	0.23	0.19
Ca	41.01	55.04	54.95	72.30	56.59	70.30	57.64	72.08	62.36	56.17	72.38	81.57
Total	100.00	100.00	100.00	100.00	100.00	100.00	100.00	100.00	100.00	100.00	100.00	100.00

73

Table G: Chlorite data from PPP04 – 7c. Cation ratios calculated as (Ca/Ca+Fe+Mn+Mg)*100

Comment	ppp7c 4	ppp7c 9	ppp7c 19	ppp7c 23	ppp7c 25	ppp7c 32
SiO2	27.14	27.74	25.52	26.27	26.19	26.68
TiO2	0.02	0.00	0.00	0.00	0.01	0.02
Al2O3	22.71	21.10	20.30	23.78	22.96	21.87
Cr2O3	0.01	0.00	0.00	0.00	0.00	0.00
FeO	20.09	20.38	28.72	19.65	20.87	20.44
MnO	1.87	1.77	1.50	2.01	1.90	1.88
MgO	15.97	16.44	11.11	15.59	15.50	16.12
CaO	0.20	0.15	0.00	0.09	0.05	0.06
Na2O	0.06	0.07	0.00	0.00	0.01	0.00
K2O	0.00	0.00	0.00	0.00	0.00	0.00
Total	88.06	87.65	87.16	87.40	87.49	87.06
Number of cations corrected for 14 oxygen						
Si	2.77	2.85	2.77	2.70	2.71	2.77
Ti	0.00	0.00	0.00	0.00	0.00	0.00
Al	2.74	2.56	2.60	2.88	2.80	2.68
Cr	0.00	0.00	0.00	0.00	0.00	0.00
Fe	1.72	1.75	2.61	1.69	1.81	1.78
Mn	0.16	0.15	0.14	0.18	0.17	0.17
Mg	2.43	2.52	1.80	2.39	2.39	2.50
Ca	0.02	0.02	0.00	0.01	0.01	0.01
Na	0.01	0.01	0.00	0.00	0.00	0.00
K	0.00	0.00	0.00	0.00	0.00	0.00
Total	9.86	9.87	9.93	9.85	9.89	9.89
Cation Ratio						
Fe	39.62	39.43	57.38	39.63	41.34	39.96
Mn	3.75	3.46	3.05	4.10	3.81	3.72
Mg	56.15	56.72	39.57	56.04	54.72	56.19
Ca	0.48	0.38	0.00	0.23	0.13	0.13
Total	100.00	100.00	100.00	100.00	100.00	100.00

Table H: Feldspar data from PPP04 – 7c. Cation ratios calculated as (Ca/Ca+Na+K)*100

Comment	ppp7c 5
SiO2	43.78
TiO2	0.00
Al2O3	36.19
Cr2O3	0.00
FeO	0.09
MnO	0.00
MgO	0.00
CaO	19.51
Na2O	0.57
K2O	0.00
Total	100.14
Number of cations corrected for 8 oxygen	
Si	2.02
Ti	0.00
Al	1.97
Cr	0.00
Fe	0.00
Mn	0.00
Mg	0.00
Ca	0.97
Na	0.05
K	0.00
Total	5.02
Cation Ratio	
Ca	94.97
Na	5.03
K	0.00
Total	100.00

Table I: Epidote data from PPP04 – 7c. Cation ratios calculated as (Ca/Ca+Fe+Mg+Mn)*100

Comment	ppp7c 6	ppp7c 12	ppp7c 22
SiO2	37.82	37.92	38.11
TiO2	0.03	0.01	0.15
Al2O3	26.34	28.14	27.38
Cr2O3	0.03	0.00	0.00
FeO	8.61	6.82	7.40
MnO	0.29	0.61	0.33
MgO	0.02	0.00	0.01
CaO	24.11	23.54	23.89
Na2O	0.00	0.00	0.00
K2O	0.00	0.00	0.00
Total	97.25	97.03	97.27
Number of cations corrected for 13 oxygen			
Si	3.16	3.14	3.16
Ti	0.00	0.00	0.01
Al	2.59	2.75	2.67
Cr	0.00	0.00	0.00
Fe	0.60	0.47	0.51
Mn	0.02	0.04	0.02
Mg	0.00	0.00	0.00
Ca	2.16	2.09	2.12
Na	0.00	0.00	0.00
K	0.00	0.00	0.00
Total	8.54	8.49	8.50
Cation ratio			
Fe	21.63	18.13	19.28
Mn	0.75	1.65	0.88
Mg	0.09	0.00	0.05
Ca	77.53	80.22	79.79
Total	100.00	100.00	100.00

76

Table J: Muscovite data from PPP04 – 7c. Cation ratios calculated as (Ca/Ca+Na+K)*100

Comment	ppp17b 15
SiO2	46.40
TiO2	0.00
Al2O3	34.96
Cr2O3	0.00
FeO	0.73
MnO	0.07
MgO	0.78
CaO	1.30
Na2O	0.50
K2O	8.38
Total	93.11
Number of cations corrected for 11 oxygen	
Comment	ppp17b 15
Si	3.12
Ti	0.00
Al	2.77
Cr	0.00
Fe	0.04
Mn	0.00
Mg	0.08
Ca	0.09
Na	0.06
K	0.72
Total	6.89
Cation Ratio	
Ca	10.66
Na	7.40
K	81.93
Total	100.00

Table J: Unknown calc-silicate data from PPP04 – 7c. Cation ratios calculated as (Ca/Ca+Mg+Fe+Mn)*100

Comment	ppp7c 7
SiO2	36.30
TiO2	0.00
Al2O3	27.01
Cr2O3	0.00
FeO	7.66
MnO	0.61
MgO	6.07
CaO	16.84
Na2O	0.00
K2O	0.00
Total	94.50
Number of cations corrected for 11 oxygen	
Si	2.59
Ti	0.00
Al	2.27
Cr	0.00
Fe	0.46
Mn	0.04
Mg	0.64
Ca	1.29
Na	0.00
K	0.00
Total	7.28
Cation Ratio	
Fe	18.84
Mn	1.50
Mg	26.60
Ca	53.06
Total	100.00

Table K: Titanite data from PPP04 – 7c.

Comment	ppp7c 10	ppp7c 28
SiO2	30.47	31.03
TiO2	34.17	30.11
Al2O3	3.28	5.49
Cr2O3	0.50	0.01
FeO	0.50	1.15
MnO	0.10	0.57
MgO	0.05	0.04
CaO	28.81	29.05
Na2O	0.02	0.00
K2O	0.00	0.00
Total	97.90	97.45
Number of cations corrected for 5 oxygen		
Si	1.01	1.04
Ti	0.86	0.76
Al	0.13	0.22
Cr	0.01	0.00
Fe	0.01	0.03
Mn	0.00	0.02
Mg	0.00	0.00
Ca	1.03	1.04
Na	0.00	0.00
K	0.00	0.00
Total	3.06	3.10

Table L: Calcite data from PPP04 – 7c.

Comment	ppp7c 15	ppp7c 20
SiO2	0.05	0.00
TiO2	0.00	0.00
Al2O3	0.06	0.00
Cr2O3	0.00	0.00
FeO	0.41	0.34
MnO	0.57	0.05
MgO	0.01	0.00
CaO	63.06	61.74
Na2O	0.00	0.00
K2O	0.03	0.00
Total	64.20	62.13
Number of cations corrected for 6 oxygen		
Si	0.00	0.00
Ti	0.00	0.00
Al	0.01	0.00
Cr	0.00	0.00
Fe	0.03	0.03
Mn	0.04	0.00
Mg	0.00	0.00
Ca	5.91	5.97
Na	0.00	0.00
K	0.00	0.00
Total	5.99	6.00

Table M: Apatite data from PPP04 – 7c

Comment	ppp7c 8	ppp7c 11
SiO2	0.10	0.00
TiO2	0.02	0.00
Al2O3	0.01	0.00
Cr2O3	0.06	0.00
FeO	0.16	0.13
MnO	0.06	0.04
MgO	0.01	0.00
CaO	54.56	54.79
Na2O	0.02	0.00
K2O	0.01	0.00
Total	55.00	54.96
Number of cations corrected for 25 oxygen		
Si	0.04	0.00
Ti	0.01	0.00
Al	0.00	0.00
Cr	0.02	0.00
Fe	0.06	0.05
Mn	0.02	0.02
Mg	0.01	0.00
Ca	24.77	24.94
Na	0.02	0.00
K	0.00	0.00
Total	24.95	25.00

Table N: Garnet data from PPP04 – 17b. Cation ratios calculated as (Ca/Ca+Mg+Fe+Mn)*100

Comment	ppp17b 10
SiO2	38.71
TiO2	0.25
Al2O3	20.05
Cr2O3	0.11
FeO	6.24
MnO	4.14
MgO	0.03
CaO	30.60
Na2O	0.06
K2O	0.00
Total	100.19
Number of cations corrected for 12 oxygen	
Si	3.00
Ti	0.01
Al	1.83
Cr	0.01
Fe	0.40
Mn	0.27
Mg	0.00
Ca	2.54
Na	0.01
K	0.00
Total	8.07
Cation Ratio	
Fe	12.57
Mn	8.43
Mg	0.11
Ca	78.90
Total	100.00

Table O: Chlorite data from PPP04 – 17b. Cation ratios calculated as (Ca/Ca+Mg+Fe+Mn)*100

Comment	ppp17b 19	ppp17b 21	ppp17b 27
SiO2	30.75	28.56	28.72
TiO2	0.98	0.61	4.55
Al2O3	17.99	19.92	18.35
Cr2O3	0.14	0.09	0.09
FeO	18.38	22.42	20.16
MnO	0.71	0.88	1.06
MgO	15.62	13.69	11.69
CaO	0.11	0.17	3.90
Na2O	0.11	0.10	0.00
K2O	2.83	1.26	0.57
Total	87.63	87.71	89.10
Number of cations corrected for 14 oxygen			
Si	3.16	2.98	2.94
Ti	0.08	0.05	0.35
Al	2.18	2.45	2.22
Cr	0.01	0.01	0.01
Fe	1.58	1.95	1.73
Mn	0.06	0.08	0.09
Mg	2.39	2.13	1.79
Ca	0.01	0.02	0.43
Na	0.02	0.02	0.00
K	0.37	0.17	0.08
Total	9.87	9.84	9.63
Cation Ratio			
Fe	39.04	46.77	42.82
Mn	1.52	1.88	2.29
Mg	59.16	50.89	44.27
Ca	0.28	0.47	10.62
Total	100.00	100.00	100.00

Table P: Feldspar data from PPP04 – 17b. Cation ratios calculated as (Ca/Ca+Na+K)*100

Comment	ppp17b 8	ppp17b 14	ppp17b 22	ppp17b 26	ppp17b 28
SiO2	43.09	44.71	46.47	60.15	59.76
TiO2	0.00	0.00	0.03	0.00	0.00
Al2O3	36.77	31.65	33.74	24.68	25.25
Cr2O3	0.00	0.00	0.02	0.00	0.00
FeO	0.13	3.21	0.26	0.16	0.24
MnO	0.00	0.08	0.01	0.00	0.00
MgO	0.01	2.83	0.02	0.00	0.00
CaO	20.25	13.98	16.75	6.02	6.49
Na2O	0.16	0.91	2.06	8.32	8.02
K2O	0.00	0.82	0.00	0.07	0.04
Total	100.41	98.18	99.36	99.39	99.81

Number of cations corrected for 8 oxygen

Comment	ppp17b 8	ppp17b 14	ppp17b 22	ppp17b 26	ppp17b 28
Si	1.99	2.12	2.15	2.69	2.67
Ti	0.00	0.00	0.00	0.00	0.00
Al	2.00	1.77	1.84	1.30	1.33
Cr	0.00	0.00	0.00	0.00	0.00
Fe	0.00	0.13	0.01	0.01	0.01
Mn	0.00	0.00	0.00	0.00	0.00
Mg	0.00	0.20	0.00	0.00	0.00
Ca	1.00	0.71	0.83	0.29	0.31
Na	0.01	0.08	0.18	0.72	0.70
K	0.00	0.05	0.00	0.00	0.00
Total	5.02	5.06	5.02	5.02	5.02
Cation Ratio					
Ca	98.58	84.25	81.80	28.45	30.79
Na	1.42	9.87	18.20	71.16	68.97
K	0.00	5.88	0.00	0.39	0.24
Total	100.00	100.00	100.00	100.00	100.00

Table Q: Epidote data from PPP04 – 17b. Cation ratios calculated as (Ca/Ca+Mg+Fe+Mn)*100

Comment	ppp17b 6	ppp17b 7
SiO2	38.83	38.49
TiO2	0.04	0.03
Al2O3	29.91	27.85
Cr2O3	0.00	0.04
FeO	5.25	7.69
MnO	0.50	1.74
MgO	0.00	0.02
CaO	23.81	22.38
Na2O	0.06	0.03
K2O	0.00	0.00
Total	98.40	98.26
Number of cations corrected for 13 oxygen		
Si	3.14	3.16
Ti	0.00	0.00
Al	2.85	2.70
Cr	0.00	0.00
Fe	0.35	0.53
Mn	0.03	0.12
Mg	0.00	0.00
Ca	2.06	1.97
Na	0.01	0.01
K	0.00	0.00
Total	8.45	8.49
Cation Ratio		
Fe	14.49	20.15
Mn	1.38	4.62
Mg	0.00	0.05
Ca	84.13	75.19
Total	100.00	100.00

Table R: Muscovite data from PPP04 – 17b. Cation ratios calculated as (Ca/Ca+Na+K)*100

Comment	ppp17b 15
SiO2	46.40
TiO2	0.00
Al2O3	34.96
Cr2O3	0.00
FeO	0.73
MnO	0.07
MgO	0.78
CaO	1.30
Na2O	0.50
K2O	8.38
Total	93.11
Number of cations corrected for 11 oxygen	
Comment	ppp17b 15
Si	3.12
Ti	0.00
Al	2.77
Cr	0.00
Fe	0.04
Mn	0.00
Mg	0.08
Ca	0.09
Na	0.06
K	0.72
Total	6.89
Cation Ratio	
Ca	10.66
Na	7.40
K	81.93
Total	100.00

Table S: Unknown calc-silicate data from PPP04 – 17b. Cation ratios calculated as (Ca/Ca+Mg+Fe+Mn)*100

Comment	ppp17b 9	ppp17b 11
SiO2	36.20	36.20
TiO2	0.00	0.01
Al2O3	26.42	26.12
Cr2O3	0.02	0.02
FeO	9.04	9.57
MnO	0.52	0.50
MgO	6.77	6.54
CaO	15.45	15.54
Na2O	0.04	0.06
K2O	0.00	0.00
Total	94.46	94.56
Number of cations corrected for 11 oxygen		
Si	2.59	2.59
Ti	0.00	0.00
Al	2.23	2.21
Cr	0.00	0.00
Fe	0.54	0.57
Mn	0.03	0.03
Mg	0.72	0.70
Ca	1.18	1.19
Na	0.01	0.01
K	0.00	0.00
Total	7.30	7.31
Cation Ratio		
Fe	21.84	23.00
Mn	1.29	1.23
Mg	29.12	27.97
Ca	47.76	47.80
Total	100.00	100.00

Table T: Ilmenite data from PPP04 – 7c. Cation ratios calculated as (Fe/Fe+Mn)*100

Comment	ppp17b 18	ppp17b 24
SiO2	0.11	0.09
TiO2	52.36	52.24
Al2O3	0.04	0.03
Cr2O3	0.26	0.28
FeO	20.05	20.43
MnO	25.53	25.20
MgO	0.01	0.01
CaO	0.13	0.11
Na2O	0.02	0.03
K2O	0.02	0.03
Total	98.55	98.44
Number of cations corrected for 2 oxygen		
Si	0.00	0.00
Ti	1.00	1.00
Al	0.00	0.00
Cr	0.01	0.01
Fe	0.43	0.44
Mn	0.55	0.54
Mg	0.00	0.00
Ca	0.00	0.00
Na	0.00	0.00
K	0.00	0.00
Total	1.99	2.00
Cation Ratio		
Fe	43.69	44.47
Mn	56.31	55.53
Total	100.00	100.00

Table U: Titanite data from PPP04 – 17b.

Comment	ppp17b 2	ppp17b 3	ppp17b 4	ppp17b 5	ppp17b 13	ppp17b 16
SiO2	30.43	30.53	30.53	30.74	30.80	30.64
TiO2	33.87	35.16	35.20	33.19	33.01	32.99
Al2O3	3.50	2.80	2.73	4.11	4.57	4.13
Cr2O3	0.20	0.36	0.11	0.15	0.18	0.20
FeO	0.55	0.39	0.70	0.65	0.49	0.56
MnO	0.28	0.03	0.24	0.22	0.12	0.27
MgO	0.00	0.01	0.01	0.03	0.01	0.01
CaO	28.82	28.87	28.94	28.64	29.43	28.99
Na2O	0.02	0.02	0.09	0.02	0.01	0.00
K2O	0.00	0.00	0.00	0.00	0.00	0.00
Total	97.68	98.16	98.55	97.75	98.62	97.79
Number of cations corrected for 12 oxygen						
Si	2.44	2.43	2.43	2.45	2.44	2.45
Ti	2.04	2.11	2.11	1.99	1.96	1.98
Al	0.33	0.26	0.26	0.39	0.43	0.39
Cr	0.01	0.02	0.01	0.01	0.01	0.01
Fe	0.04	0.03	0.05	0.04	0.03	0.04
Mn	0.02	0.00	0.02	0.02	0.01	0.02
Mg	0.00	0.00	0.00	0.00	0.00	0.00
Ca	2.47	2.46	2.47	2.45	2.50	2.48
Na	0.00	0.00	0.01	0.00	0.00	0.00
K	0.00	0.00	0.00	0.00	0.00	0.00
Total	7.35	7.32	7.34	7.36	7.38	7.37

Table V: Sulfide data from PPP04 – 7c.

Comment	ppp17b 12	ppp17b 17	ppp17b 23	ppp17b 25
SiO2	0.23	0.15	0.17	0.16
TiO2	0.17	0.18	0.23	0.52
Al2O3	0.13	0.07	0.05	0.06
Cr2O3	0.35	0.32	0.35	0.37
FeO	73.60	77.30	77.31	76.71
MnO	0.14	0.13	0.13	0.23
MgO	0.09	0.08	0.06	0.08
CaO	0.16	0.12	0.09	0.10
Na2O	0.10	0.08	0.08	0.10
K2O	0.03	0.02	0.04	0.03
Total	75.00	78.46	78.52	78.35
Cations				
No.	126.00	131.00	137.00	139.00
Si	0.00	0.00	0.00	0.00
Ti	0.00	0.00	0.00	0.01
Al	0.00	0.00	0.00	0.00
Cr	0.00	0.00	0.00	0.00
Fe	0.97	0.98	0.98	0.97
Mn	0.00	0.00	0.00	0.00
Mg	0.00	0.00	0.00	0.00
Ca	0.00	0.00	0.00	0.00
Na	0.00	0.00	0.00	0.00
K	0.00	0.00	0.00	0.00
Total	0.99	0.99	0.99	0.99

Appendix D: Microprobe Pictures

Figures 1.1. 1.2, &1.3: Spot locations for PPP04 – 19. The number on the figures correspond to the last two numbers in the microprobe tables
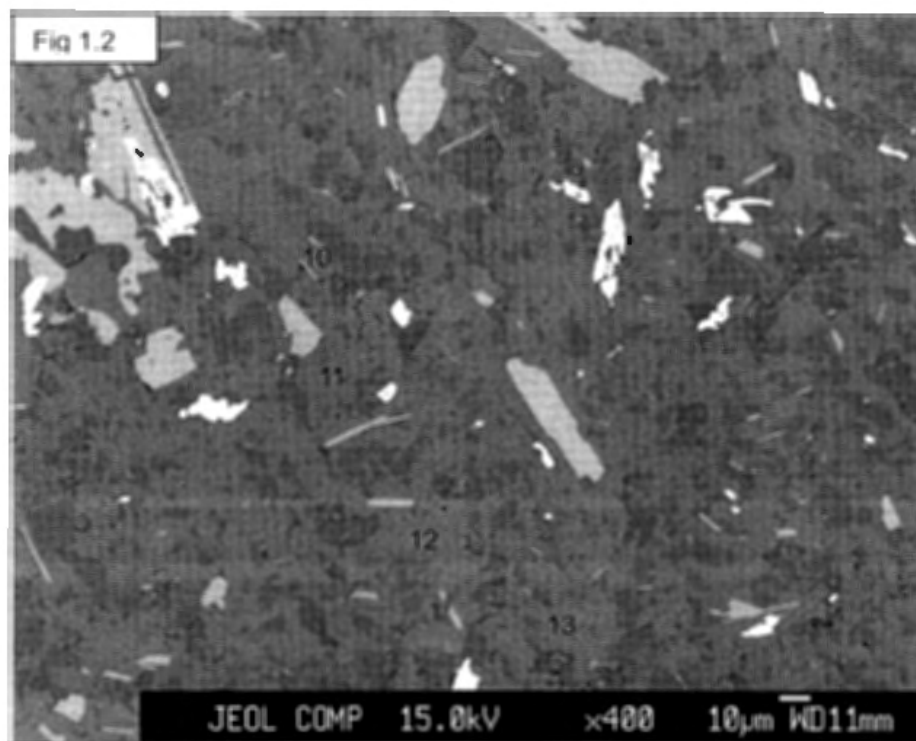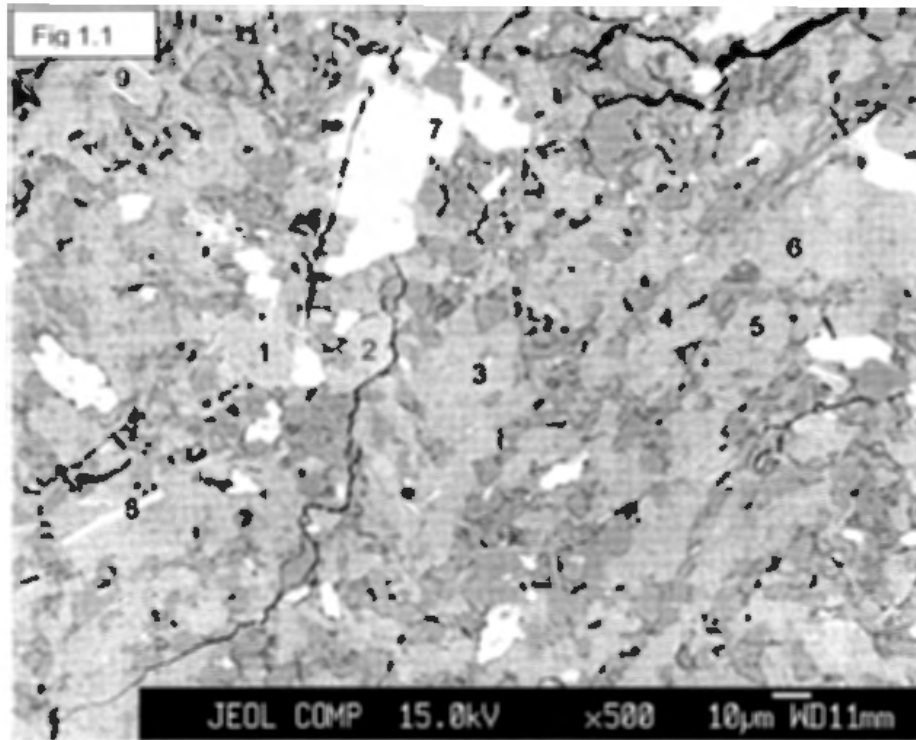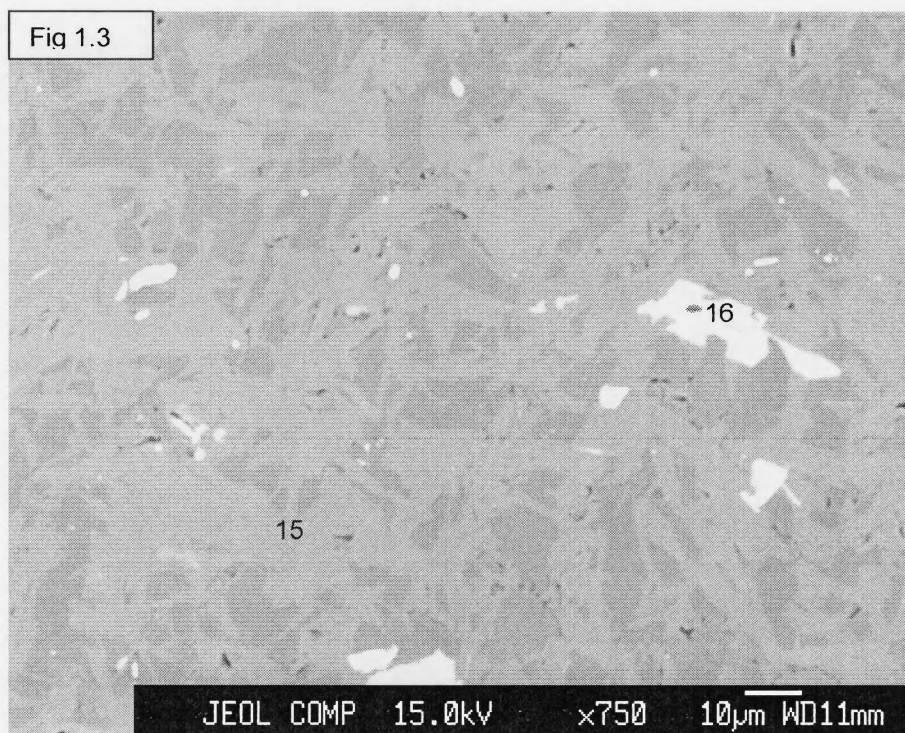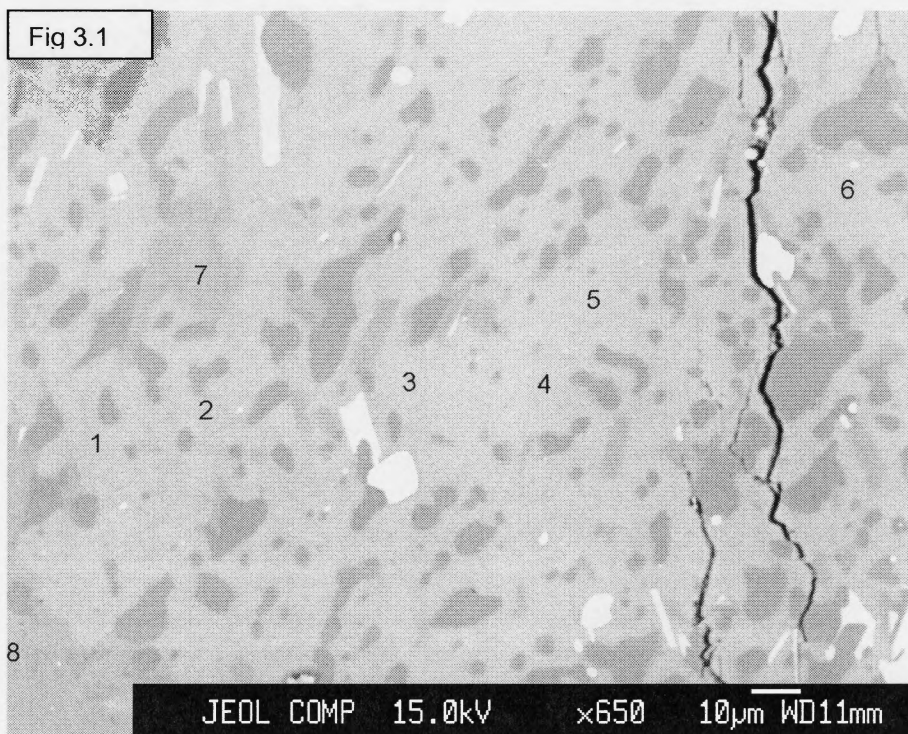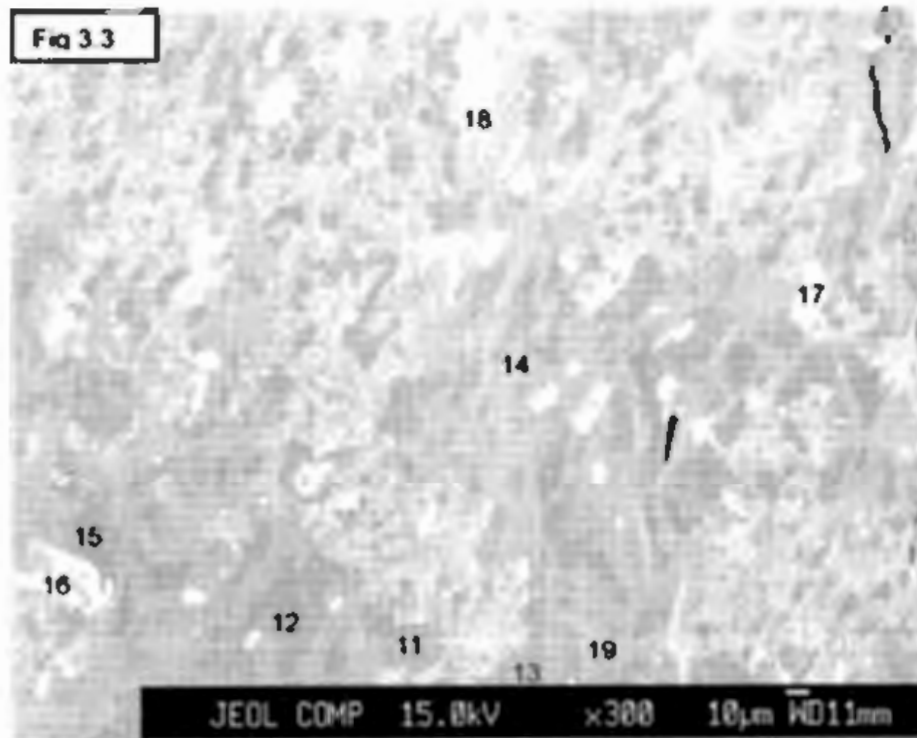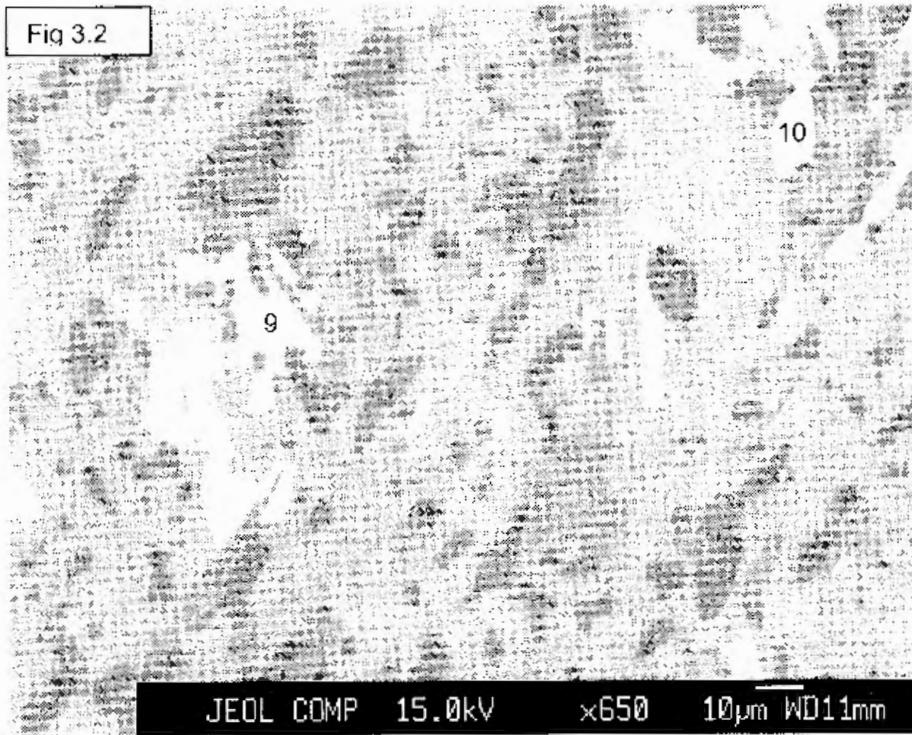
Note: point 14 is just out of field of view

Figures 2.1 & 2.2: Spot locations for PPP04 – 5b. The number on the figures correspond to the last two numbers in the microprobe tables
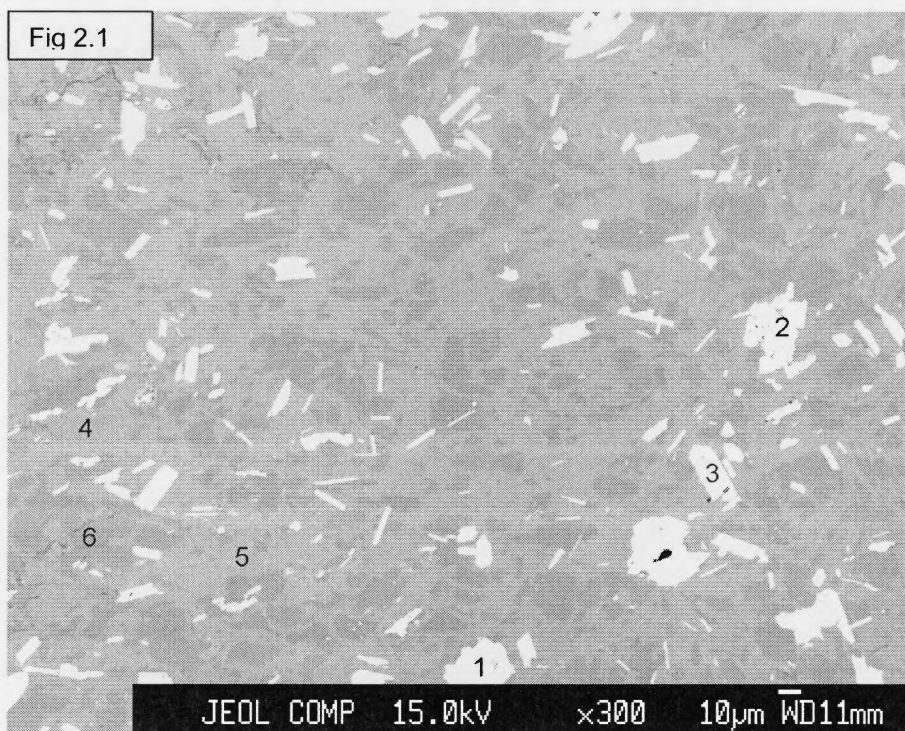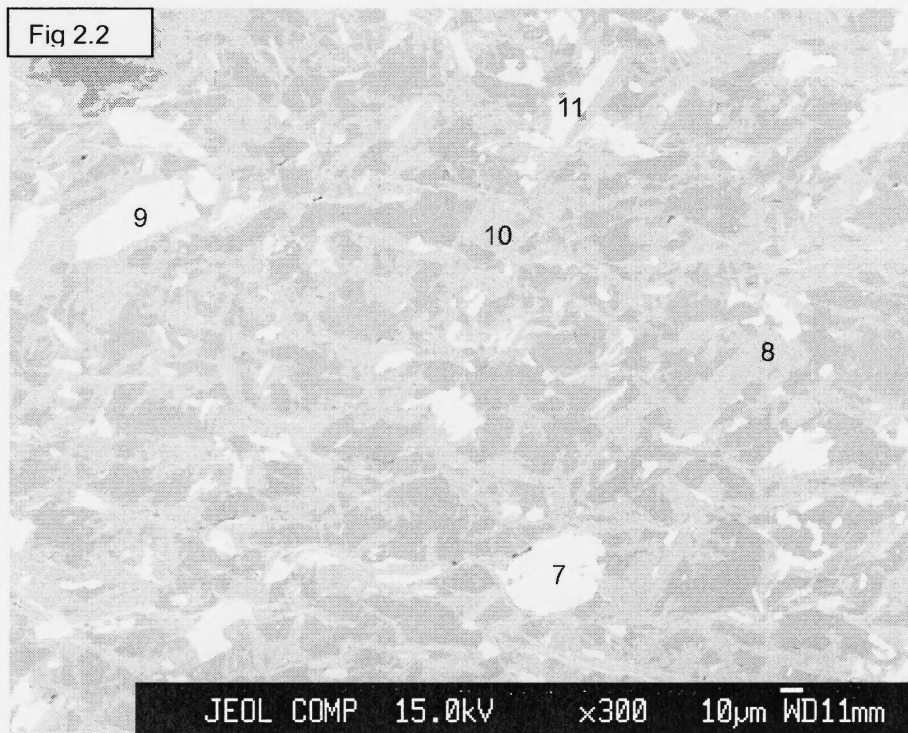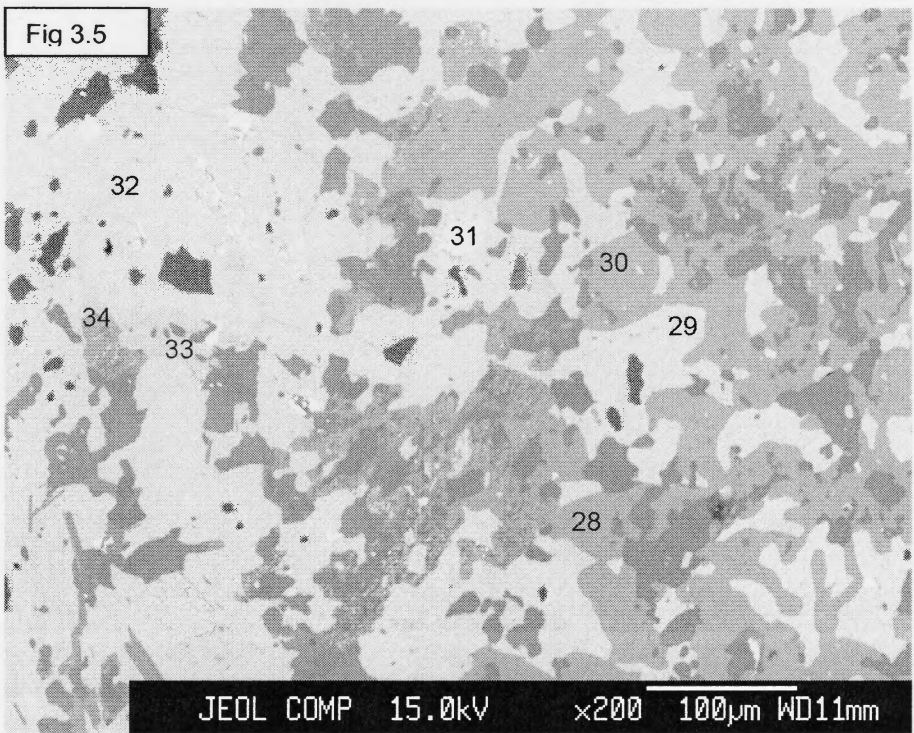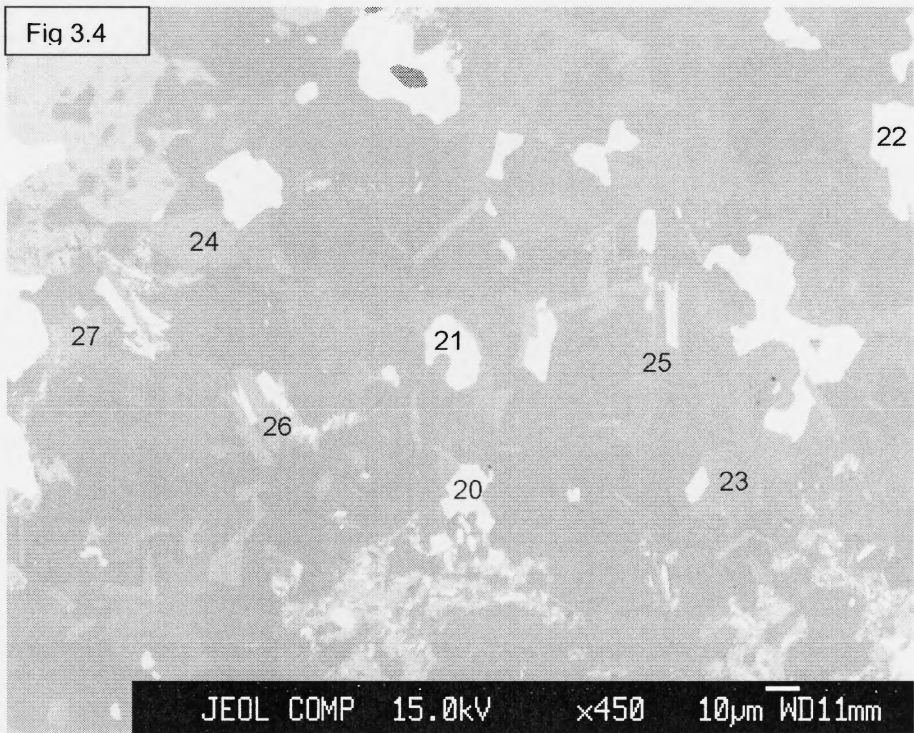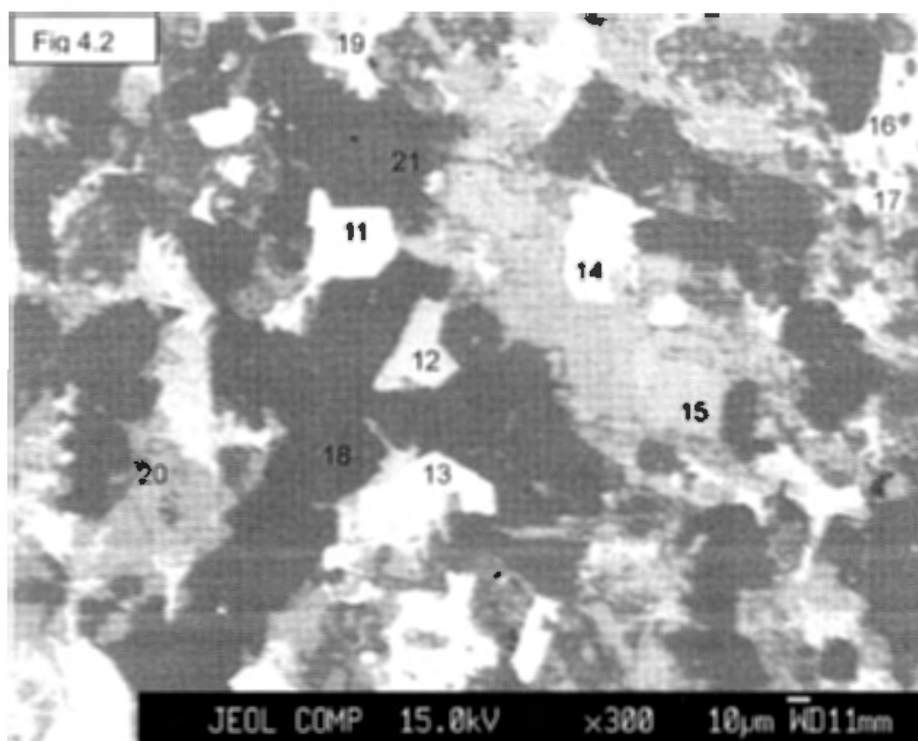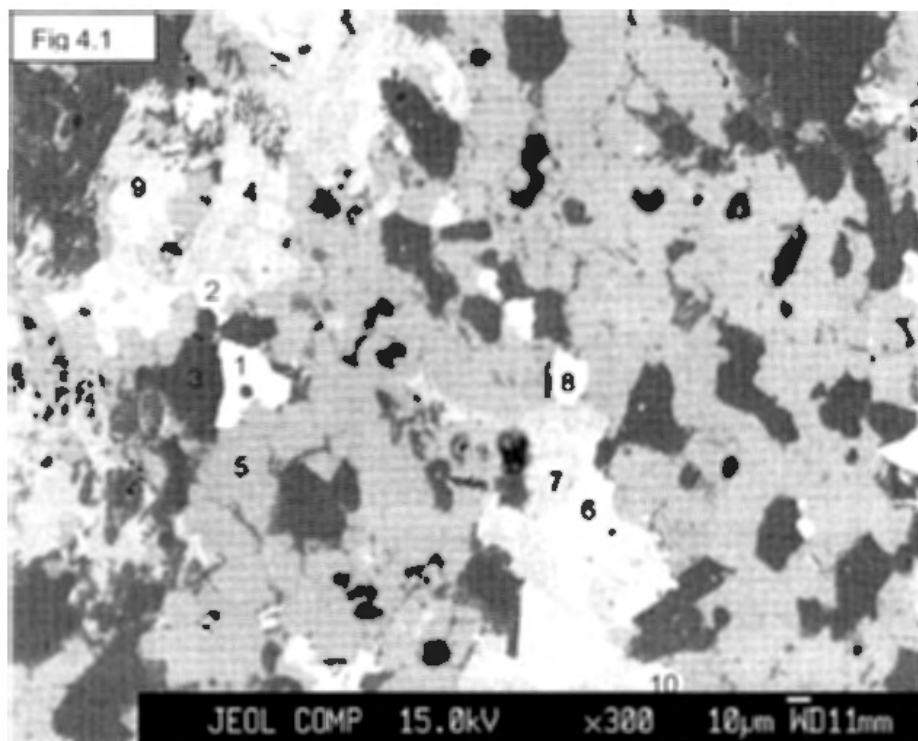
Figures 3.1, 3.2, 3.3, 3.4, & 3.5: Spot locations for PPP04 – 3. The number on the figures correspond to the last two numbers in the microprobe tables

Fig 3.2

JEOL COMP   15.0kV   x650   10µm WD11mm

Fig 3.3

JEOL COMP   15.0kV   x300   10µm WD11mm

Fig 3.4

JEOL COMP   15.0kV   ×450   10µm WD11mm

Fig 3.5

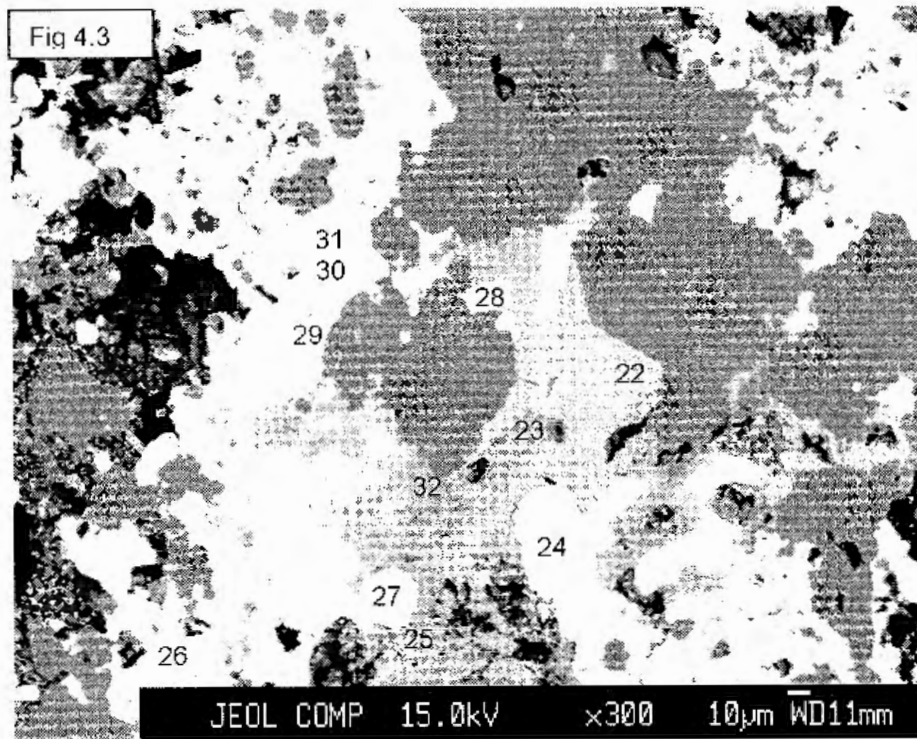JEOL COMP   15.0kV   ×200   100µm WD11mm

Figures 4.1, 4.2, & 4.3: Spot locations for PPP04 – 7c. The number on the figures correspond to the last two numbers in the microprobe tables

Figures 5.1, 5.2, 5.3, & 5.4: Spot locations for PPP04 – 17b. The number on the figures correspond to the last two numbers in the microprobe tables

Fig 5.2

JEOL COMP 15.0kV ×150 100µm WD11mm

Fig 5.3

JEOL COMP 15.0kV ×300 10µm WD11mm

Fig 5.4